THE FAILURE PROCESS IN COLUMNAR-GRAINED ICE

Ъy

Lorne W. Gold

A thesis submitted to the Faculty of Graduate Studies and Research in partial fulfillment of the requirements for the degree of Doctor of Philosophy.

Interdisciplinary Programme in Glaciology, McGill University, Montreal. 24 March, 1970.

ACKNOWLEDGEMENTS

The information presented in this thesis was obtained from a series of experiments carried out at the National Research Council in Ottawa over a period of five years. This work was the culmination of a series of studies that had their start when the author was given the opportunity to do research on the properties of ice and snow in the NRC'c Division of Building Research in 1950. Early studies soon demonstrated the unique research opportunities offered by the material, ice, and the author had the good fortune to be able to exploit these opportunities because of the continued interest, support and encouragement of Dr. R.F. Legget, the Director of the Division from 1947 to 1969.

The interest of the author in snow and ice soon brought him into contact with allied work at McGill University - initially Professor J.S. Marshall and the Stormy Weather Group, and subsequently Professor E.R. Pounder and his Ice Physics Group, Professor F. Muller and Professor J. Jonas. He benefited greatly from these associations and wishes to express his gratitude for the time that has been shared with him.

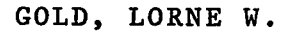
One of the privileges enjoyed by the author was great freedom in the pursuit of his research interests. For this he is particularly indebted to Dr. Legget.

The author wishes to express his appreciation for the encouragement and support received from Professor Pounder, and for his comments and recommendations concerning this thesis. He wishes also to express his thanks to Professor Jonas for his constructive suggestions and helpful discussions.

The investigations reported in this thesis were undertaken after preliminary studies of the elastic and creep properties of ice, and of some of the factors associated with crack formation. The following students assisted in the early work during summer periods: R. Wallace, 1958; A. Bunner, 1959; F. Wilson, 1960; P. Mitenko, 1961; D. Dunlop, 1962; F. Fyfe, 1964. Their contribution to the investigations that led to the undertaking of the more detailed studies on crack formation and failure is gratefully acknowledged. The author wishes also to acknowledge with thanks the assistance of L.E. Goodrich in the observations of the cracking activity at -31°C.

The author is indebted to McGill University for allowing him to use his research at the National Research Council as the subject of this thesis, and to the National Research Council for their permission to use this work in this way.

Finally, he wishes to acknowledge with special thanks the technical assistance of Mr. W. Ubbink during the five years of this study, and the assistance of Miss L. Lacombe in the typing and assembling of the thesis.



THE FAILURE PROCESS IN COLUMNAR-GRAINED ICE

Submitted for the Degree of Doctor of Philosophy
Interdisciplinary Programme in Glaciology

Information is presented on the stress, strain, temperature and time dependence of crack formation in columnar-grained ice. It was observed that cracks began to form during creep when the constant compressive stress exceeded about 6 kg/cm^2 . For stresses less than about 10 kg/cm^2 , the cracking activity was confined primarily to the primary creep stage. When the stress was greater than about 12 kg/cm^2 , crack formation brought on the failure condition before the secondary creep stage could be established.

It is shown that prior to the onset of failure, the cracking activity was essentially random, and probably involved two
independent processes - one with a probability of crack formation dependent on the strain, and one with a probability
independent of the strain. Observations are presented on the
probability distribution for crack density, width and orientation.
The possible effect that modes of deformation and recovery might
have on the temperature and strain dependence of the cracking
activity is discussed.

TABLE OF CONTENTS

| Ac | Acknowledgements | | | | |
|-----|------------------|------------------------------|----|--|--|
| ΑЪ | Abstract | | | | |
| Tal | ble o | f Contents | v | | |
| 1. | INT | RODUCTION | 1 | | |
| 2. | PROI | PERTIES OF ICE | 6 | | |
| | 2.1 | Crystal Structure | 6 | | |
| | 2.2 | Lattice Imperfections | 10 | | |
| | | 2.2.1 Point Defects | 11 | | |
| | | 2.2.2 Dislocations | 15 | | |
| | | 2.2.3 Substructure | 18 | | |
| | 2.3 | Polycrystalline Ice | 19 | | |
| | 2.4 | Deformation | 24 | | |
| | | 2.4.1 Single Crystals | 24 | | |
| | | 2.4.2 Granular Ice | 33 | | |
| | | 2.4.3 Columnar-grained Ice | 37 | | |
| | | 2.4.4 Degree of Freedom | 42 | | |
| | | 2.4.5 Modes of Deformation | 46 | | |
| | 2.5 | | 60 | | |
| 3. | FAIL | | 66 | | |
| | 3.1 | Definitions | 66 | | |
| | 3.2 | Crack Initiation | 69 | | |
| | 3.3 | Crack Propagation | 75 | | |
| | 3.4 | Cavity Formation | 87 | | |
| | 3.5 | | | | |
| | 3.6 | Failure of Rock and Concrete | 90 | | |
| | 3. 0 | or wook and concrete | 7/ | | |

| 4. | SPEC | IMEN PREPARATION AND EXPERIMENTAL PROCEDURES | 104 | | |
|----------------------------|-------|--|-----|--|--|
| | 4.1 | Preparation of the Ice | 104 | | |
| | 4.2 | Preparation of the Specimens | 106 | | |
| | 4.3 | Conduct of Experiments | 107 | | |
| 5. | TIME | TO FORMATION OF FIRST CRACKS | 114 | | |
| | 5.1 | Observations | 115 | | |
| | 5.2 | Discussion | 120 | | |
| | 5.3 | Conclusions | 129 | | |
| 6. | CRACE | KING ACTIVITY DURING CREEP | 130 | | |
| | 6.1 | Results of Observations on Crack Formation | 130 | | |
| | 6.2 | Creep Behaviour | 152 | | |
| | 6.3 | Discussion | 171 | | |
| 7. | STATI | STICS OF THE CRACKING ACTIVITY | 183 | | |
| | 7.1 | Spatial Distribution of Cracks | 184 | | |
| | 7.2 | Crack Orientation | 194 | | |
| | 7.3 | Crack Widths | 198 | | |
| | 7.4 | Crack Density | 206 | | |
| | 7.5 | Discussion | 218 | | |
| 8. | Conc1 | usions | 222 | | |
| 9. | Recom | mendations for Future Research | 225 | | |
| Sibliography 2 | | | | | |
| Claim of Original Work 246 | | | | | |

THE PROCESS OF FAILURE IN COLUMNAR-GRAINED ICE

1. INTRODUCTION

Ice is such a natural and familiar part of our environment that we tend to overlook or take for granted the consequences of its unique characteristics. It is the solid form of one of the few substances that expands on freezing. Because it floats on the surface of its melt, it helps maintain an environment suitable for the survival of life through winter periods in cold areas. The frictional properties of its surface contribute both to the pleasures of skating and the hazards of travel. It is able to accumulate to such depths in some regions that it flows under its own weight and, in so doing, contributes to the continual reshaping of the earth's surface. It will fracture in a brittle manner, even at its melting temperature, when struck lightly with a hammer.

The behaviour of ice when under stress is a subject of some importance for engineering. Structures built in cold regions must often be designed to withstand the forces that ice can exert. Ice covers are sometimes used for transportation purposes, and it is important to know the amount of weight that can be placed safely onto covers of given thickness and quality.

Both of these problems require for their solution a knowledge of the ultimate strength of ice and its deformation behaviour, particularly at failure, for given load conditions. For most engineering materials, the information required to establish the safe working stress and stress at failure can usually be obtained by appropriate laboratory tests. These tests, often empirical in nature and supplemented by experience in use, help to establish the service conditions from both a safety and economic point of view. When consideration is given to problems associated with ice, however, several factors are encountered in a combination rare in engineering practice.

One of the most significant of these is that the temperature of the ice is close to that at which it melts. Its homologous temperature is usually greater than 0.8. For practically all engineering problems ice is in a high temperature state and exhibits behaviour to be expected for this condition.

Another factor is that the condition of interest is usually that associated with the maximum force that ice is able to sustain or exert. The ability of the engineer to predict the failure condition, and the deformation behaviour leading up to and during this condition, is in an inadequate state of development. This is particularly true for failure at high temperature.

Still another factor is that man normally does not have the control over the manufacture and use of ice that he has for most engineering materials. He must work or contend with it in the condition provided by nature. As the material is a product of nature, it is subject to random variations in properties such as density, grain size and structure, and impurity content. These properties, determined by the conditions existing during growth, can have a significant influence on deformation behaviour and strength.

Considerable information has accumulated concerning problems such as the bearing capacity of ice covers and the force that they can exert against structures. This information has been largely empirical, derived from field experience and performance. An empirical basis for design can be adequate for many problems, but it is not satisfactory for situations that do not conform with past experience. recent years problems have arisen for which a greater understanding of the deformation and failure behaviour of ice was required. It has also been thought that some structures may have been overdesigned because of ignorance of the forces that ice can exert under given conditions. Attention has been given, consequently, to studies of the deformation and strength properties of ice with the thought that the information obtained could provide a more rational basis for estimating maximum stresses or establishing a reasonable factor of safety.

The properties of ice make it a particularly interesting material for the study of deformation and failure, quite apart from the engineering need for this information. transparent, and so it is possible to observe directly during experiment some of the structural modifications associated with deformation and the failure process. It has a crystallographic symmetry that has a marked influence on how it responds to load. For some conditions of loading it will behave in a ductile manner; for some in a quite brittle manner; and for still others it will exhibit a combination of brittleness concurrent with an overall ductile response. possible to control the grain structure and texture of ice during the freezing of water, and to thereby obtain material that can be used to study how these factors affect deformation behaviour. The combination of the above properties makesice a particularly interesting material for studies of the process of failure at high temperatures.

During a study of the deformation behaviour of ice, it was noted that internal cracks formed during compressive creep when the stress exceeded a fairly critical value. These cracks were isolated events, and tended to be stable in size. Crack formation was continuous and if the stress was sufficiently large, gradually broke down the structure until the specimen failed. The behaviour appeared to be reproducible,

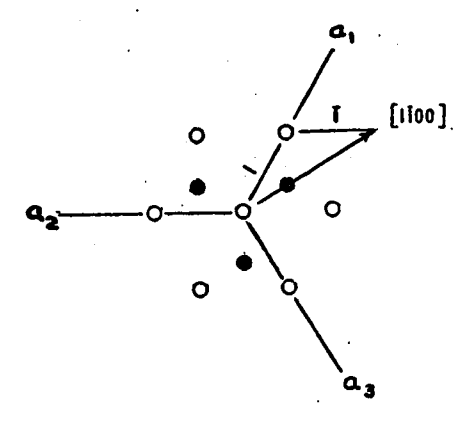
and so indicated the possibility of describing the failure condition for ice in a way suitable for engineering requirements and for providing greater insight into the failure process. Observations were undertaken to determine the factors that controlled crack formation, and how the cracking activity depended on stress, time, strain and temperature. Concurrent observations were made on the creep behaviour and on some of the deformation features that developed. the results of this study that are reported in this thesis. They are presented and discussed with reference to the properties of ice, the behaviour of other materials, and current thinking concerning crack formation and failure. review of the properties of ice of importance in the failure process is presented in Section 2. Crack initiation, propagation and failure are discussed in Section 3. The experiments are described in Section 4, and the results presented and discussed in Sections 5, 6 and 7.

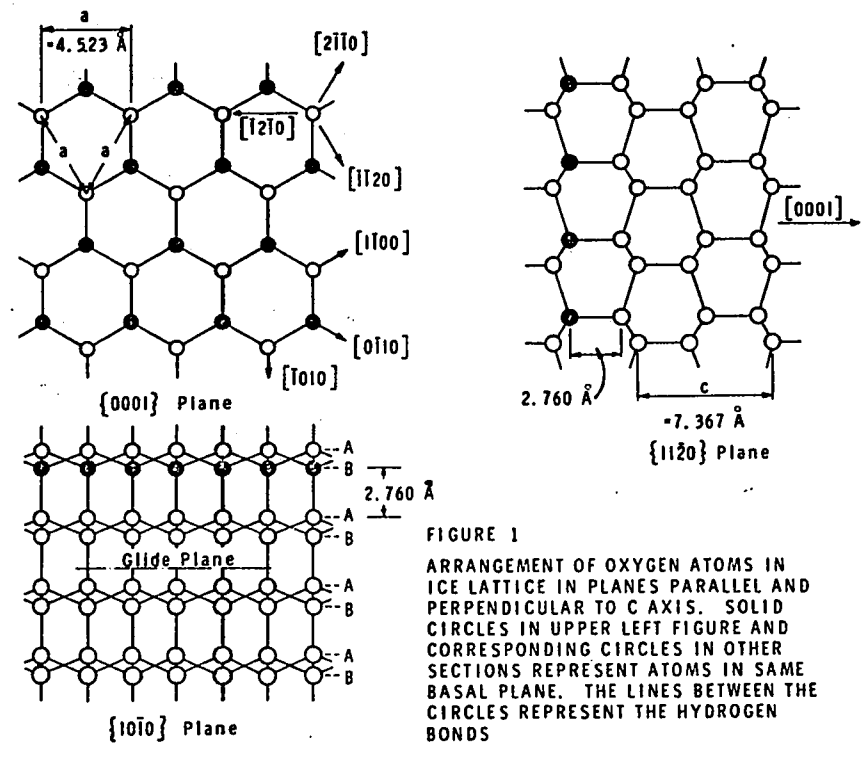
2. PROPERTIES OF ICE

2.1 Crystal Structure

Ice is composed of hydrogen bonded oxygen atoms. X-ray studies, such as those of Barnes (1929) and Owston (1953), have shown that each oxygen atom is at the centre of an almost perfect tetrahedron. The four corners of the tetrahedron are occupied by the neighboring oxygen atoms. It has been deduced from X-ray studies that the ice lattice has hexagonal symmetry, and that there are four oxygen atoms in the unit cell. Figure 1 shows the arrangement of the oxygen atoms in planes parallel and perpendicular to the symmetry, or c-axis, of the crystal.

The distance between oxygen atoms at 0°C is 2.760A and the angle between the hydrogen bonds 109.5°. At this temperature the c/a ratio for the unit cell is 1.629, just a little less than the axial ratio for an exactly regular tetrahedral arrangement (1.633). There is evidence that the distance between oxygen atoms in the plane of symmetry, or basal plane, is just slightly greater than in the direction of the c-axis (0.01Å at 0°C). Information on the structure of ice, including the temperature dependence of the lattice parameters, is reviewed by Dorsey (1940), Lonsdale (1958) and Owston (1958).





{1010} Plane

In figure 1, the atoms denoted by open circles are all on the same plane. Those denoted by solid circles are in the plane immediately adjacent (eg A and B). Each of these planes can be considered as a layer of "close packed" atoms, as is done in discussions of the molecular structure of metals (eg Reed-Hill, 1964). The ice structure can be considered as built up of identical layers of atoms, A and B. Looking in the direction of the c-axis, the oxygen atoms in one set of layers are located along lines defined by the intersection of the bisectors of the angles of the equilateral triangles formed by three adjacent atoms in the second set of layers. The stacking sequence of the layers is ABBAABB.....

The Miller indices of the three principal directions in the ice lattice are shown in figure 1: the reference axes with an example direction are shown at the top of the figure. A displacement of a layer a distance 4.25\AA in $<11\overline{2}0>$ directions, that is, along the line of closest packing of atoms, places each oxygen atom in a position exactly equivalent to its initial one. The sides of the familiar snow crystal in the shape of a hexagonal plate are parallel to the $<11\overline{2}0>$ directions; the arms of the dentritic snow crystals are extensions in the $<11\overline{2}0>$ directions.

Hydrogen atoms are difficult to detect with X-rays because they scatter the rays so weakly. For this reason

their position within the ice lattice has not been as well established as that of the oxygen atoms, and much of the evidence concerning it is indirect. On the basis of available evidence, Bernal and Fowler (1933) proposed the following rules concerning the position of the hydrogen atoms:

- the hydrogen atoms are located on the lines connecting adjacent oxygen atoms;
- 2. there is only one hydrogen atom between two adjacent oxygen atoms;
- 3. each oxygen atom has two hydrogen atoms attached to it at a distance of about 1A.
 (i.e. the water molecule is preserved in the ice crystal lattice).

Each oxygen atom in the ice lattice has four bonds with neighboring oxygen atoms. There are, therefore, six different ways in which the hydrogen atoms can be placed about the oxygen atom so as to satisfy the Bernal-Fowler rules. A preference for any one of these six arrangements would cause ice to have pyro- and piezo-electric properties. Since there is no evidence of this, it must be concluded that if the hydrogen atoms obey the Bernal-Fowler rules, all six possible arrangements are equally probable.

Pauling (1935) assumed such a statistical behaviour. In addition to the Bernal-Fowler rules, he also postulated that

the interaction between non-adjacent molecules is such that it will not stabilize any one of the many possible configurations. With this model he was able to give a reasonable explanation for the residual entropy possessed by ice at 0°K.

X-ray measurements by Owston (1953, 1958); neutron scatter measurements by Wollen et al (1949) and Petersen and Levy (1957) on D₂O ice; proton magnetic resonance measurements by Kume (1961); and measurement of dielectric properties (see Granicher et al, 1957), support the Pauling statistical model. These observations indicate that there is short range order in the position of the hydrogen atoms as required by the Bernal-Fowler rules, but that long range order is not present. The observations of Petersen and Levy show that the spatial average of the positions of the hydrogen atoms is equivalent to the atom in each bond spending 50% of its time about 1A from one oxygen atom, and the remainder in the corresponding position relative to the second. It is now generally accepted that the Pauling statistical model is a reasonable description of the position and behaviour of the hydrogen atoms in the ice lattice.

2.2 Lattice Imperfections

Strength, plasticity and viscosity are structure sensitive properties. They are controlled primarily by imperfections that exist or are induced into the crystal lattice. It is

useful to have an appreciation of the imperfections that occur in the ice lattice, and the energy associated with their formation and movement, when considering the strength and deformation behaviour of ice.

2.2.1 Point Defects

The most common point defects in pure crystals are atoms or molecules missing from their normal positions in the lattice (vacancies), or in abnormal interlattice positions (interstitials). Vacancies in particular play an important role in deformation at high homologous temperatures (Nabarro, 1948; Herring, 1950; Garofalo, 1965; Weertman, 1968). They provide a means by which matter can be effectively transferred from one region of a crystal to another due to differences in the Gibbs free energy.

A vacancy is formed, conceptually, by removing an atom or molecule from its position in the lattice and placing it on the surface of the crystal. Removing a molecule of water from the interior of ice involves the breaking of four hydrogen bonds. Two hydrogen bonds are formed when the molecule is attached to the surface. The energy of the hydrogen bond is about 0.25eV, and so the energy of formation of a vacancy should be about 0.50eV (Kräger, 1964). Gränicher (1958) obtained 0.53eV for the energy of formation of a vacancy.

^{*} leV = 23.05 kca1/mole

Granicher also estimated the energy of formation of an interstitial water molecule to be about 0.7eV. This suggests that interstitial water molecules play a smaller role in mass transport in ice than vacancies. It has been suggested by Haas (1962) that interstitial water may participate in the diffusion process if its energy of formation is reduced by the formation of bonds with neighboring molecules.

Several studies have been made of the activation energy of self-diffusion of $\mathrm{H}_2^3\mathrm{O}$ and $\mathrm{H}_2\mathrm{O}^{18}$ in ice. $\mathrm{H}_2^3\mathrm{O}$ and $\mathrm{H}_2\mathrm{O}^{18}$ refer to molecules of water tagged with the isotopes of hydrogen and oxygen, H^3 and O^{18} , respectively. The results of some of these studies are summarized in Table 1. A calculation by Ramseier (1967) indicates that self-diffusion of $\mathrm{H}_2^3\mathrm{O}$ occurs by the vacancy mechanism, and involves the whole molecule. The approximate equality of the activation energy for self-diffusion of $\mathrm{H}_2^3\mathrm{O}$ and $\mathrm{H}_2\mathrm{O}^{18}$ supports this conclusion.

Bjerrum (1951, 1952) discussed point defects that can occur due to violations of the Bernal-Fowler rules. A translation of a hydrogen nucleus from one of its stable positions in the bond to the second produces ionic defects i.e.

Subsequent similar translations of hydrogen nuclei can separate these two ions so that they become independent of each other. A rotation of a water molecule can remove a hydrogen nucleus from its bond position, and place it into a bond that is already occupied. This creates a hydrogen vacancy or unoccupied bond called an L defect; and a hydrogen "interstitial" or doubly occupied bond called a D defect. Subsequent rotation of water molecules can separate these two defects and make them independent. Ionization and rotational defects provide the basis for currently accepted models describing the electrical properties of ice (Granicher et al, 1957; Granicher, 1963; Jaccard, 1965).

Kräger (1964) suggested that L and D defects may be associated with vacancies. An energy calculation indicated thet association of a vacancy with a D defect is preferred. Haas (1962) suggested that the defects may be associated also with interstitials. It is considered that the L and D defects play a role in mechanical relaxation. Their possible effect on the motion of dislocations is discussed in the following section. It appears that the hydrogen atom may have a significant effect on the deformation behaviour of ice at high temperatures. Activation energies associated with the formation of orientation and translation defects involving hydrogen atoms are given in Table 1.

TABLE I

Activation energies for formation of point defects and self diffusion in ice.

| Defect or Process | Activation Energy | Source | |
|---|--|--|--|
| | e.V. | | |
| Vacancy | 0.53 | Granicher, 1958 | |
| Interstitial | 0.70 | Gränicher, 1958 | |
| Orientational defect (pair) | 0.68 ± 0.04 | Jaccard, 1959 | |
| L defect | 0.235 ± 0.01 | Jaccard, 1959 | |
| Ion pair defect | 1.2 ± 0.1 | Jaccard, 1959 | |
| Diffusion | | | |
| * T ** T_ + T T_L T_L T_L T T & | 0.62 ± 0.03 0.62 ± 0.07 0.63 ± 0.02 0.63 ± 0.03 0.58 ± 0.05 0.63 ± 0.05 0.67 ± 0.08 0.65 ± 0.05 | Blicks et al, 1966 Blicks et al, 1966 Dengel et al, 1963 | |
| † 0 ¹⁸ | 0.68 ± 0.13 | Delibaltas et al, 1966 | |

^{*} T: Tritium ice (H_2^30) .

^{**} \parallel : Diffusion in the <0001> direction.

⁺ \perp : Diffusion perpendicular to the <0001> direction.

[†] 0^{18} : Ice containing water molecules tagged with the 0^{18} isotope.

2.2.2 Dislocations

Etch pits can be produced on the surface of ice using a solution of polyvinyl formal (formvar) in ethylene dichloride (Higuchi, 1958). There is evidence that some of the pits mark the site of emergence of dislocations. Bryant and Mason (1960) observed etch channels in the <11 $\overline{2}$ 0> direction associated with pits in the basal plane and suggested they were due to edge dislocations. They were not able to match pits on parallel faces of ice plates 100 μ thick.

Muguruma (1961, 1963, 1965) observed that the density of etch pits in both the basal and prism planes was of the order of 10^6 to $10^7/\mathrm{cm}^2$ at the surface, and about $10^5/\mathrm{cm}^2$ about 100 μ below the surface. He suggested that the increase in density of the pits near the surface was due to the formation of dislocations by the mechanical polishing technique used to prepare the surface for etching.

Muguruma and Higashi (1963) subjected undeformed single crystals with an initial etch pit density of 10^5 to $10^6/\text{cm}^2$, to non-basal glide of 3%. The etch pit density on the basal plane increased to about $10^7/\text{cm}^2$. Etch channels associated with the pits indicated dislocations moving in the < $10\overline{10}$ > and < $11\overline{20}$ > directions. They concluded that the channels could be caused by pure screw dislocations in the $\{10\overline{10}\}$ or $\{11\overline{22}\}$ planes with Burgers vector in the < $11\overline{20}$ > direction. It was

considered that the motion of dislocations created vacancy trails, and that nearby impurities precipitated into the trails. They suggested that the etch channels, which were formed about 24 hours after the deformation, were due to the presence of the vacancy trails.

Muguruma, Mae & Higashi (1966) studied the formation of voids during non-basal glide. The voids formed in layers parallel to the basal plane, and were aligned in the $\langle 11\overline{2}0\rangle$ direction. Their formation appears to be similar to that of vacancy discs observed in zinc foil by Price (1963), and is strong evidence that non-basal glide involves non-conservative motion of dislocations.

Interesting information on dislocation networks in ice hase been obtained with X-ray topography. Webb and Hayes (1967), using tabular dendritic crystals 0.1 to 0.3 mm in thickness, observed that most of the dislocations lie in the basal plane. Higashi et al (1968), found the same condition for specimens about 1 mm thick.

Webb and Hayes found that newly formed crystals had large areas (0.5 cm²) free of dislocations. The dislocations appeared to originate at inclusions during deformation. There was a strong tendency for the dislocations to be of the screw type with Burgers vector $\overline{b} = a/3 < 11\overline{20} >$.

Evidence was obtained for the reaction.

 $a/3<11\overline{2}0> + a/3<1\overline{2}10> = a/3<2\overline{11}0>$

Climb appeared to take place during annealing, transforming dislocations of $\langle 11\overline{2}0 \rangle$ type to edge dislocations lying approximately in the $\langle 0001 \rangle$ direction. There was evidence of cross slip on pyramidal planes, probably $\{1\overline{1}01\}$, but no evidence of partial dislocations and stacking faults. They suggested that etch pits on the basal plane would show only a small fraction of the dislocation structure visible by X-ray topography because the dislocations tend to be parallel to the (0001) plane.

Higashi et al (1968) and Fukuda and Higashi (1969) also found the principal Burgers vector to be a/3 <11 $\overline{2}$ 0>. The dislocations in the basal plane tended to be curved and roughly parallel to <11 $\overline{2}$ 0> and <10 $\overline{1}$ 0> directions, suggesting that they were not tied strongly in a Peierls valley.

The evidence obtained to date indicates that dislocations in ice lie primarily in the basal plane, and are of the screw or almost screw type with Burgers vector a/3 <11 $\overline{2}$ 0>. Dislocations tend to be curved, but with a general <11 $\overline{2}$ 0> and <10 $\overline{1}$ 0> direction. Short edge dislocations in the <0001> direction may be present, particularly after annealing following deformation. By far the easiest mode of deformation

is by dislocation glide on basal planes, and pyramidal cross-slip.

Bjerrum (1952) pointed out that disorder in the hydrogen atoms could have a significant influence on plastic deformation. Glen (1968) has given consideration to the consequence of this disorder for the motion of dislocations. The passage of a dislocation through the ice lattice will shift the oxygen atoms a distance of one Burgers vector. Each hydrogen bond crossing the glide plane must be broken and reformed. the position of the hydrogen atom in the bond is random, additional orientation and ionization defects will be formed unless there is diffusion of these defects to and from the dislocation. Glen used a simple argument based on the energy of formation of orientation defects to show that if there was no diffusion of the defects it would require a shear stress of the order of 4300 bars to move a dislocation through the lattice. Since it is known that plastic flow can occur in ice for shear stress of the order of one bar, Glen concluded that the motion of dislocations through ice must involve the diffusion of L, D and ionization defects.

2.2.3 Substructure

Workman (1953) observed a substructure in ice. This structure, which consisted of bundles of coordinated hexagonal

prisms 1/2 to 20 microns in width, and 1 to 10 microns in length, was examined in greater detail by Truby (1955). Gentile and Drost-Hansen (1956) reported that the structure was not present immediately after ice was formed. They found that it developed in new ice if it was stored at -20°C for one to two weeks. These investigators suggested that the structure resulted from the condensation of vacancies into disc-shaped voids that subsequently collapsed to form dislocation rings.

Zajac (1962) concluded from a study of primary and secondary extinction of X-rays that ice has a substructure. His analysis showed that the subgrains making up the structure were of the order of 5 microns in size, and that the misorientation between adjacent blocks was of the order of 2 minutes of arc.

The existence of a substructure in ice is still a matter of debate. No evidence of it has been reported from the X-ray topographic studies. The question of its existence is of some importance with respect to deformation and failure because of the possible interaction between the structure and dislocations.

2.3 Polycrystalline Ice

The way in which polycrystalline ice responds to a load is dependent on the texture of the grains. This was recognized

by McConnel and Kidd in their studies published in 1888.

Measurements of the deformation behaviour of ice are meaningful only if adequate information is given on the shape and size of the grains, and the characteristics of their crystallographic orientation. Much of the published information on strength and deformation is of doubtful value because of the lack of this information.

The characteristics of the grain structure of ice are very dependent on the thermal and mechanical conditions associated with nucleation and growth. Michel (1969) and Michel and Ramseier (1969) have developed a classification for naturally occurring ice covers based on their genesis, structure and texture. This classification provides a suitable framework for reporting observations on strength and deformation behaviour.

If ice forms on a calm surface, the first crystals are tabular, extending out over the surface of the water. The grains that result are large with irregular boundaries. There is a marked preference for their symmetry or <0001> direction to be perpendicular to the surface. If the surface of the water is agitated when freezing begins, or if freezing is initiated by snow, the first layer of ice will have a granular texture with random crystallographic orientation. Michel and Ramseier refer to this first layer formed as primary ice.

Secondary ice develops from the primary as freezing progresses parallel to the direction of heat flow. The secondary ice often has a columnar texture, with the long direction of the columns parallel to the direction of growth, and crystallographic orientation controlled by that of the primary ice.

Hillig (1958) found that ice grows more readily perpendicular to the <0001> direction than parallel to it. This behaviour can lead to the development of a preferred crystallographic orientation in ice, as discussed by Perey and Pounder (1958) and observed by Gold (1960). Ketchem and Hobbs (1967) and Ramseier (1968) have studied in some detail the factors that control the growth of one grain relative to its immediate neighbors.

If the primary ice layer has a preferred orientation with the <0001> direction in the direction of growth, this will be retained in the secondary ice. There will be a tendency for the average grain diameter to increase with growth due to the squeezing out of unfavourably oriented grains. If the primary ice has a random orientation, there will be a marked tendency for the secondary ice to develop a preferred orientation with the <0001> direction perpendicular to the direction of growth. This preferred orientation can be well developed by the time the ice is 2 cm thick. The <0001> direction will have a random

orientation in the plane perpendicular to the growth direction.

Average grain diameter increases with growth to a greater extent than for ice with the <0001> direction in the direction of freezing.

Granular ice can form, for example, by the flooding of snow on top of an ice cover. This ice often has a whitish appearance, and the grain size is usually less than 5 mm. Michel and Ramseier call such ice "tertiary ice". The classification that has been developed by them is summarized in Table II.

Substructure can develop in ice during formation, particularly if supercooling or impurities are present.

Observations of this structure are described in papers by Harrison and Tiller (1963a) and Macklin and Ryan (1965). Sea ice provides an extreme natural example of the strong control impurities can have on the structure and substructure of polycrystalline ice (Weeks and Assur, 1968).

One of the characteristics of water is the small value of the partition coefficient $k = S_1/S_w$, where S_w and S_1 are the impurity contents of the water and resulting ice respectively. Because of this, ice is relatively much purer than the melt from which it is formed. The build-up of impurities in front of the ice-water interface can cause morphological instability which leads to their entrapment in the grain

TABLE II

Genetic Classification of Ice (Michel and Ramseier, 1959)

Primary Ice (ice formed initially)

- P1 C axis preferred vertical; crystal size large to extra large; crystal boundaries of irregular shape.
- P2 C axis orientation random to preferred vertical superimposed on random; crystalsize medium to extra large; crystal shape tabular or needle.
- P3 Ice cover initiated by frazil; C axis orientation random; crystal size small to medium; crystal shape equiaxed and tabular.
- P4 Ice cover initiated by snow; C axis orientation random; crystal size small to medium; crystal shape equiaxed.

Secondary Ice (develops from primary)

- Sl Columnar-grained; C axis vertical orientation; crystal size increases with depth, and is usually large to extra large; grain shape irregular.
- S2 Columnar-grained; C axes tend to become perpendicular to long direction of columns with growth; crystal size small to large, increasing more rapidly with depth than type S1.

Tertiary Ice

Snow ice; C axis orientation random; grains equiaxed; grain size small to medium.

Grain Size

small: Grain diameter less than 1 mm.

medium: Grain diameter between 1 and 5 mm.

large: Grain diameter between 5 and 20 mm.

very

large: Grain diameter greater than 20 mm.

boundary region, as exemplified by the freezing of sea water. This is discussed by Harrison and Tiller (1962, 1963a), Weeks and Assur (1968), and Rohatgi and Adams (1966). The value of the partition coefficient is found to be about 10⁻⁴ or less. (Harrison and Tiller, 1963b; Anantha and Chalmers, 1967; Weeks and Lofgren, 1967).

2.4 Deformation

2.4.1 Deformation of Single Crystals

As early as 1888 it was reported that single crystals of ice deformed "like a pack of cards" (McConnel and Kidd, 1888; McConnel, 1891). Greater insight into this behaviour was provided by the experiments of Glen and Perutz (1954), Steinemann (1954a, 1958) and Nakaya (1958). These studies demonstrated conclusively that deformation of single crystals of ice occurs most easily by glide on basal planes, and that it is much more difficult to induce glide on non-basal planes.

Observations on the creep behaviour of crystals oriented for basal glide in tension or compression, have exhibited, in general, a power law relationship between strain rate, stress and time, and an exponential relationship between strain rate and temperature. An equation of the following form is usually

assumed when analyzing results of experiments:

$$\dot{\gamma} = A\tau^n t^m \exp (-Q/kT) \tag{1}$$

where $\mathring{\gamma}$ is the shear strain rate; τ the shear stress; t the time; Q the apparent activation energy; T the temperature in degrees absolute; k Boltzman's constant and A, n, and m are constants.

Butkovich and Landauer (1959), Glen and Jones (1967), and Jones and Glen (1967) found m to be about 0.5 for strain less than 5%. There is some evidence that it may decrease with decreasing temperature. The value of n is found to be between 1.5 and 4 for shear stress greater than 0.5 bar (Steinemann, 1958; Butkovich and Landauer, 1959; Readey and Kingery, 1964; Higashi et al 1964, 1965; and Jones and Glen, 1967). Observations show that n tends to increase with stress and decrease with strain. Values obtained for the apparent activation energy, Q, are summarized in Table III.

The critical resolved shear stress for slip on the basal plane at temperatures warmer than -40°C is very low, probably less than 0.2 bars (Steinemann, 1954b, 1958, Wakahama, 1967). There is no evidence of work hardening during basal glide, and annealing has no or very little effect on subsequent deformation. Glen and Perutz found little X-ray asterism developed during deformation of up to 100%. These observations indicate that there is little interaction between dislocations, and that the Peierls force is not very large.

TABLE III

Apparent activation energy for deformation of single crystals of ice.

| Activation Energy | · · · · · · · · · · · · · · · · · · · | |
|----------------------|--|--------------------------|
| eV | Method | Source |
| | Basal Glide | |
| 0.62 ± 0.07 | $\dot{\gamma}$ = Const. | Readey and Kingery, 1964 |
| 0.69 | $\dot{\gamma}$ = Const. | Higashi et al, 1964 |
| 0.69 | 3 point bending of beams | Higashi et al, 1965 |
| 0.68 ± 0.04 | τ = Const. -10°C> T >-50°C | Jones and Glen, 1967 |
| 0.41 ± 0.04 | τ = Const. -50°C> T >-90°C | Jones and Glen, 1967 |
| 0.79 ± 0.04 | <pre></pre> | Jones and Glen, 1967 |
| 0.45 ± 0.03 | γ̈́ = Const. -55°C> T >-90°C | Jones and Glen, 1967 |
| 0.48 | $\dot{\gamma}$ = Const. Chemically polished | Muguruma, 1969 |
| 0.65 | γ̈́ = Const. Mechanically polished | Muguruma, 1969 |
| | Non-basal glide | |
| 0.72 | $\dot{\gamma}$ = Const. | Higashi et al, 1968 |

There appears to be little tendency for a preferred slip direction on the basal plane. Glen and Jones (1967) give evidence for a slight preference in the <1120> direction.

These results are in agreement with the conclusion drawn from the X-ray topographic and other observations that dislocations in the basal plane are probably not strongly tied to their Peierls valley. Kamb (1961), however, showed that if the value for the stress exponent, n, is less than 4, the absolute value of the difference between the direction of the shear stress and the direction of glide will be less than 3°.

Ice that has not been deformed previously has an upper yield stress when subjected to a constant rate of basal glide in tension or compression. This effect has been studied by Readey and Kingery (1964); Higashi et al (1964); and Jones and Glen (1967). Over the temperature range -1.5°C to -80°C, yield is observed to occur at a strain of about 1%. The strain to yield tends to increase with increasing strain rate and decreasing temperature. As with the creep experiments, there is no evidence of work hardening or recovery even after annealing at temperatures close to the melting point.

It is found that the stress at yield has the following dependence on strain rate and temperature.

$$\tau_{y} = C'\dot{\gamma}^{1/m} \exp\left(\frac{E}{kT}\right) \tag{2}$$

where m, C' and E are constants

Raising each side of equation (2) to the power m and rearranging gives:

$$\dot{\gamma} = C \tau_y^n \exp\left[-\frac{Q}{kT}\right] \tag{3}$$

where Q = mE, and m has been replaced by n so as to put equation (3) in the same form as equation (1).

The values found for n and Q are similar to those obtained from creep experiments. Values for the apparent activation energy are given in Table III.

The behaviour of ice single crystals during a constant rate of strain test is consistent with Johnston's (1962) theory for yield. Johnston assumed, on the basis of observations made on the movement of dislocations due to a shear stress, that the number of dislocations increased linearly with strain and their velocity was proportional to τ^n . Direct observations of the movement of dislocations in ice have not been made so it is not known if their behaviour agrees with the assumptions underlying Johnston's theory. When observations are fitted to the theory, reasonable values are obtained for the initial dislocation density (about $10^5/\text{cm}^2$) and the dislocation velocity (about 50Å/sec at -50°C).

There is evidence that the maximum stress associated with yield is sensitive to the initial dislocation density and the condition of the surface of the specimen. Muguruma (1969)

found that the yield stress was larger for specimens prepared by chemically polishing with alcohol, than for specimens prepared by mechanically polishing. Higashi et al (1965) observed the same behaviour for the bending of ice beams. This effect was attributed to dislocations induced in the surface by the mechanical polish. Muguruma found also that crystals containing low angle boundaries had a lower yield stress, and suggested this was because the boundaries were good sources and sinks for dislocations. The initial slope of the stress - strain curve did not appear to be sensitive to the initial dislocation density, but rather depended on the elastic properties of the specimen in combination with the testing machine.

Some observations have been made on the spacing of the slip lines associated with basal slip. Wakahama (1967) found for the mean spacing between slip lines

$$(\tau - 0.2) d = 0.45 \times 10^{-3}$$
 (4)

where τ is the shear stress in kg/cm², and d is the spacing in cm.

Readings and Bartlett (1969) observed both fine and coarse slip lines. The fine lines were associated with shear stress less than about 0.2 bar. Their observations on the spacing of the coarse lines were in general agreement with those of Wakahama; i.e. $^1/d$ was found to be proportional to $(\tau - 0.2)$ kg/cm².

Observations on the behaviour of ice during non-basal glide at constant rate of strain have been reported by Higashi (1967) and Higashi et al (1968). An initial linear increase in stress with strain is observed. This is followed by yield at about one percent strain, and subsequent work hardening extending over several percent. The rate of work hardening depends on the angle between the stress and the {1010} plane. Maximum rate of work hardening occurred when this angle was 60°. In this case there are two {1010} planes at 60° to the stress, indicating that the maximum rate of work hardening may be due to interaction between the dislocations gliding on the two planes. The rate of work hardening was relatively insensitive to strain rate and temperature.

It was found that the strain rate and temperature dependence of the maximum stress at yield had the same form as for basal glide under constant strain rate conditions (see equation 3). The value for the exponent of the stress, n, was found to be 6.5, considerably larger than for basal glide. The apparent activation energy had about the same value as for basal glide, and is given in Table III.

It was observed that for the same strain rate and temperature, the resolved shear stress required to cause yield on non-basal planes was almost twenty times that for yield on the basal plane. The shear stress at yield on the $\{10\overline{1}0\}$ planes

was found to be independent of θ , the angle between the stress and the plane. It tended to increase with increasing strain rate and decreasing temperature.

Voids formed in the work hardening phase of non-basal deformation (Muguruma et al, 1966; Mae, 1968). The voids had a hexagonal shape, were in planes parallel to the basal plane and aligned in the <1120> direction. They tended to aggregate into rows of cavities after the stress had attained its maximum value. The strain to the first appearance of voids increased with strain rate. It was also observed that the lower the temperature or larger the strain rate, the greater was the strain to failure. These observations suggest that non-basal glide is associated with the formation of vacancies and that the voids grow by vacancy diffusion.

The electrical properties of ice have been found to be greatly affected by doping the ice with hydrogen fluoride or ammonia. It is considered that the effect is due to the change in the concentration of orientation and ionization defects by the impurity ions. Since the HF molecule has only one hydrogen atom, its inclusion in the ice lattice will create a corresponding number of L defects. It will also bring about the reaction

$$H_{2}O + HF \neq H_{3}O^{+} + F^{-}$$

and the concentration of D defects and OH ions will be depressed. Similarly, since NH has an extra hydrogen atom, its inclusion into the lattice will increase the D and OH defects, and suppress the L and H O defects. If the movement of dislocations through ice is controlled by these defects, changing their concentration should affect the deformation behaviour.

Jones (1967) and Jones and Glen (1969) have studied the deformation behaviour of HF and NH doped ice. HF has a definite softening effect and the addition of NH a slight hardening effect. It was concluded from the study that the velocity of the dislocations is controlled primarily by the concentration of L defects; additional D defects do not appear to result in softening, and may even cause some hardening.

The equality of the activation energies for time dependent deformation and diffusion for ice single crystals indicates that the deformation is controlled by the diffusion process. This is considered to be the general situation for the deformation of materials at high homologous temperatures (Weertman, 1968). The studies of Jones and Glen, however, indicate that orientation defects also play a significant role. It is not possible to say on the basis of activation energies which mechanism may be controlling the movement of the dislocations as the energies of formation and migration of vacancies and L and D defects are about the same.

Measurements of activation energy indicate that there is a change in the mechanisms controlling dislocation movement at about -50°C. This behaviour is still to be clarified.

Jones and Glen (1967) found that failure occurred at -90°C with no significant deformation, even for a resolved shear stress of 13.8 bar applied for 200 hours. It is of interest that for this stress, time and an activation energy of 0.41 eV, a strain of 2 to 3% should have occurred.

2.4.2 Granular Ice

The behaviour in creep of granular or type T1 (see Table II) ice, grain size about one to two mm., has been studied by Glen (1953, 1955), Steinemann (1954b, 1958), Jellinek and Brill (1956), Butkovich and Landauer (1960), Halbrook (1962) and Dillon and Andersland (1967). The time dependence of the creep strain shows the three stages normally associated with the creep of granular materials: a primary or transient stage; a secondary stage in which the rate of creep tends to a constant value; and a tertiary stage in which the creep rate accelerates. The principal interest in the creep behaviour of ice has been with respect to the flow of glaciers, and attention has concentrated on the secondary stage.

The critical resolved shear stress for granular ice is less than 0.2 bars. During primary and the initial part of the secondary creep, the strain is observed to be approximately proportional to the square root of the time. For stress less

than about one bar, the flow appears to be Newtonian, with the strain rate proportional to the stress. This indicates that in this stress range Nabarro-Herring creep probably controls the deformation behaviour.

It is observed for stress greater than about one bar, that the steady state creep rate of granular ice has a power-law dependence on the stress, similar to that for single crystals deforming by glide on the basal plane. The value of the exponent of the stress, n, appears to increase with stress. Steinemann (1954b) obtained a value of about 2 for a stress of 2 bars, increasing to a little over 4 when the stress was 12 bars. Observations of the steady state creep rate at $T \simeq -5$ °C are plotted against stress in figure 2.

Jellinek and Brill (1956) found that their observations of the creep of granular ice had the following dependence on stress and time:

$$\varepsilon = A\sigma \quad t \tag{5}$$

where ϵ is the creep strain at time t, σ is the applied stress and A a constant.

It is usual in the analysis of creep results to relate the creep rate at a given amount of strain into the secondary stage, to the stress. If equation (5) is differentiated to obtain the strain rate, and also used to substitute for t in

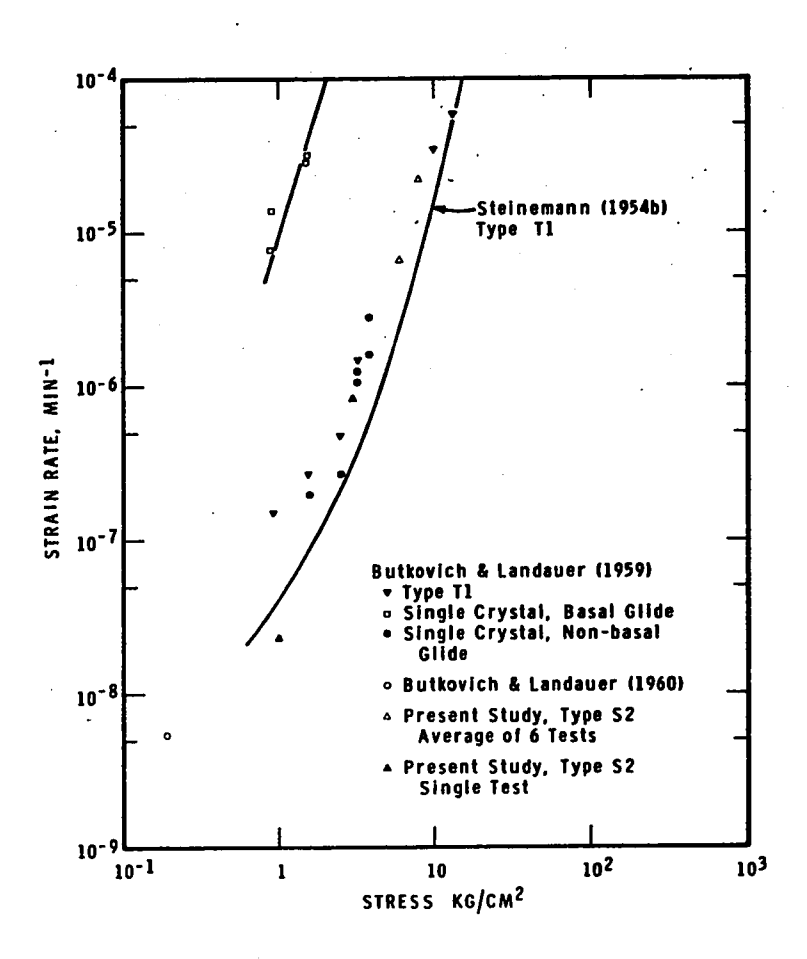


FIGURE 2 STRESS DEPENDENCE OF MINIMUM CREEP RATE; TEMPERATURE - -5°C

the resulting equation, the value obtained for the exponent, n, of the stress (for the condition ϵ = constant) is in agreement with that found by Glen (1955) and Steinemann (1954b).

Steinemann (1954b) and Jonas and Müller (1969) found that ice can recrystallize during strain. Steinemann's observations on thin sections showed that this occurred for strains of between 1 and 2%, depending on the stress, and was associated with the onset of tertiary creep. Steinemann (1954b) and Glen (1955) both observed that the average grain size obtained from thin sections prepared after deformation well into the secondary stage, decreased with increasing stress.

Some information has been obtained by Halbrook (1962) and Dillon and Andersland (1967) on the behaviour of granular ice during deformation conditions approaching constant rate of strain. Strain rates in the range 6.5 x 10⁻³ to 3.33% per min. were used. Yield was found to occur at a strain of about 1 to 2%. The maximum stress at yield increased with increasing rate of strain. It was found that yield in the constant strain rate tests occurred at about the same strain as recrystallization and the beginning of the tertiary creep stage for the same type of ice.

The deformation behaviour of granular ice appears to have an Arrhenius type dependence on temperature. Apparent activation

energies that have been determined show a wide scatter in value. This probably is indicative of the current lack of understanding and control of the factors that affect the temperature dependence of the deformation behaviour of polycrystalline ice. Values for the apparent activation energy of granular ice are given in Table IV.

2.4.3 Columnar-grained Ice

Bromer and Kingery (1968) studied the creep behaviour of columnar-grained type S1 ice (see Table II), subjected to stress of less than about 2 bars applied perpendicularly to the long axis of the columns. The strain rate was found to be proportional to the stress and inversely proportional to the square of the grain size, as predicted by Nabarro-Herring creep. Butkovich and Landauer (1960) observed that the strain rate of columnar-grained type S2 ice, with load applied in the long direction of the columns, was also proportional to the stress for stress less than about 0.20 bars.

Krausz (1963) and Gold (1965) have studied the deformation behaviour of type S2 ice for stresses greater than about 4 bars applied perpendicularly to the long direction of the columns. It was observed that during primary creep the creep rate of previously undeformed type S2 ice goes through a maximum at a strain of about 0.25%. This was considered due to the development of new modes of deformation. If the ice was deformed

TABLE IV

Apparent activation energies for polycrystalline ice.

| Activation Energy eV | Type of Ice and Method | Source |
|----------------------------|----------------------------------|---------------------------------|
| | | |
| 0.62 | T1; $\tau = Const.$ small stress | Butkovich and Landauer, 1960 |
| 0.50 | T1; τ = Const. small stress | Dillon and Andersland, 1967 |
| 1.40 | T1; τ = Const. large stress | Glen, 1955 |
| 0.70 | T1; τ = Const. | Jellinek and Brill, 1956 |
| 0.61 | Tl; Creep thick walled cylinder | Jellinek, 1962 |
| 0.52 | S1; τ = Const. small stress | Bromer and Kingery, 1968 |
| 0.70 | S2; $\dot{\gamma}$ = Const. | Muguruma, 1969 |
| 0.91 | S2; τ = Const. -5> T >-15°C | Gold, present investigation |

more than 1%, annealed, and then subjected to the same load applied initially, the effect was no longer present.

If the observations for stress greater than 4 bars are analyzed assuming a power law stress dependence for the secondary stage creep rate, the values for the exponent of the stress, n, are about the same as for granular ice.

Information on the stress dependence of the strain rate during creep of columnar-grained ice for temperatures of -5°C and -10°C, is shown in figures 2 and 3. Additional information on the creep of type S2 ice was obtained from the present study, and is presented in Section 6.

There is little information on the behaviour of columnargrained ice under conditions of constant rate of strain.

Preliminary observations by Gold (1968) indicated yield in the
range of strain corresponding to the maximum in the strain
rate during the primary stage of creep. There was also evidence of a second yield at a strain corresponding to the
initiation of the tertiary stage in creep.

Muguruma (1969) has studied the deformation behaviour of type S2 ice with specimens 5 mm thick and 25 mm wide. The ice was subjected to a compressive stress perpendicular to the long direction of the columns under conditions of constant rate of cross-head movement. He found that the maximum stress at yield had a dependence on strain rate and also temperature

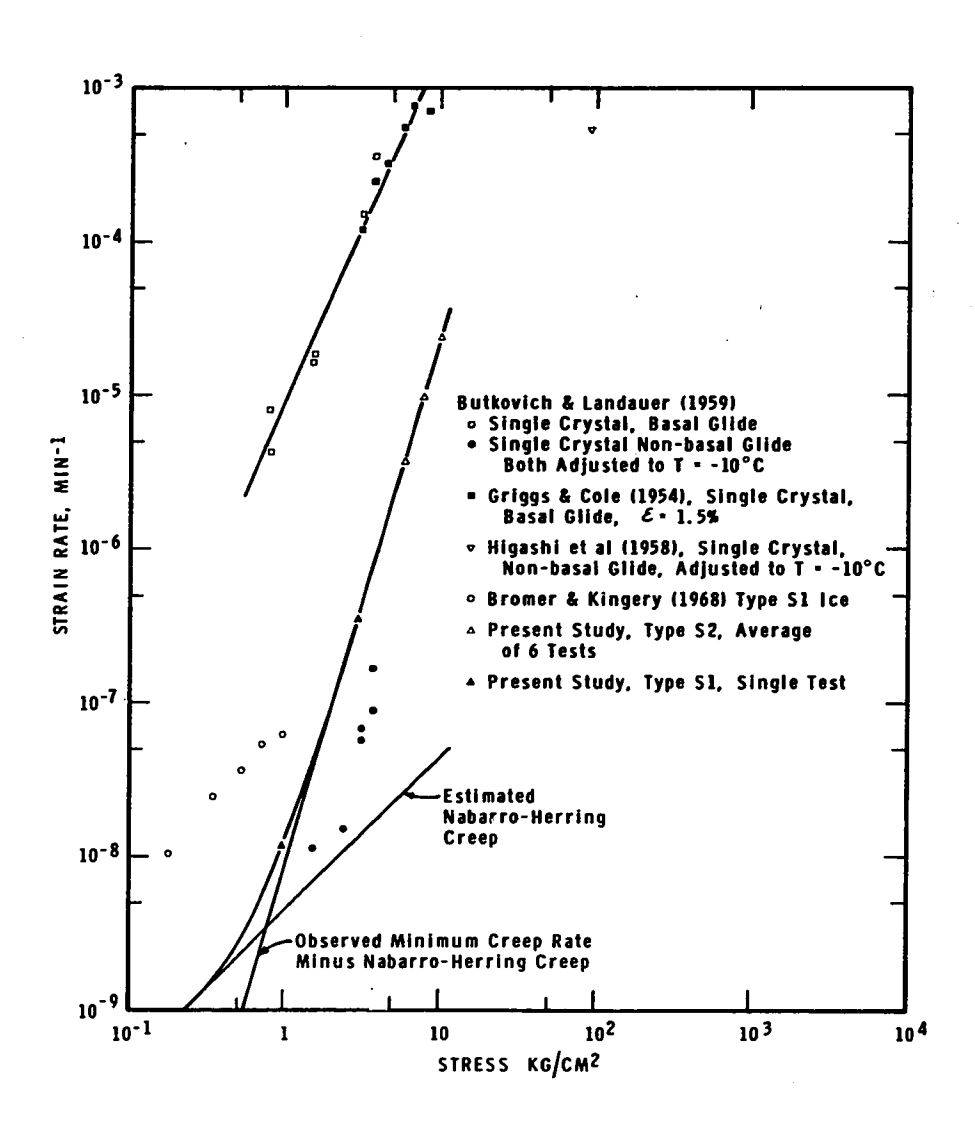


FIGURE 3
STRESS DEPENDENCE OF MINIMUM CREEP RATE; TEMPERATURE - -10°C

as given by equations (2) and (3). The value obtained for the stress exponent, n, was in agreement with that obtained for granular ice. The apparent activation energy was also similar, and is given in Table IV. Muguruma found that the yield behaviour of the columnar-grained ice was the same for mechanically and chemically polished surfaces. He concluded from this that the dislocations associated with the deformation are not generated at the surface, but rather internally and probably at the grain boundaries.

Krausz (1968a) has developed the following expression for the dislocation velocity from rate theory assuming that the activation energy depends linearly on the stress, and that the energy barrier and activation volume in the forward direction are different from those in the backward direction:

$$v = A_f \exp \left(\frac{v_f^{\tau} eff}{kT}\right) - A_b \exp \left(-\frac{v_b^{\tau} eff}{kT}\right)$$
 (6)

where v is the dislocation velocity, A_f and A_b are constants for given T, V_f and V_b are the forward and backward activation volumes, and τ_{eff} is the effective shear stress acting on the dislocation.

This equation was found to describe well the stress dependence of the dislocation velocity reported for several crystals.

Krausz (1968b, 1969) used this theory to analyze strain

relaxation measurements made with columnar-grained type S2 ice.

He obtained

0.4 x
$$10^{-20}$$
 cm³ < V_f < 9 x 10^{-20} cm³
0.5 x 10^{-20} cm³ < V_b < 22 x 10^{-20} cm³,

and concluded that strain relaxation in ice can be described fully by the asymmetrical form of the rate theory. The symmetrical form of the rate theory has been used in all applications to date for ice, and the implications of the findings of Krausz have still to be explored.

2.4.4 Degrees of Freedom

The deformation of a polycrystalline material is completely determined by measuring the three principal strains and the three shear strains. If the deformation is one of constant volume, then only five of these strains are independent. Von Mises (1928) and Taylor (1938) used this geometric fact as the basis for the argument that if a polycrystalline aggregate is to undergo an arbitrary, constant volume change in shape, each grain must have at least five independent slip systems. The consequence of this requirement has been discussed by several authors (Gold, 1963a; Groves and Kelly, 1963; Kocks, 1964; Tegart, 1964a). If the grains do not have sufficient degrees of freedom for deformation, stresses will build up, particularly in the grain boundary

regions, until a sufficient number have been initiated, or the deformation is no longer one of constant volume (i.e. voids or cracks form).

The constraints imposed on grains by neighboring grains are one of the main sources of increased strength of an aggregate over its constituent crystals. It is often assumed that the tensile stress, σ , necessary to produce a given strain or strain rate in the polycrystal, is related to the corresponding critical resolved shear stress, $\tau_{\rm c}$, for the single crystal by

$$\sigma = m\tau_{c} \tag{7}$$

The value of m is dependent on the crystallographic symmetry of the constituent crystals and the ways in which they can deform. Calculations of it for face-centred cubic crystals have been made by Bishop and Hill (1951) and Taylor (1958). In general, the smaller the number of degrees of freedom for deformation, the larger is m.

Attention has been given to the conditions that must be satisfied at the grain boundaries for deformation there to be compatible with the imposed deformation (Gilman, 1953; Livingston and Chalmers, 1957; Hauser and Chalmers, 1961). When deformation is initiated, dislocations move into the grain boundary regions. The boundaries present a barrier to

the movement of the dislocations; the strength of this barrier depends upon the ease with which slip is initiated in neighboring grains. Because of the barrier, dislocations pile up. The stress associated with the pile-ups depends in part upon the degree of incompatibility of the grains in their boundary regions.

When consideration is given to the resistance of a polycrystal to deformation, two size effects are apparent - a grain size effect and a specimen size effect (Armstrong, 1961). It is found that yield and some types of fracture are related to grain size by an equation of the following form (Petch, 1953; Dieter, 1961, p.121)

$$\tau = \tau o + kd^{-\frac{1}{2}}$$
 (8)

where T is the shear stress associated with yield or fracture, To is the friction stress opposing the motion of dislocations (for no grain boundary restraints), k is a parameter determined by the resistance to shear caused by the grain boundary regions, and d is the grain size.

Armstrong et al (1962), Smith and Worthington (1964) and McEvily and Johnston (1967) discussed the role that crystal-lographic orientation and availability of slip systems play in the grain size effect and in determining the value of k in equation (8). Similar discussion was presented by Smith and

Worthington (1965) for brittle to ductile transition criteria.

The stress on an adjacent grain due to a dislocation pile-up at the boundary is given by (Johnston et al, 1965; Tegart, 1966, p. 176):

$$\tau_{\mathbf{r}} = (\tau - \tau_0) \left(\frac{\mathbf{d}}{\mathbf{r}}\right)^{\frac{1}{2}} \tag{9}$$

where τ_r is the shear stress at distance r from the head of the pile-up.

If yield is to propagate from one grain to an adjacent grain, τ_r must be large enough to cause slip to occur. Equation (9) shows that the stress is greatest close to the boundary, and it is in this region that multiple slip is observed to begin. The term kd $-\frac{1}{2}$ in equation (8) is a measure of the extra stress required to generate slip, or initiate equivalent modes of deformation in the neighboring grains at each end of slip bands. In general, the higher the stress concentration developed at the grain boundary, the greater will be the volume of crystal involved in the development of additional slip systems.

When there are few grains in the cross-section of a specimen (e.g. less than about 20), the full confining effect of grains upon their neighbors is not mobilized. As the number of grains in the cross-section increases, the value of m in equation (7) increases to i's stable value. For specimens with relatively few grains, the specimen size effect,

which tends to be independent of grain size, dominates. When there are more than about 20 grains in the cross-section, the true grain size effect is observed.

2.4.5 Modes of Deformation

With this appreciation of the importance of degrees of freedom for deformation for the plastic and viscous behaviour of materials, it is of interest to consider the modes of deformation that occur in polycrystalline ice. Observations on slip line formation, movement of etch pits, dislocation networks and yield, show that the resistance to deformation on non-basal planes is at least an order of magnitude greater than on basal planes. Although the critical resolved shear stress for glide in the basal plane is about 0.2 bars, indirect experimental evidence indicates that for type S1 ice the main mode of deformation for stress less than one bar is Nabarro-Herring creep (Bromer and Kingery, 1968). No surface evidence of glide was observed in a specimen of type S2 ice subjected to a compressive stress of 1 kg/cm². The specimen was deformed for over 400 days and the total creep was about 0.63%. Evidence of basal glide was clearly visible at this creep strain for stress of 3 kg/cm^2 .

Deformation bands of the type described by Gervais et al (1953), were observed in thin sections prepared within one-half hour after the removal of a stress of 3 kg/cm 2 from type S2 ice

deformed about 1% in creep at -10°C. Gold (1965) showed, using a thermal etching technique, that low angle boundaries associated with the deformation bands did not form until the strain had exceeded about 0.1%. The boundaries were often continuous from one grain to the next, changing direction abruptly at the grain boundaries. Examples are shown in figures 4a and b. Formation of deformation bands and associated low angle boundaries provide a rotational degree of freedom for deformation about a line in the basal plane.

Nakaya (1958), Higashi and Sakai (1961) and Higashi et al (1965) have studied low angle boundary formation during the bending of beams made from single crystals. Observations on the stress induced movement of low angle boundaries by Higashi and Sakai indicated that they are made up of edge dislocations. Their occurrence also indicated that dislocation climb must take place, and this in turn implies the very probable presence of a significant vacancy concentration (Weertman, 1968). Groves and Kelly (1969) suggested that dislocation climb may allow for some crystals a change of shape that cannot be produced by active slip systems.

It was observed by the author that voids did not grow in the specimen of type S2 ice deformed 0.63% under a creep stress of 1 kg/cm^2 . They did appear during the initial part of the deformation of a type S2 specimen subjected to a compressive

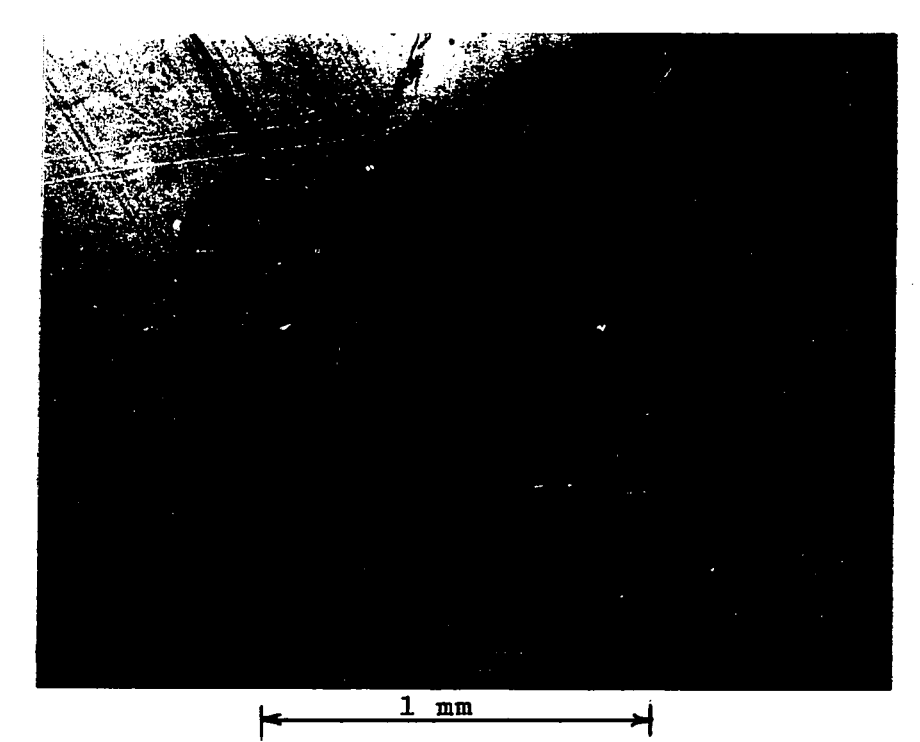


Figure 4a) Low angle boundaries initially perpendicular to the glide bands; type S2 ice deformed about 5% under a stress of 12 kg/cm².

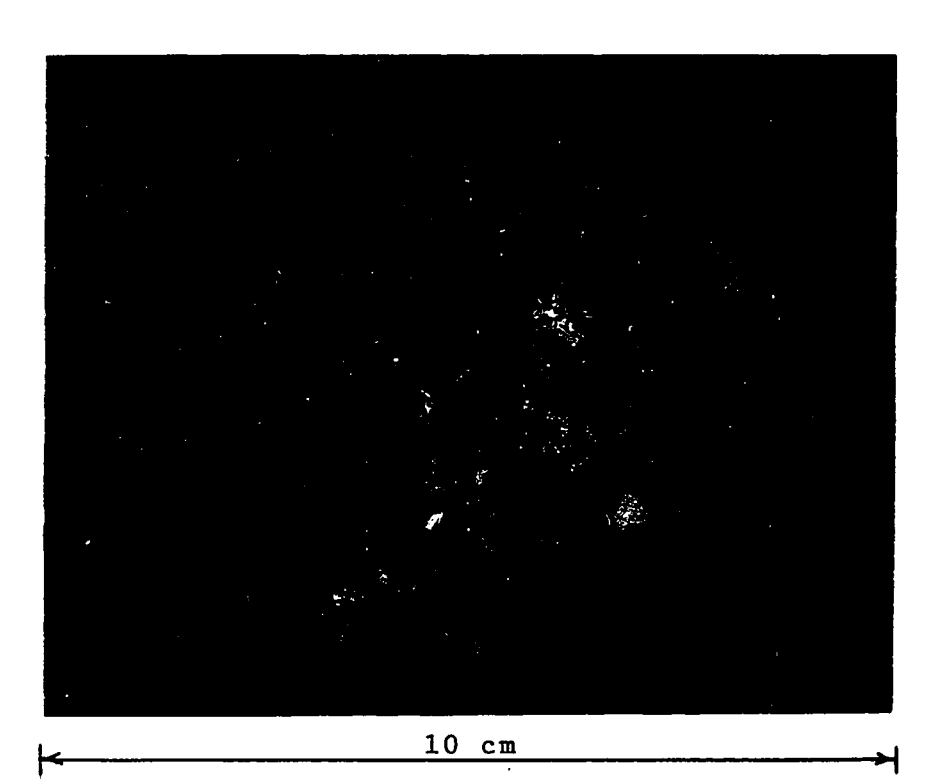


Figure 4b) Deformation bands observed in a thin section with polarized light; type S2 ice deformed about 6% under a stress of 9 kg/cm².

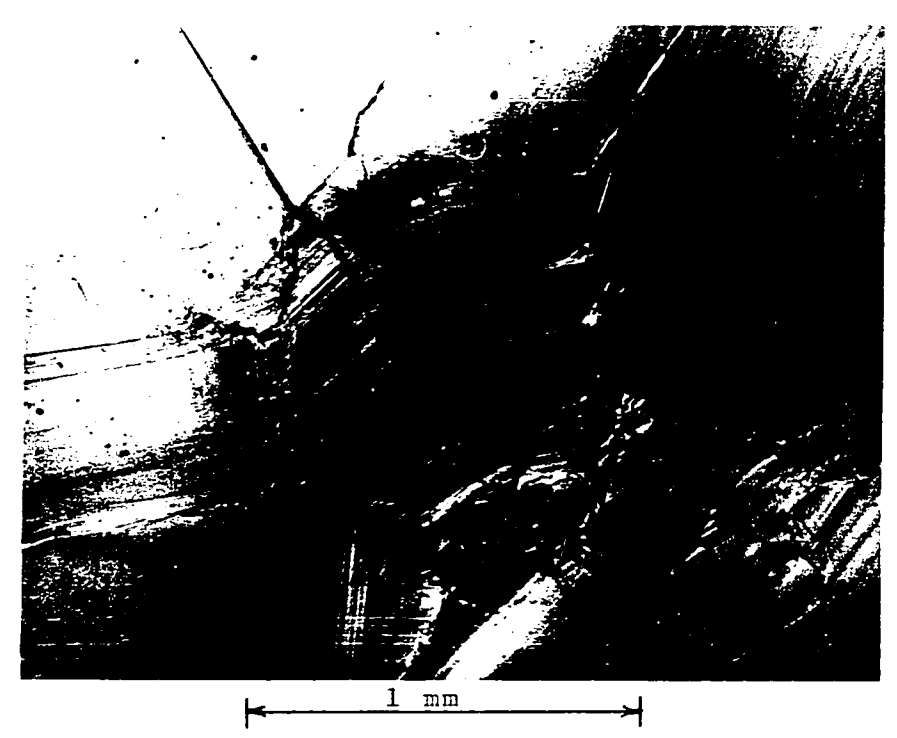


Figure 4a) Low angle boundaries initially perpendicular to the glide bands; type S2 ice deformed about 5% under a stress of $12~\rm kg/cm^2$.

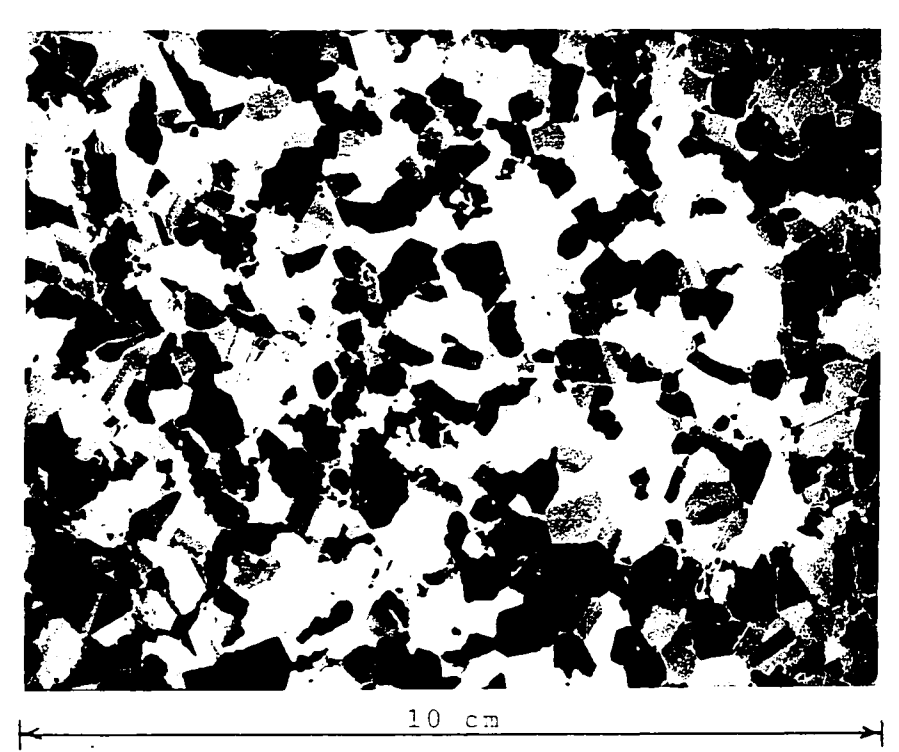


Figure 4b) Deformation bands observed in a thin section with polarized light; type S2 ice deformed about 6% under a stress of 9 kg/cm².

stress of 3 kg/cm², but subsequently disappeared. These observations indicated that for small stresses (small rates of strain), the deformation modes that occur in ice are adequate to allow the change in shape to be essentially one of constant volume.

Void formation was observed during the compressive creep of type S2 ice subjected to stress between 4 and 8 kg/cm². The voids formed in the grain boundary region in planes that tended to be parallel to the applied stress. Examples are shown in figures 5a and b. Their occurrence indicates active formation of vacancies, and tensile stresses perpendicular to the plane in which they formed.

Gold (1963a, 1965, 1966) observed that severe distortion occurred in the grain boundary regions of type S2 ice for stress greater than 3 kg/cm². (See figures 4a,5b and 6a). This distortion was associated with polygonization, apparent non-basal glide, and crack formation or "fragmentization". Grain boundary migration also occurred. Markings were observed on the surface of some grains that were interpreted as evidence of cross-slip. Examples are shown in figures 4b and 6b. These structural changes appeared to be initiated at a strain of about 0.01%, and to develop most actively in the range of 0.01 to 0.25%.

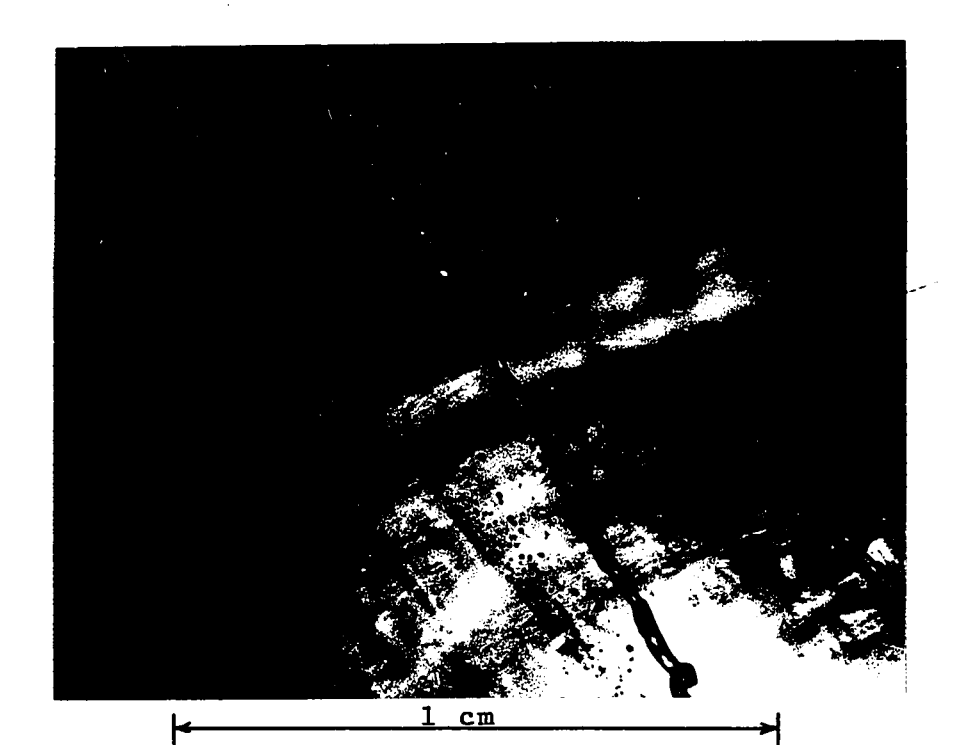


Figure 5a) Example of cavity formation in type S2 ice. The long columnar void is associated with a triple point. The ice deformed 5.6% under a compressive stress of 8 kg/cm².



Figure 5b) Example of highly deformed region where cavities have formed. Note cavities below surface, and trace of slip lines and low angle boundaries. The ice deformed 5.6% under a compressive stress of 8 kg/cm².

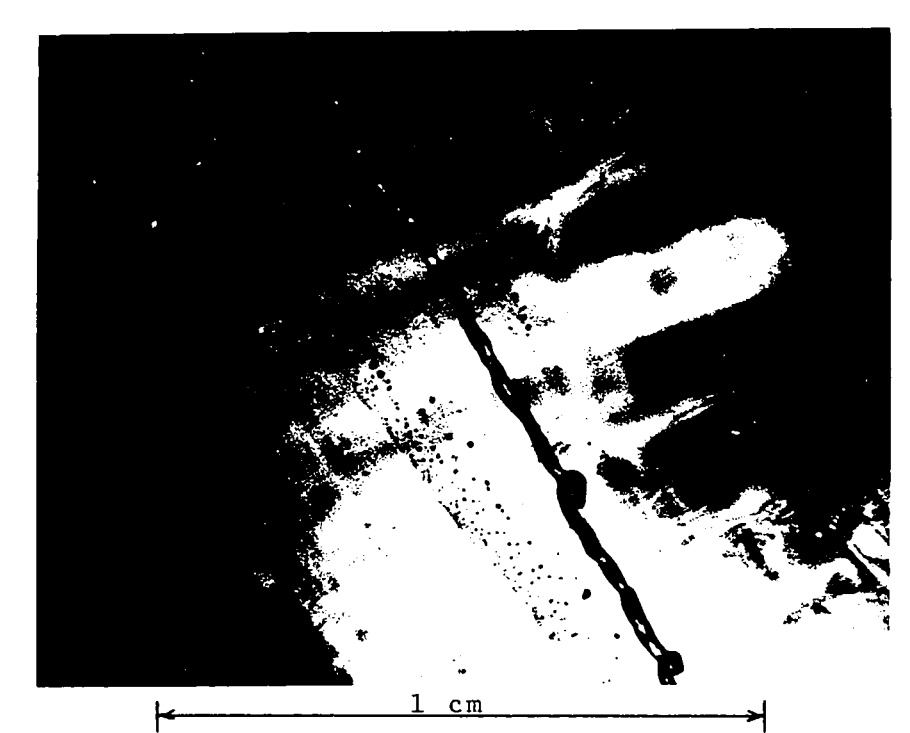


Figure 5a) Example of cavity formation in type S2 ice.
The long columnar void is associated with a triple point. The ice deformed 5.6% under a compressive stress of 8 kg/cm².



Figure 5b) Example of highly deformed region where cavities have formed. Note cavities below surface, and trace of slip lines and low angle boundaries.

The ice deformed 5.6% under a compressive stress of 8 kg/cm².

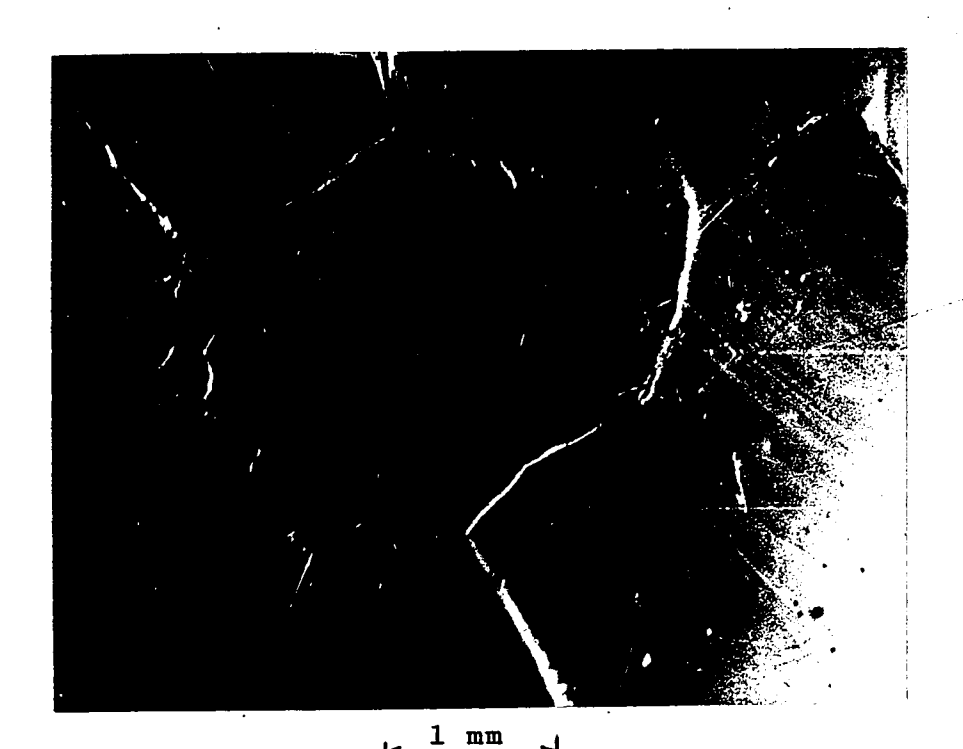


Figure 6a) Example of grain boundary migration. Note how the boundary has been distorted in upper right corner. The ice was deformed 3.0% under a compressive stress of 9 kg/cm².

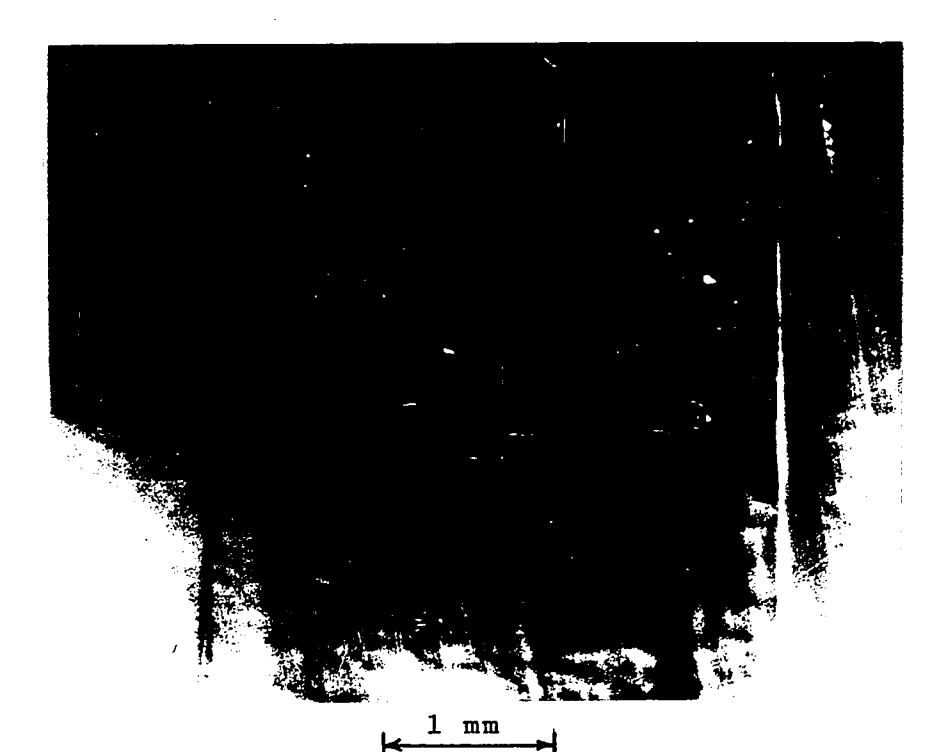


Figure 6b) Example of non-basal glide.

(.



Figure 6a) Example of grain boundary migration. Note how the boundary has been distorted in upper right corner. The ice was deformed 3.0% under a compressive stress of 9 kg/cm²,

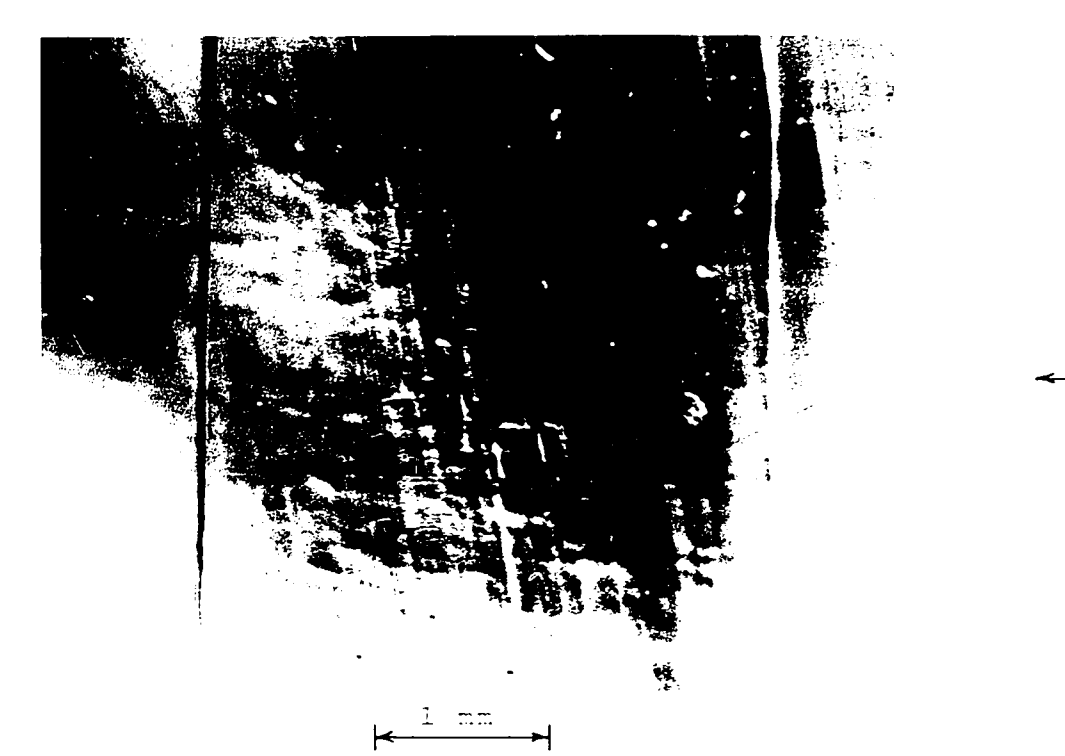


Figure 6b) Example of non-basal glide.

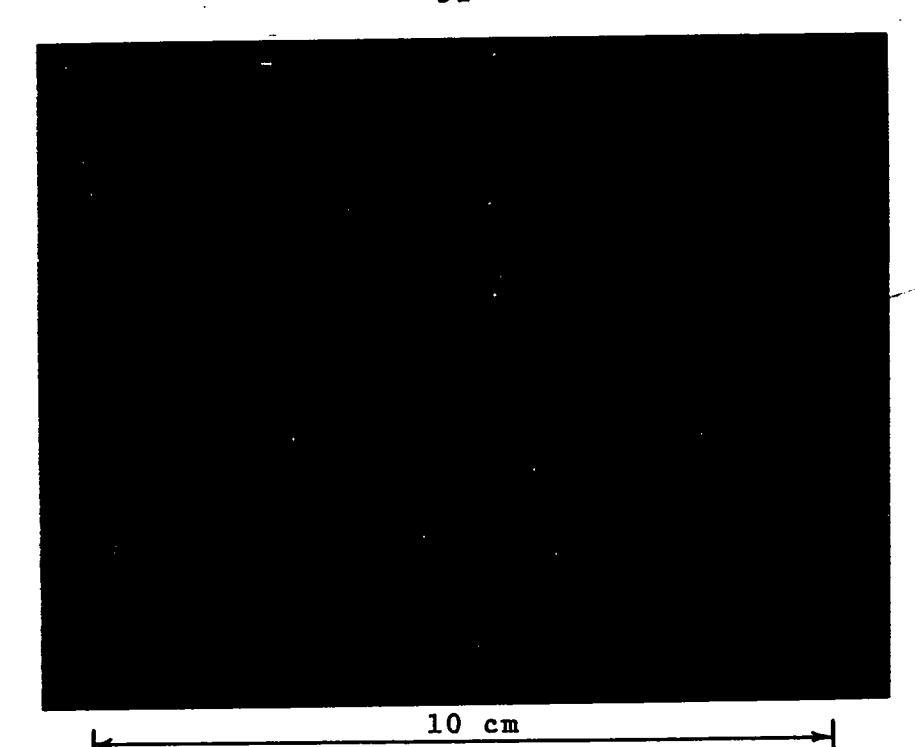


Figure 6c) Break-up of columnar-grained structure by deformation. The upper part is a thin section of undeformed ice. The lower part was deformed 5% under a stress of 8 kg/cm².

Surface deformation features showed that away from grain boundaries, the grains in S2 ice changed shape mainly by glide on basal planes and rotation about low angle boundaries. Accommodation between grains took place primarily in the severely distorted grain boundary region, as can be seen in figure 4b. The distorted region enlarged as the ice deformed, until it finally consumed the whole grain. Thin sections of deformed specimens viewed with polarized light indicated that the columnar structure was gradually transformed in this way to a granular one (figure 6c). The break-up of the columns was associated with the secondary creep stage.

Tegart (1964b) suggested that the creep rate of polycrystalline ice is controlled by non-basal glide. suggestion is supported by the information presented in figures 2 and 3. It can be seen in figure 2 for $T = -5^{\circ}C$, that the stress dependence of the strain rate of type S2 ice is almost the same as single crystal ice oriented for non-basal Steinemann's observations indicated that granular, type glide. $^{
m T1}$ ice has actually a higher resistance to deformation. single crystal measurements shown in figure 3 were adjusted to T = -10°C by assuming an apparent activation energy of 0.68 eV. In this case, single crystals oriented for non-basal glide exhibit a slightly higher resistance to deformation than type S2 ice. On the other hand, single crystals oriented for easy glide have a creep rate in the same range of strain, about two orders of magnitude larger for a given stress.

In figure 3 the assumed Nabarro-Herring creep at small stress is extrapolated to large stress. The straight line, A - B, is closely equal to the observed steady state creep rate minus the extrapolated Nabarro-Herring component. This suggests that some of the variation in the stress exponent, n, observed by Steinemann and Glen, may be due to the contribution of the Nabarro-Herring creep.

It can be seen from figures 2 and 3 that the stress required to produce a given strain rate in type S2 ice is about ten times that required for ice oriented for easy glide. This indicates that during deformation, the resistance to flow by glide on basal planes must be considerably less than that due to incompatible grain boundaries and grains with their basal plane tending to be parallel or perpendicular to the applied stress. Significant stress concentrations must be set up in grain boundary regions at the ends of slip bands in grains with their basal planes between about 20° to 70° to the applied stress. Since the creep rate of type S2 ice for a given stress is about equal to that for ice oriented for non-basal slip, the back-stress associated with the dislocation pile-ups in grains in which easy glide is significant, must be equal to about 90% of the resolved shear stress. This suggests that for a very significant proportion of the grains the resistance to deformation is mobilized mainly in the grain

boundary region. The severe lattice distortion that is observed in that region is evidence for this.

One of the interesting modes of deformation observed for ice is crack formation. Gold (1963a, 1967) found that crack formation occurred in type S2 ice during compressive creep when the applied stress exceeded about 6 kg/cm². When the stress was applied perpendicularly to the long direction of the columns, the plane of the cracks tended to be parallel to the applied stress. The cracks were long and narrow, with their long direction in the long direction of the grains. They usually involved only one or two grains. Their formation was a brittle event; once formed they did not appear to grow significantly with continued deformation. Low angle boundaries perpendicular to the plane of the crack, were observed at the edge and central regions. The cracks opened by rotation at low angle boundaries, as shown in figure 7a.

About two-thirds of the cracks that formed during creep at -10°C were transcrystalline. These cracks tended to propagate parallel or perpendicularly to the basal plane of the grains in which they formed. Examples are shown in figures 7a, b and c. As the plane of the cracks also tended to be parallel to the applied stress, this indicated that the cracks formed in grains so oriented that they could not deform readily - i.e., at "hard sites" within the structure. This behaviour was also observed for grain boundary cracks (see figure 7d).



Figure 7a) Crack parallel to the basal planes. Note the role played by low angle boundaries in opening of the crack.



Figure 7b) Crack parallel to the basal planes in one grain and perpendicular to them in the adjacent grain. Note that one edge of the crack is associated with a grain boundary, indicating that initiation may have occurred in this region.

 σ

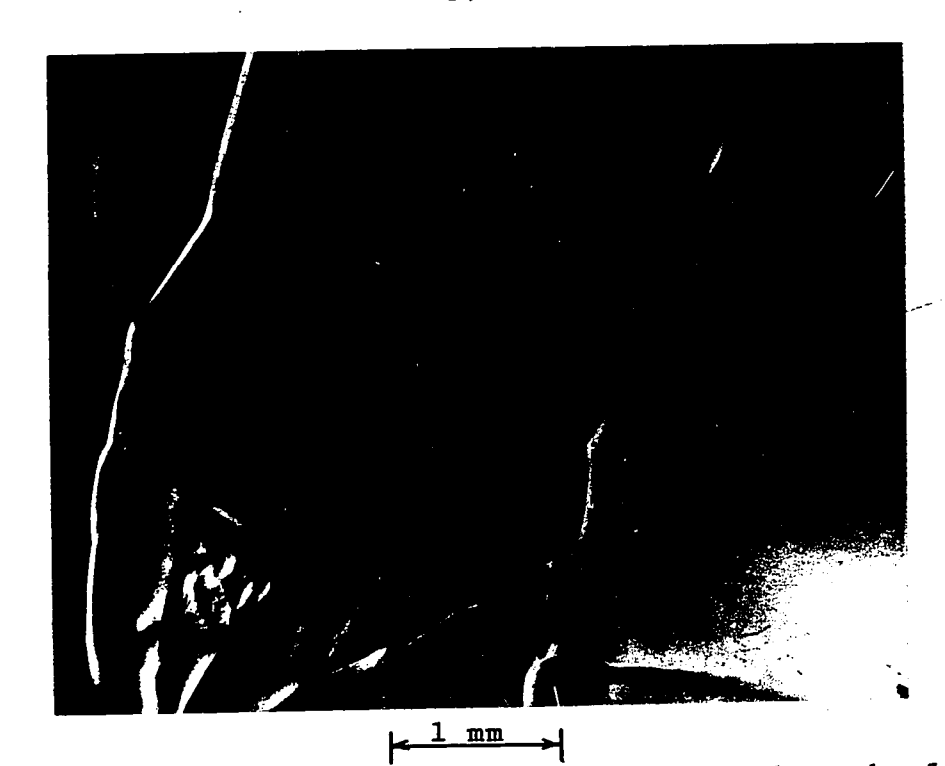


Figure 7c) Crack parallel to basal planes as shown by low angle boundaries. Note that one edge of the crack is associated with a grain boundary.

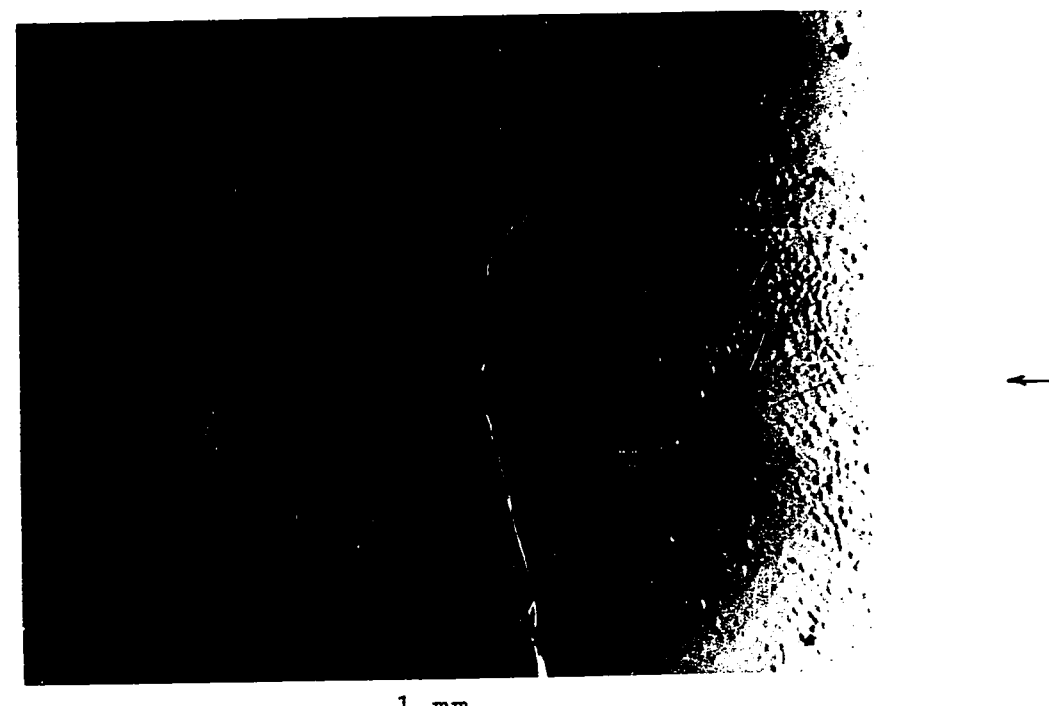
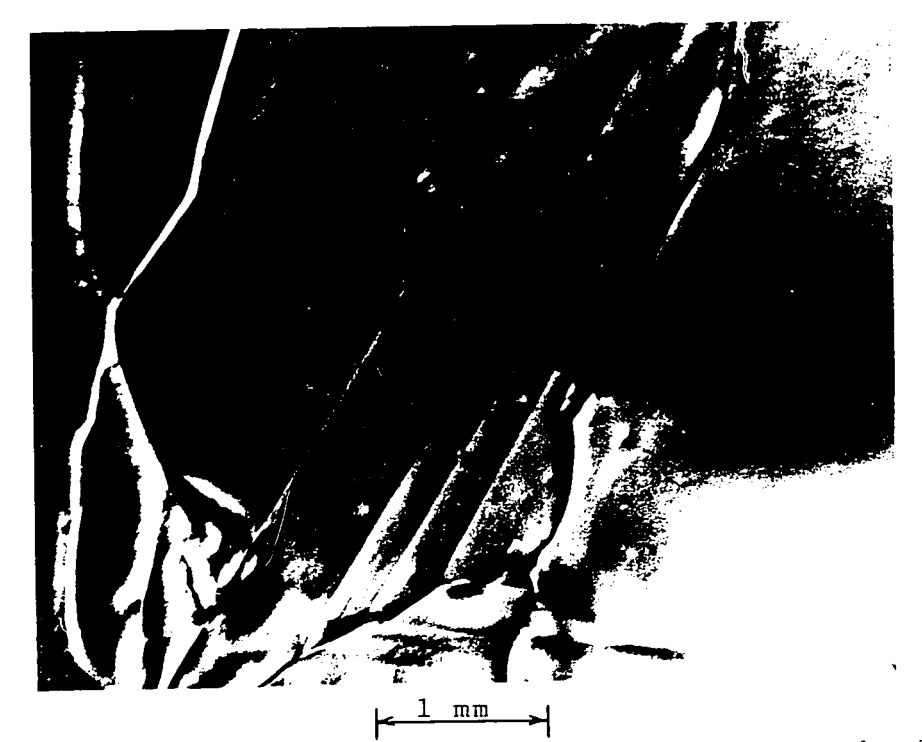


Figure 7d) Grain boundary crack. Note that the basal plane of one grain is almost perpendicular to boundary.



σ

Figure 7c) Crack parallel to basal planes as shown by low angle boundaries. Note that one edge of the crack is associated with a grain boundary.

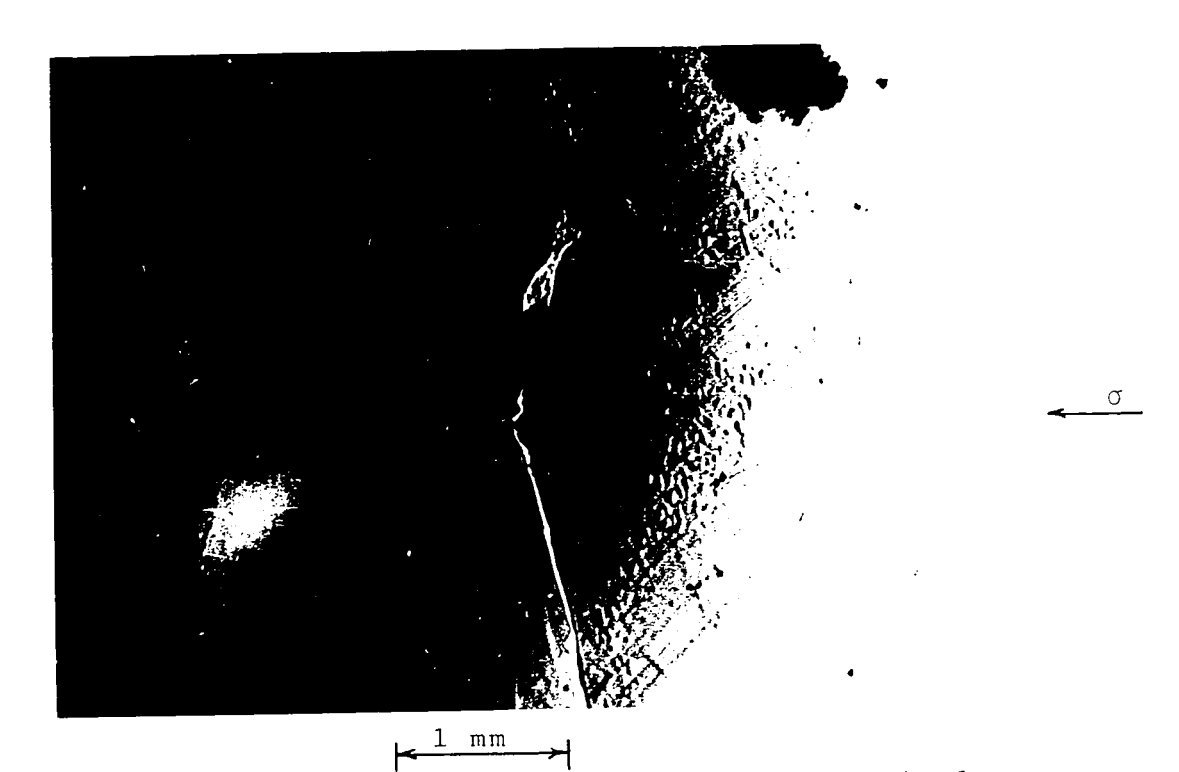


Figure 7d) Grain boundary crack. Note that the basal plane of one grain is almost perpendicular to boundary.

The deformation modes that have been observed in ice are consistent with what is known about its deformation behaviour, and point defects and dislocation networks that occur in it. Tegart (1964) pointed out that hexagonal metals tend to be more ductile the larger the number of effective, active deformation modes. Ice has only two degrees of freedom for easy glide and these are in the basal plane. Observations show that Nabarro-Herring creep appears to provide for polycrystalline ice adequate freedom for deformation for the strain rates associated with stress less than about 1 kg/cm2. For larger strain rates, however, both Nabarro-Herring creep and basal glide are inadequate, and the applied stress increases into the range associated with non-basal glide. Significant nonuniform internal stresses must develop as well because of the marked anisotropy in the resistance to dislocation movement. These stresses can be large enough to initiate other modes of deformation, such as grain boundary migration, formation of low angle boundaries, dislocation climb, cross-slip, and void and crack formation.

The difference in the deformation behaviour of the different types of ice illustrates the important role played by the degree of compatibility of grain boundaries. Grains in previously undeformed type S2 ice have, initially, only one degree of freedom for easy glide when the load is applied perpendicularly to the long direction of the columns. This is

in the direction of the resolved shear stress on the basal plane. Type S2 ice under this condition of load undergoes essentially two dimensional deformation for about the first 2% strain (i.e. there is no significant strain in the long direction of the columns). Type S1 columnar-grained ice has no degrees of freedom for easy glide for load applied parallel or perpendicularly to the columns, because the shear stress resolved on the basal plane is zero. Both types S1 and S2 ice show a marked yield within the first 0.5% strain, and, as mentioned in section 2.4.3, this is considered due to the development of new modes of deformation. Granular, type T1 ice, on the other hand, does not appear to exhibit yield for this range of strain for compressive stresses up to about 20 kg/cm², and is relatively more ductile in its behaviour.

Type S2 ice with the load applied perpendicularly to the columns is relatively more prone to crack formation than granular ice. Type S1 ice, and type S2 with the load applied parallel to the long direction of the columns, are quite brittle in their behaviour. Under conditions of rapid rate of loading, failure can occur before yield, and in some cases it is explosive.

It can now be appreciated why polycrystalline ice can be a useful and interesting material for the study of crack formation and the failure process. The small number of degrees

of freedom for deformation ensures that the internal stresses necessary for crack formation are induced by relatively little strain. The crack forming process and the associated deformation can be made two dimensional by using a columnar-grained structure. By varying the structure it is possible to produce significant changes in the nature of the constraints imposed on grains and, thereby, to study their effect on failure behaviour. In addition to providing these possibilities, ice is transparent so that it is possible to observe characteristics of the failure processes as deformation proceeds.

2.5 Strength of Ice

Observations as early as 1884 by Ludlow, and 1894 by
Beach et al, had demonstrated that under some conditions of
loading polycrystalline ice yields in an apparently plastic
manner, whereas for other conditions failure is abrupt and
brittle. The crushing strength was found to be greatly
variable, ranging from almost 7 kg/cm² to over 100 kg/cm².

It was appreciated that the strength depended upon temperature,
rate at which the load was applied, type of ice, and direction
of the stress relative to the grain structure.

The reasons for the great variation in the strength of ice can be readily appreciated, at least from a qualitative point of view, from the knowledge that has been developed concerning the strength of materials and the factors that

affect strength. Studies of the strength of ice, however, have not usually been carried out with sufficient completeness or control to allow the influence of each factor to be determined or taken into account. Much of the information available on the strength of ice, therefore, is qualitative and of doubtful value except from that point of view. Reviews on this subject have been prepared by Voitkovski. (1960); Weeks and Assur (1968) and Gold (1968).

Brown (1926) pointed out that the term "compression or crushing strength of ice is meaningless in itself. behaviour of ice in compression is different at the same rates of loading at different temperatures, and at different rates of loading at the same temperatures. to obtain characteristic compression fractures the load must be applied rapidly, so that the ice has no opportunity to flow." Brown observed that if columnar-grained ice was loaded in compression parallel to the long direction of the grains at a rate of about 15 kg/cm²/sec, conical type fractures were obtained. When the load was applied at the same rate perpendicularly to the long direction of the columns, a "tent-like" ductile yielding occurred. Similar behaviour was reported by Bell (1911). observed that close to 0°C, columnar-grained ice with the load applied perpendicularly to the long direction of the columns, would spread out or flow without fracture at stresses up to about 35 kg/cm 2 .

The brittle behaviour of polycrystalline ice at high rates of loading, and ductile behaviour at low rates, indicated that ice has a brittle to ductile transition point. The conditions associated with this transition have not been studied systematically. Jellinek (1958) found that the tensile strength of granular ice at about -5°C increased with increasing rate of loading to a maximum at a rate of about 0.2 kg/cm²/sec. The strength then decreased to a relatively constant value for rate of loading in excess of about 0.5 kg/cm²/sec. It was recommended by Butkovich (1958) that all measurements of the strength of icebecarried out at this rate of loading, or greater, in order to obtain results independent of the rate.

This may be true for tests in which the ice fails in tension, as failure is probably associated with the formation of the first large crack. The work of Brown (1926), Butkovich (1955) and Halbrook (1962) showed that at this rate of stressing both columnar and granular ice still behave in a ductile manner in compression. Peyton (1968) found for sea ice, which has a ductility that is probably not much greater than that of granular ice, that the rate of loading had to exceed at least 10 kg/cm²/sec to obtain compressive strengths independent of the rate. This result is in line with that of Brown for columnar-grained ice.

Butkovich (1954, 1955) studied the compressive, tensile and shear strength of columnar and granular ice. He found that the compressive and torsional shear strengths of columnar-grained ice are more temperature dependent than for granular ice and columnar-grained ice in tension. He found also that the compressive strength of columnar-grained ice was greater when the load was applied parallel to the long direction of the columns than when applied perpendicularly to it.

Butkovich (1955, 1958) presented evidence of the influence of cross-sectional area on the crushing strength of ice.

Jellinek (1958) found that the strength of granular ice in tension depended on the volume of the ice being tested. He interpreted his results in terms of the probability that the ice would contain a flaw at which failure would be initiated.

Jellinek recognized that his results could be influenced by the constraints imposed at the points of application of the load, but he did not attempt to evaluate this effect. In general, insufficient attention has been given to the effect of specimen size, ratio of specimen width to length, and conditions at the point of application of the load, in observations of the strength of ice.

Several observers have noted internal crack formation during creep in constant load tests, during yield in controlled rate of strain tests, and prior to failure in strength tests

(e.g. Brown, 1926; Butkovich, 1954; Dillon and Andersland, 1967; Muguruma, 1969). Gold (1960) studied the influence of crack formation on the creep behaviour of type S2, columnargrained, ice at -10°C. That study indicated that crack formation occurred when the applied compressive load exceeded a fairly critical value. If the stress was less than what appeared to be a well defined range, cracking activity increased and subsequently decreased until it was practically non-existent in the secondary creep stage. If the stress exceeded this range, cracking activity was continuous. The resulting breakdown of structure, which tended to be concentrated in zones parallel to the planes of maximum shear, appeared to be a contributing factor to the onset of tertiary creep.

This behaviour was an interesting contrast to that observed by Steinemann for granular ice. He found that tertiary creep was associated with recrystallization. This difference in behaviour may be due to the difference in the constraints existing between the grains. Steinemann used thin sections for his observations, and so the specimens were probably in a state of plane stress. Gold used large specimens, and because of the nature of the deformation of type S2 ice, the region in which a crack formed was probably in a state of plane strain.

It was clear from the observations that brittle crack formation in ice had a significant effect on its deformation behaviour, even when it was ductile. It was also apparent that cracking activity depended in a measurable and reproducible way on time, stress and strain. A series of observations were subsequently undertaken to obtain information on the factors controlling cracking activity and the formation of individual cracks (Gold, 1963a, b, 1966, 1967).

The observations on the factors controlling the formation of individual cracks have shown that their formation is consistent with current ideas concerning crack initiation and propagation in crystalline solids. It will be useful to review some of the information now available concerning crack initiation, crack propagation and failure before presenting the results of the present study of the role that crack formation plays in the failure of ice.

3. FAILURE

3.1 Definitions

The failure or fracture of a material can occur in numerous ways. There has been a rapid increase in appreciation of this, and in understanding of the conditions associated with and responsible for the different types of failure. The subject is of such interest and importance that it is reviewed regularly (e.g. Smekol, 1936; Hollomon, 1948; Orowan, 1948; 1950; Zener, 1948; Petch, 1954; Low, 1954, 1963; Stroh, 1957; Cottrell, 1958, 1963, 1964; Davis and Dennison, 1958-59; Pugh, 1967; Sullivan, 1967; Kenny and Campbell, 1968).

Sufficient information has accumulated concerning failure to provide a basis for classification of the various types.

Sullivan (1967) presented a good discussion of classification of failure; the following remarks are based mainly on his paper. These remarks go beyond the needs of the present study, but are presented to provide a framework in which to report and discuss the results. It should be emphasized that at this stage in the development of knowledge concerning failure, any classification will be arbitrary to some extent, and that many of the terms defined are concerned with a spectrum of conditions or behaviour rather than something distinct.

Fracture is defined as a separation across a geometrical surface. It is to be distinguished from rupture, which is defined as a process in which slip operates on a macroscopic scale to produce separation (e.g. slipping off along a glide plane, drawing down to a point without significant microcracking or void formation). The occurrence of rupture implies the operation of sufficient degrees of freedom for deformation to ensure that a grain always conforms, by slip alone, to the imposed change in shape and the constraints of neighboring grains.

Fracture can occur by several mechanism acting alone or in combination. Some of the principal mechanisms are cleavage, plastic, creep, and shear fracture. Cleavage fracture is a transgranular separation perpendicular to the plane of the fracture, caused by tensile forces usually acting across a well defined plane. Plastic fracture is a separation because of structural breakdown due to intensive slip. It is commonly agreed that the first step in plastic fracture is the formation of internal voids. Creep fracture also involves separation because of the breakdown of the structure due to slip. The distinction between creep and plastic fracture is that the former is time dependent (high homologous temperatures) and the latter essentially time independent. Shear failure is a separation because of loss of cohesion due to relative motion parallel to the plane of failure.

mode, behaviour and appearance. Mode refers to the path followed by the failure plane; e.g. along grain boundaries (intercrystalline or intergranular), across grain boundaries (transgranular). Behaviour is concerned with the amount of deformation prior to failure. Brittle behaviour implies little deformation and ductile implies extensive deformation. The boundary between these two types of behaviour is not clearly defined. They can be associated with any of the mechanisms of fracture. Appearance refers to descriptive characteristics of the fracture surface, usually as observed at low magnification.

Failure is a structure sensitive phenomenon. The processes associated with it may be confined to the immediate vicinity of the surface of separation, or they may be distributed throughout the material, causing a gradual deterioration in structure and finally the formation of the failure surface. Two distinct stages are associated with both cases: initiation and propagation. Initiation involves the creation of a discontinuity in structure from which a separation can develop. It may occur at only one site in the material, or at several, depending upon the conditions present. Propagation is the subsequent extension of the initial separation as a crack.

3.2 Crack Initiation

The formation of cracks involves the creation of new surface. This requires work which must be done by the forces causing separation. Much effort in the study of failure has been devoted to clarifying how the work of the external forces acts to produce new surface.

It was recognized from the nature of crack formation, and from the fact that observed strengths are smaller by orders of magnitude than the theoretical maximum, that there exist mechanisms whereby the work done by external forces can be made available for creation of new surface at specific locations. Inglis (1913) showed that surface notches and internal cracks provide such locations, for the stress concentration at their roots could be large enough to overcome the force of attraction between atoms. Failure brought about in this way, however, requires the preexistence of such flaws, and in many cases the material does not contain any of sufficient size to account for the low strengths observed.

Evidence accumulated indicating that plastic or viscous flow occurred prior to the formation of a crack (Petch, 1954; Dieter, 1961, p. 200; Smith, 1968a). Zener (1948) made the suggestion that crack initiation might occur by the coalescence of the leading dislocations in a pile-up. The pile-up could

be caused, for example, by blocking of dislocations in their glide plane at grain boundaries or inclusions. This suggestion focused attention on the stress concentrations that exist at the head of pile-ups, or similar strain discontinuities in solids, and the energy conditions that must be satisfied on a microscale if a crack is to be initiated.

The stress field near the head of a pile-up is given by

$$\tau_{ij} = \frac{\tau_e}{2} \left(\frac{\ell}{r}\right)^{\frac{1}{2}} f_{ij} (\theta)$$
 (10)

where

 τ_{ij} are the components of the elastic stress field at the point $P(r,\theta)$, to is the shear stress acting on the dislocations, ℓ is the length of the pile-up, and $f_{ij}(\theta)$ is a function of θ , the angle between the glide plane of the dislocations and the vector \dot{r} to the point $P(r,\theta)$. (Stroh, 1957; Head, 1960; Basinski and Mitchell, 1966; Smith and Barnby, 1967.).

This field can be calculated by either assuming a pile-up of n discrete dislocations (Eshelby, Frank and Nabarro, 1951; Stroh, 1954), or a continuous distribution of dislocations (Eshelby, 1949; Head and Louat, 1955). The number of dislocations in the pile-up is given by

$$n = \frac{\pi(1-v)}{Gb} \tau_e \ell \tag{11}$$

where G is the shear modulus, v Poisson's ratio and v the length of the Burgers vector.

The elastic stress field associated with other types of strain discontinuities, including cracks, can be obtained by replacing them with an equivalent distribution of dislocations (Cottrell, 1963).

From equation (10) it is seen that a singularity exists in the stress field at the head of the pile-up. It is considered that the stress in this region is so large compared to the applied stress that crack initiation under these conditions is controlled essentially by the characteristics of the pile-up (Davidson et al, 1966; Dower, 1967; Francois and Wilshaw, 1968). Criteria for crack initiation for various situations can be obtained by assuming the pile-up to be equivalent to or associated with a hypothetical crack. The criteria are obtained by determining the stationary values for the total energy of the system in terms of the local conditions near the tip of the propagating hypothetical crack (Smith, 1965; Smith and Barnby, 1967). Criteria have been obtained by this approach, or an equivalent one, by Stroh (1954, 1958); Gilman (1958); Bilby and Hewitt (1962); Bullough (1964); Chen (1964); Priestner and Louat (1965); Smith (1965, 1966a, b, 1968b); and Smith and Barnby (1967). These studies have shown that the effective

shear stress required to initiate a crack is given by

$$\tau_{e} = \Lambda \sqrt{\frac{\gamma}{k}}$$
 (12)

where A is a parameter determined by the elastic constants of the material and geometric factors; γ is the work or energy associated with the formation of unit area of new surface.

where

Substituting for & in equation (12) using equation (11), and squaring, gives

$$\tau_{e} n = \frac{B\gamma}{b}$$

$$B = \frac{\pi(1-\nu)}{G} A^{2}$$
(13)

Some of the criteria that have been obtained for given conditions are presented in Table V.

The criteria for crack nucleation obtained using dislocation theory do not involve the width of the crack. This indicates that once the condition given by equation (12) is satisfied, the crack will be initiated and continue to increase in size as long as there is sufficient energy in the pile-up to do the work associated with the formation of new surface.

Several studies have indicated that crack formation in crystalline material is associated with the motion of dislocations, and dislocation interactions. Gilman (1958) observed

TABLE V

Criteria for Crack Initiation

Plane Strain Conditions

 $\frac{\frac{\text{MODEL}}{s}}{s}$ $\theta = 70.5^{\circ}$

CRITERION

$\tau_{e} \geq \left[\frac{3\pi\gamma E}{16(1-v^{2})k}\right]^{\frac{1}{2}}$

$$n = \frac{3\pi^2 \gamma}{8\tau_e b}$$

$$\frac{1}{2}$$
 Stroh, 1957

$$\tau_{e} \simeq \left[\frac{\pi \gamma E}{4(1-v^{2})\ell}\right]^{\frac{1}{2}}$$

$$n = \frac{\pi^2 \gamma}{2\tau_e b}$$

*Smith and Barnby, 1967

SOURCE

*Smith and Barnby show crack nucleation criterion almost independent of $\boldsymbol{\theta}$ for

$$0 \le \theta \le 90^{\circ}$$

that cracks formed in zinc in blocked slip bands. Stokes et al (1958, 1959, 1961) and Johnston (1960) obtained evidence that crack formation in $M_{\rm g}{\rm O}$ was associated with pile-ups at grain boundaries and kink bands, and with the intersection of slip bands. Stokes et al (1961) showed that the fracture behaviour of MgO depended on the relative orientation, number, thickness and spacing of the slip bands. Similar observations have been made by Westwood (1961); Clarke et al (1962); Weiderhorn (1963); Wronski and Fourdeux (1964); Argon and Orowan (1964); Briggs et al (1964); Ku and Johnston (1964); Beevers and Halliday (1968); and Kamdar and Westwood (1968). Gold (1966) found that the shape of cracks in ice was consistent with models of crack initiation by dislocation pile-ups. This can be seen in the photographs presented in figure 7. Relevant reviews have been prepared by Low (1963) and Sullivan (1967).

The role that degrees of freedom for deformation plays in crack initiation in polycrystalline materials can now be appreciated. The maximum stress that will develop at a dislocation pile-up, or similar source of strain concentration, will depend upon the degree of compatibility of grain boundaries, the ease with which multiple slip is initiated within the constituent crystals, and the modes of deformation that can develop within a grain (e.g. bend planes, kink bands, twinning, dislocation climb, etc.). It would be expected that cleavage

crack formation would occur more readily in materials that have few degrees of freedom for deformation, as it is in such materials that there is a good probability that stress concentrations will exceed the cohesive strength before they can be relieved by initiating other modes of deformation.

3.3. Crack Propagation

The stress field at a point $P(r,\theta)$ near the tip of a crack, according to elastic theory, is given by equations of the form

$$\tau_{ij} = \sqrt{\frac{K}{2\pi r}} f_{ij} (\theta)$$
 (14)

where

r is the distance of the point P from the tip in the plane perpendicular to the edge; K is a parameter that depends upon the elastic constants, the size and geometry of the crack, and the applied stress; and $f_{ij}(\theta)$ depends only on the angle θ between the vector \vec{r} and the plane of the crack (Sneddon, 1946; Kenny and Campbell, 1968).

Equations (14) are of the same form as equations (10) for the stress in the vicinity of the head of a pile-up. They also have a singularity at the tip of the crack. During propagation the stress in this region must be so large that the material is no longer behaving elastically. It is usually not possible

to calculate the plastic or viscous work associated with the deformation near the tip during propagation. Assumptions must be made, either implicitly or explicitly, concerning the behaviour near the tip when determining criteria for crack extension.

One of the first calculations of a criterion for crack extension was that of Griffith (1921). He was able to circumvent the difficulty caused by the singularity in the stress and strain fields by applying the first law of thermodynamics. Consider a long, narrow crack of width 2c (see figure 8). Let the work done by external forces during a small extension, dc, of the width of the crack, be dw. If the corresponding change in strain energy is -du, then the net work available for crack extension is

$$dF = dW - du \tag{15}$$

Griffith assumed that the work expended in increasing the width of a long, narrow crack an amount dc is $2\gamma dc$ per unit length. The criterion for crack extension can then be expressed as

$$\frac{d\mathbf{F}}{d\mathbf{c}} = \frac{d(W - \mathbf{u})}{d\mathbf{c}} \ge 2\gamma \tag{16}$$

i.e. the work done by the external forces plus the change in strain energy must be equal to or greater than the work required

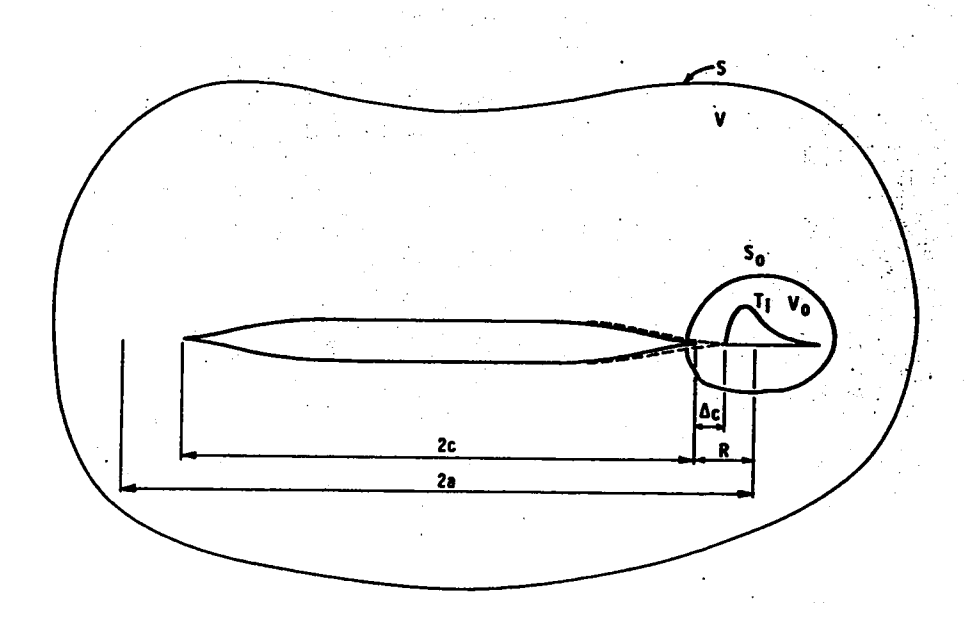


FIGURE 8
CRACK EXTENSION, TI REPRESENTS THE COHESIVE STRESS AT THE CRACK TIP

to form the new surface. This criterion has been evaluated for several crack geometries and stress conditions. Some of the results are presented in Table VI.

Griffith identified γ with the surface energy of the material, which implies that there is no plastic or viscous flow at the crack tip during propagation, i.e. the material is elastic everywhere. This assumption has been found to be reasonably valid for a brittle material such as glass. It cannot be true if crack propagation is associated with plastic flow. Orowan (1950) and Irwin (1948, 1960) suggested that for such cases the work available for crack propagation should be equated to the sum of the surface energy and the work P, associated with plastic and viscous flow. The criterion for crack extension in this case becomes

$$\frac{dF}{dc} = \frac{d(W - u)}{dc} = G \ge (2\gamma + P) \tag{17}$$

For many situations $P > 2\gamma$, and the effect of surface energy on crack propagation can be neglected.

For a "fixed grip" situation, the work of crack extension clearly must come from the strain energy stored in the material. From equation (17), it can be appreciated that the energy required for crack propagation can always be calculated using elastic theory. For this reason G has been called the strain

TABLE VI

Criteria for Crack Propagation

MODEL

CRITERION

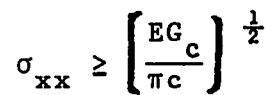
SOURCE

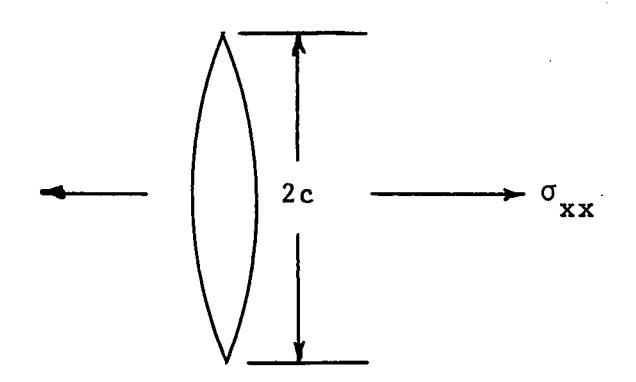
Long narrow crack, plane stress

$$\sigma_{xx} \geq \left[\frac{EG_c}{\pi c}\right]^{\frac{1}{2}}$$

Griffith, 1921; Tetelman

and McEvily, 1967, p. 53





Long narrow crack, plane strain

$$\sigma_{xx} \geq \left[\frac{EG_c}{\pi c (1-v^2)}\right]^{\frac{1}{2}}$$

Orowan, 1934; Tetelman and McEvily, 1967, p. 53

Penny shaped crack, plane strain

$$\sigma_{xx} \geq \left[\frac{\pi E G_c}{4c(1-v^2)}\right]^{\frac{1}{2}}$$

Sack, 1946; Tetelman and McEvily, 1967, p. 53

TABLE VI (Cont.)

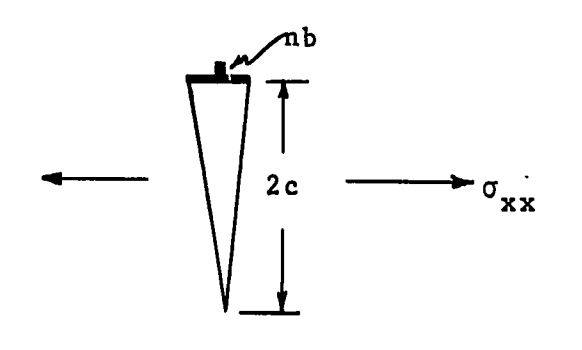
CRITERION

SOURCE

Long narrow crack, plane strain (approximate solution)

$$\tau_e \sigma_n L \geq \frac{EG_c}{\pi(1+\nu)}$$

Stroh, 1958



MODEL

Long narrow crack, plane strain, (nucleated by coalescence of n dislocations)

Size of dislocation crack = Griffith crack

$$\sigma_{xx} \geq \frac{G_{c}}{nb}$$

$$2c_{crit} = \frac{n^2b^2E}{2\pi(1-v^2)G}$$

for
$$\sigma_{xx} = 0$$

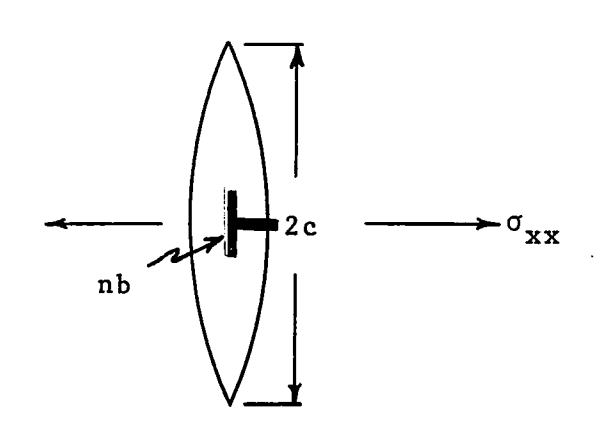
$$2c = \frac{n^2b^2E}{8\pi(1-v^2)G}$$

8

Bullough, 1964

TABLE VI (Cont.)

MODEL



CRITERION

Long narrow crack, plane strain, (nucleated by coalescence of n dislocations)

Size of dislocation crack = Griffith crack

$$\sigma_{xx} \geq \frac{2G}{nb}$$

$$2c_{crit} = \frac{n^2b^2E}{4\pi(1-v^2)G_c}$$

for
$$\sigma_{xx} = 0$$

$$2c = \frac{n^2b^2E}{8\pi(1-v^2)G_c}$$

SOURCE

Bullough, 1964

 α

energy release rate. The critical value of G associated with the initiation of crack propagation is defined as

$$G_{c} = (2\gamma + P) \tag{18}$$

The Griffith approach to crack extension involves the calculation of the total energy of a body as a function of the crack width. Because of the singularity in the stress field at the crack tip, it would be expected that the energy for an infinitesimal extension of the crack would come mainly from this region. Attention has been given, therefore, to establishing criteria for crack extension based on the conditions that exist at the tip. This approach could also be valid for the Irwin-Orowan criteria if the plastic work were confined to a sufficiently small region.

Consider the long narrow crack of width 2c shown in figure 8. Let the crack extend by a small amount Δc when the material within the contour S, enclosing volume V, goes from the initial state, a, to the final state, b. If inertial effects are neglected, it can be shown that the Griffith fracture criterion can be expressed as

$$\int_{\mathbf{v}} \left[\int_{\mathbf{a}}^{\mathbf{b}} \left(\sigma_{\mathbf{i}\mathbf{j}}^{\mathbf{b}} - \sigma_{\mathbf{i}\mathbf{j}} \right) d\varepsilon_{\mathbf{i}\mathbf{j}} \right] d\mathbf{v} \geq 2\gamma \Delta c$$
 (19)

where σ_{ij} and ϵ_{ij} are the stress and strain components respectively (see Sanders, 1960;

Cottrell, 1963; Rice, 1965, 1968; and Rice and Drucker, 1967).

Assume that the region at the crack tip in which plastic and viscous flow occurs is small compared to the width of the crack. Let this region for both the initial state, a, and final state, b, be enclosed in a finite volume V containing the crack tip. It can be shown (e.g. Rice, 1965; Rice and Drucker, 1967) that the criterion for crack propagation can also be expressed as

$$\geq -\lim_{\Delta c \to 0} \frac{1}{\Delta c} \int_{\Delta c} \left[\int_{a}^{b} T_{i} du_{i} \right] dc = G = 2\gamma + P \quad (20)$$

where T_i is the cohesive stress acting across Δc from the initial to the final state (i.e. the stress perpendicular to the plane of the crack experienced by each point on the crack surface in going from the elastic state far from the tip, to the final, stress free state, on the surface).

The important point of the foregoing discussion is that when the plastic or viscous work is confined to a region small compared to the crack width, the path of integration used to

as it includes the tip. This implies that the Griffith criterion for fracture, although obtained from an overall energy balance, can be derived from the stress and strain fields in the immediate vicinity of the tip. That is, the work required to extend the crack must be available from the highly stressed region at the tip. Observations have shown that for many situations of practical interest, most of the plastic and viscous deformation associated with crack extension does involve a depth of material that is small compared to the crack width.

Irwin (1957, 1960) assumed this to be so, and determined the change in strain energy associated with a small extension of the crack using equations (14) and (17). This provided a relationship between K, the "stress intensity factor" in equation (14) and G, the strain energy release rate. The stress and strain fields in the vicinity of the tip are determined by K. Crack propagation can be expected when K attains a critical value, K_c, that is characteristic of the material, temperature, geometry of the specimen and crack, and the rate of application of the load (if the material is viscous). For the plane stress condition

$$K_c^2 = E G_c \tag{21}$$

and for plane strain

$$K_{c}^{2} = \frac{E G_{c}}{1 - v^{2}}$$
 (22)

where E is Young's modulus.

The critical value of K_c for given conditions is often referred to as the "fracture toughness". Evaluation of K_c in terms of applied stress, crack length and specimen dimensions is a normal stress analysis problem. Its determination and application for various elastic and elastic-plastic conditions is of great interest in fracture mechanics (see ASTM, 1965).

Cottrell (1963) has considered the conditions at the tip of a propagating crack using dislocation theory. His study provides additional insight into the conditions for which the Griffith criterion, and the modification of it by Orowan and Irwin, are valid. He assumed that in the region $c^2 < x^2 < a^2$ in figure 8, the stress is constant and equal to the yield stress, σ_y . It was found that the Griffith formulation is valid when $\sigma_a < < \sigma_y$, where σ_a is the applied stress. An equivalent condition is

$$R = a - c < c$$

which is the condition assumed by Rice (1965, 1968), Rice and Drucker (1967) and implicit in the formulation of Irwin. The study also showed that in the low stress limit, R is independent

of the width of the crack (i.e. a material property) and that when the Griffith condition is just satisfied, the stress field at the tip is independent of the applied stress and crack width.

There has been considerable discussion as to which is the more difficult phase of crack formation: initiation or propagation (see Smith and Barnby, 1967). From the foregoing discussion it can be appreciated that this depends upon the properties of the material, the characteristics of the source of stress concentration, and the nature of the applied stress. It is generally considered that initiation is the more difficult phase, but propagation can be if the associated plastic or viscous flow is large. In this case the Griffith or Irwin formulation would probably be invalid.

It can be expected that the critical stress intensity factor or strain energy release rate for ice will depend significantly on the temperature and rate of straining. The only information available on this was obtained by Gold (1963b) under conditions of crack arrest associated with thermal shock. He calculated the strain energy release rate for these conditions to be about 300 ergs/cm²; i.e. $G/_2 = \frac{1}{2}(2\gamma + P) \simeq 150 \text{ ergs/cm}^2$. This value is not too different from the surface energy for ice, about 100 ergs/cm², indicating that P must be quite small.

Because of the small value of the strain energy release rate, it can be concluded that the Griffith-Irwin-Orowan formulation is valid for the conditions associated with a rapidly running crack in ice. It is probably valid as well for a slowly propagating crack because of the deformation properties of the material, but there is no experimental evidence as yet to support this assumption.

When the external stress field is taken into consideration in a study of crack initiation by dislocation pile-ups, the critical crack widths are given by the roots of a binomial equation (see Stroh, 1957; Bullough, 1964). The smaller root corresponds to the equilibrium width of the dislocation crack and is essentially independent of the applied stress. The larger root corresponds to the Griffith crack width. The critical condition occurs when the two roots are equal, for then the dislocation crack can act as a Griffith crack. From a knowledge of the role of small scale stress concentrations in crack initiation, and the factors controlling crack propagation, it can be appreciated why a superimposed hydrostatic pressure will suppress propagation but have little effect on initiation (see Davidson et al, 1966; Dower, 1967; Francois and Wilshaw, 1968).

3.4 Cavity Formation

For some conditions of stress and temperature, the increase

in volume that may be required because of incompatible grain boundaries occurs by the formation of voids rather than cracks. It is considered that these cavities grow by the stress-induced diffusion of vacancies (Seigle and Resnick, 1955; Balluffi and Seigle, 1957; Hull and Rimmer, 1959; Ratcliffe and Greenwood, 1965). Observations have shown that they generally develop in the vicinity of grain boundaries subject to a tensile stress, particularly at low creep rates, with the number of cavities decreasing with increasing angle between the stress and the normal to the boundary (Greenwood et al, 1954; Davies et al, 1968). There is also evidence that they may form in association with grain boundary sliding at higher rates of strain (Gittins and Williams, 1967). Theoretical studies showed that the condition that must be satisfied for voids to grow by receiving vacancies when no hydrostatic pressure is present, is given approximately by

$$\sigma = \frac{2\gamma}{r\cos^2\theta} \tag{23}$$

where σ is the applied stress, r is the radius of the void, and θ is the angle between the stress and the normal to the boundary near which the voids are forming. (Balluffi and Seigle, 1957; Hull and Rimmer, 1959; Speight and Harris, 1967).

Void nucleation is considered to be heterogeneous, and to take place, for example, at impurities, preexisting voids, gas bubbles and grain boundary ledges. (Boettner and Robertson, 1961; Gifkins, 1959, 1963; Low, 1963). The growth of voids is diffusion controlled and therefore depends on the time.

Gold (1963) has observed void formation in columnar-grained ice during creep under compressive loads. The voids formed in the region of grain boundaries running generally parallel to the applied stress, at stresses less than and extending into the range associated with cleavage crack formation. In the light of experimental evidence concerning the conditions associated with cavity formation, their presence indicated that local tensile stresses developed during the compressive creep of the ice.

Figure 5a is an example of void formation in type S2 ice. The voids had formed in the central part of the specimen, and the specimen was subsequently cut so as to bring them closer to the surface. Figure 5b is an example of substructure developed in the region of void formation, indicating the severe deformation that has occurred. The surface was polished and thermally etched using a technique described by Krausz (1961).

Theoretical studies concerning crack nucleation and observations on cavity formation, indicate that strain is a major factor controlling both events. For a material that is able to creep or flow viscously, time must also be important, for it would be expected that dislocations and point defects could move out of regions of stress concentration (e.g. head of dislocation pile-ups) by thermally activated processes, and thus increase the time necessary to establish a critical condition. The observations that have been made on columnargrained ice show that for this material at sufficiently low rates of strain, the conditions required for cleavage crack nucleation during compressive creep are not obtained, and that the time available is adequate for cavity nucleation and growth to provide the additional freedom for deformation required by incompatible grain boundaries. It should be noted also that no evidence was seen (at magnification of about 25x) of cavity formation in the vicinity of cracks, or throughout the specimen if a sufficient number of cracks had formed.

The process (cavity or crack formation) that predominates depends on the level of the applied stress, or rate of strain. Similar observations on the stress dependence of crack and cavity formation have been reported for other materials (McLean, 1956; Heslop, 1962; Williams, 1967) and discussed theoretically by Waddington (1968). Cottrell (1963) pointed out

cavity formation is the most efficient mechanical method of bringing about the separation of material, because the movement of vacancies to voids can occur in a thermodynamically reversible manner, and so the maximum fraction of the work of deformation is converted into energy of new surface. The stress required for slow growth of cavities would, therefore, be expected to be smaller than that required for crack nucleation and propagation.

3.5 Mechanisms of Failure

A reasonable picture can now be developed of the mechanisms of failure of an elasto-viscous or elasto-plastic material that behaves in a brittle manner under some conditions of temperature, stress and rate of strain. In the study of deformation behaviour it is usual to assume that the stress and strain at a point are well behaved in the mathematical sense, and can be described by continuum theory. It is realized, however, that in real materials properties affecting the stress and strain are not uniform but can vary spatially in a random manner. These variations may be due to dislocations and their interactions, imperfections such as voids or inclusions, changes in orientation across grain boundaries, etc. Because of these variations, the stress and strain can be expected to vary also from point to point in a random manner about an average value. Because the dimensions of imperfections are normally at least

an order of magnitude smaller than those associated with measurements, measured values of stress and strain can usually be assumed to be equal to the average values.

Fluctuations in stress and strain over small distances are of little significance if the deformation is in the elastic range. They become of particular importance, however, if the behaviour to be observed is structure sensitive, as is crack initiation, crack propagation and yield. The occurrence of these phenomena is evidence of a non-uniform stress field and a heterogeneous structure.

If a load is applied so rapidly that no or little viscous or plastic deformation occurs, the non-uniformity in the stress is due mainly to heterogeneities causing elastic stress concentrations. Crack formation in this case would tend to be associated with inclusions, preexisting microcracks and pores. and stress concentrations at grain boundaries due to the anisotropy in the strain of adjacent grains. If viscous or plastic flow can occur, it will relieve elastic stress concentrations. The resistance offered by grain boundaries and other impediments to the movement of dislocations, and the anisotropy in the deformation behaviour, now become the principal causes of a non-uniform stress field. The more difficult it is to initiate and maintain multiple slip relative to slip on the primary glide plane, the greater will be the

variance in the stress about the average value. For some materials (e.g. ice), the resistance to multiple glide is sufficiently large to cause the tensile stresses necessary for cleavage crack formation even during creep in compression (see Bartenev and Zuyev, 1968).

Consider now a visco-elastic material (i.e. its deformation behaviour is time dependent) deforming in tension. The more rapid the rate of strain the more probable is crack formation due to stress concentration of the type associated with dislocation pile-ups. Under these conditions there is a good possibility that when a dislocation crack is initiated, it will be of sufficient size to propagate as a Griffith crack, and failure will occur. The behaviour of the material will tend to be brittle.

As the rate of strain is reduced there will be a greater probability that the dislocation crack, when formed, will not be large enough to propagate as a Griffith crack (Muguruma, 1969). There will also be greater opportunity for the stress at the head of pile-ups and about micro-cracks and voids to be relieved by viscous flow. It would be expected, therefore, that greater strain would be required to develop a separation of sufficient size to propagate as a Griffith crack. At still lower rates of strain, cavity formation by the diffusion of vacancies, and other modes of deformation, maintain the maximum

tensile stress below that required for cleavage crack formation. With further reduction in rate of strain, even void formation is suppressed, and the deformation must occur by mechanisms that are essentially ones of constant volume.

As the rate of strain is decreased, or the temperature increased, the behaviour tends to become more ductile. Transitions in behaviour are often quite pronounced, and this is reflected in the strain to failure and the strain energy release rate. The magnitude of the brittle to ductile transition and the range of rate of strain over which it occurs, depends on the material, structural characteristics such as grain size and texture, temperature, state of stress and impurity content. The transition is often associated with a change in the mechanism by which failure is brought about (e.g. a change from predominantly cleavage crack formation to void formation). A discussion of the brittle to ductile transformation in steel, which is plastic rather than viscoelastic, is given by Hahn et al (1959), Louat and Wain (1959), Dieter (1961), Waddington and Lofthouse (1967). elastic case is discussed by Mullendore and Grant (1963), Davidson et al (1966), and Bartenev and Zuyev (1968). Conditions associated with brittle and ductile failure in tension are discussed by Cottrell (1963), Low (1963), Garofalo (1965), Tegart (1966), Sullivan (1967) and Kenny and Campbell (1967).

The situation is somewhat different for compression. For this load condition tensile stresses associated with incompatible grain boundaries and heterogeneities are local in character. These regions of tensile stress would be expected to be only of the order of grain diameter in size. Cleavage crack and void formation would tend to place an upper limit on this stress, or relieve it altogether. As the region of tensile stress is limited in extent, cleavage cracks would be expected to be stable in size once formed. For large stress, however, the cracks may propagate in the shear mode (Brace, 1960; Murrell, 1964). Morrison (1963), Udd (1963) and Brace and Bombolalsio (1963) have observed that when conditions in brittle materials are suitable for crack extension due to a compressive stress, the crack tends to curve into and propagate parallel to the applied load.

If the compressive stress is below that required for crack propagation, each localized crack event need have little effect on the ability of the material to carry the load.

These events can be looked upon as a form of work softening, however, as they relieve internal constraints on the deformation. Evidence of this was obtained for ice by the author (Gold, 1965), and mentioned in Section 2.4.3. Krausz and Gold (to be published) have found crack formation in ice to be associated with yield in constant rate of strain tests.

The removal of lateral constraints to deformation by continuing crack formation would gradually reduce the resistance of the material to shear. If failure is not initiated by conditions over the area where the load is applied, it would be expected that at some fairly critical average distance of crack separation failure would develop. Observations of this behaviour for type S2 ice were described in Section 2.5.

As the conditions associated with the development of failure in compression are different from those for tension, it would be expected that the brittle to ductile transition need not occur over the same range of strain rate and temperature. The stable nature of cleavage cracks and their work softening effect allows them to be compatible with ductile behaviour in compression, when for the same stress in tension the material may be quite brittle. This behaviour is most certainly true for ice (Gold, 1968).

Bridgman stated in 1949 that "fracture is prepared for, at least in some cases, by the reversible creation by the stress itself of alterations in the structure; when these alterations have proceeded to a critical degree the structure becomes unstable and fracture ensues". Fracture from this point of view is the climax to a series of events that have modified the internal structure of the material. In some cases it may require only one of these events to bring about

failure, as in cleavage due to tension. In others, the onset of instability may be due to a series of events that gradually break down the structure until it can no longer carry the load. This is often the case for brittle materials such as ice, concrete and rock.

3.6 Failure of Rock and Concrete

It is instructive to review briefly some of the information that has been obtained concerning the failure behaviour of concrete and rock. There is evidence that cracks begin to form in concrete when the compressive stress is 25% to 30% of the ultimate strength (Jones, 1952; Rüsch, 1959). The plane of the cracks tends to be parallel to the applied stress, as for ice. Jones (1958) and Hansen (1968) observed cracks on the surface of specimens when the load exceeded about 50% of the ultimate. The cracks formed abruptly, and always in the cement paste. They usually propagated in the paste until they encountered a void or aggregate particle. Blakey and Beresford (1955) found that the stress-strain behaviour of beams in three point loading was linear up to the onset of "micro-cracking". When this condition was attained, surface strains became non-This was attributed to crack formation at the surface. uniform. It is considered that crack initiation in concrete is due to the difference in the elastic properties of the aggregate and the cement paste.

End conditions are found to have a marked influence on the nature of the failure. If the ends are constrained, a pyramidal section immediately under the platens is free of cracks. Hansen (1968) found that this was associated with a barrel type failure. Jones (1958) considered failure to be due to the pyramidal section being forced into the centre section damaged by cracking. If the ends were unconstrained, cracks extended right to the platen.

Hansen (1968) pointed out that crack formation relieves transverse tensions, and new cracks should not be able to form within several aggregate diameters of existing ones. The number of cracks that form should depend on the size of the specimen and the average diameter of the aggregate. This point is relevant also to crack formation in ice during compressive creep.

Isenberg (1968) found that in biaxial loading the nature of the failure depended on the ratio of the principal stresses. In tension experiments, the failure changed from cleavage to crushing at a critical ratio of the compressive stress to the transverse tensile stress. Smith and Brown (1941) found that with increased confining pressure, the mode of failure in compression changed from splitting to shear. At high confining pressures the specimens appeared to flow laterally.

Kaplan (1961) and Romualdi and Batson (1963) have successfully applied Irwin's fracture mechanics to crack propagation in concrete. Hansen found that the failure of concrete became time dependent when the load exceeded about 90% of the ultimate. This finding led him to suggest that failure strength should be related to the condition for which a crack is not stable under a sustained load. Isenberg suggested that structures should be designed with reference to the stress necessary to initiate microcracking. These comments indicate the way in which some of the more recent findings concerning crack formation and failure are being given attention even for one of the commonest of building materials.

There is evidence that cracks exist in rocks prior to loading. When a compressive load is applied it is found that the initial part of the stress-strain curve is not linear, and this has been attributed to the closing up of preexisting cracks by the stress (Simmons and Brace, 1965; Brace et al, 1966). Brace and Orange (1966) found that the resistivity of rocks increased with stress over the non-linear part of the stress-strain curve, providing additional evidence of the closing up of preexisting cracks. The cracks were considered to form during the cooling of the rock from its molten state. Walsh and Brace (1964) and Walsh (1965a, b, c) have presented theoretical discussions of the influence of cracks on the elastic and failure behaviour of rocks. Simmons and Brace

found that the effect of the assumed cracks was removed by confining pressures of two to three kb. For pressures larger than this, the expected interrelationships were found to exist between the elastic constants.

The stress-strain curve is again found to become nonlinear for uniaxial compressive loads greater than 0.3 to 0.7
of the ultimate strength (Bridgman, 1949; Brace et al, 1966;
Orowan, 1966). This is considered to be due to the reopening
of the preexisting cracks (Brace, 1960; McClintock and Walsh,
1962; Brace and Orange, 1966). Observations have shown that
the cracks tend to be parallel to the applied load, as for
concrete and ice. When propagating cracks were inclined to
the load, they tended to curve so as to run parallel to the
compressive stress (Brace and Bombolalsio, 1963; Morrison,
1963; Udd, 1963). Failure could occur by the running together
of cracks, or by the breakdown of the material between them
(i.e. cataclasis).

The mode of failure depends upon the rock type and composition, structure, stress field and temperature. Strong rocks in uniaxial compression usually fail abruptly in a brittle manner. Yield and crack formation may be uniformly distributed throughout soft rock specimens, resulting in a more ductile behaviour and a barrelling type of failure. Faulting, or a localized offset due to shear, can occur when the glide, yield

or cataclastic flow is not general throughout the specimen, but localized.

The development of a fault plane may or may not result in separation or total loss of resistance to shear. The fault may be confined to a plane, in which case the resistance to shear may be due to the friction between the two surfaces, or to a zone in which the material is highly cracked or crushed and has a cataclastic texture.

Griggs and Handin (1960, Mogi (1966) and Byerlie (1968), found pressure to have a marked effect on the brittle and ductile behaviour of rocks. At no or low confining pressure, failure may be abrupt as shown by curves D and C in figure 9. With increasing confining pressure there is a greater probability for a more gradual breakdown of structure by crack formation and yield, and the development of a fault zone. Under these conditions a yield point may be observed as illustrated by curve B. The approximately constant stress attained after yield is the resistance offered by the material in the fault zone to continuing shear. Deformation at this point is confined almost entirely to the fault zone. It is observed that for some materials this stress has a Coulomb-Rankine type behaviour.

At still higher confining pressures the resistance to glide in incipient fault zones is sufficiently great that yield

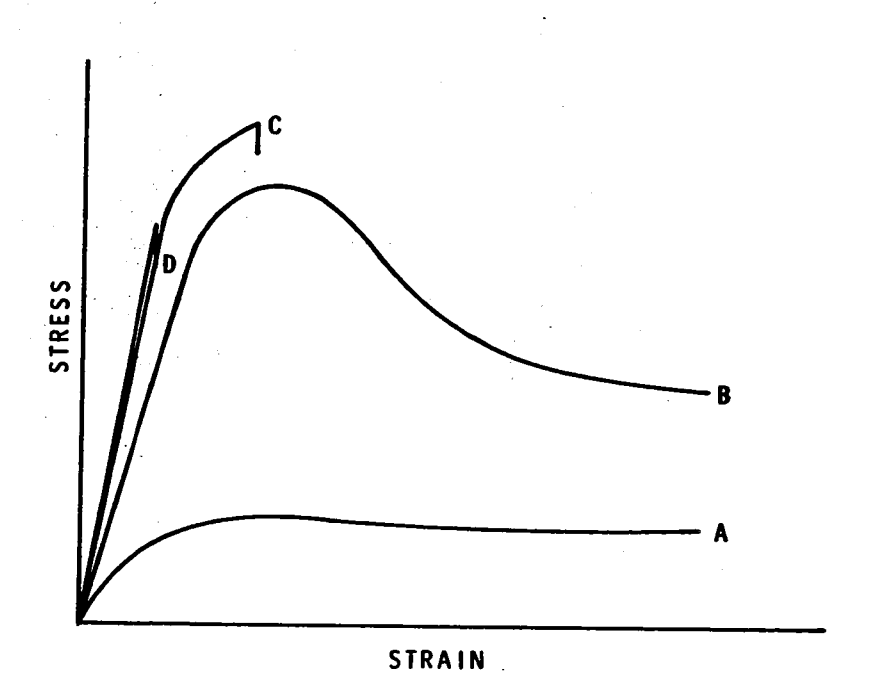


FIGURE 9

STRESS-STRAIN BEHAVIOUR FOR ICE SUBJECT TO A CONSTANT RATE OF STRAIN. AS THE STRAIN RATE IS INCREASED THE BEHAVIOUR IS TRANSFORMED FROM A THROUGH TO D.

is forced to occur more uniformly throughout the specimen.

Under this condition of load, rock becomes much more plastic in its behaviour and after yield the stress is almost independent of strain. With some rocks a form of work hardening is observed at high confining pressures.

The particular behaviour exhibited depends upon the type of rock, structure and conditions of loading. For ductile materials, the ductile to brittle transition depicted in figure 9 can be produced by increasing the rate of strain.

Observations that have been made on ice show that for small rates of strain, types S1, S2 and T1 have a behaviour similar to curve A. As the rate of strain is increased, the behaviour is gradually transformed through B, C to D. The failure behaviour of ice, therefore, is quite comparable to that of rocks, although the stress fields necessary to produce similar behaviour are very different. The failure behaviour of this whole class of visco-elastic to brittle materials, furthermore, is consistent with what is now known concerning the inhomogeneous nature of materials, and crack initiation and propagation.

4. SPECIMEN PREPARATION AND EXPERIMENTAL PROCEDURES

The observations on the failure process in ice were made in the cold room of the Snow and Ice Section of the Division of Building Research, National Research Council, Ottawa. This room has all the facilities necessary for preparing ice, machining specimens and carrying out the load tests. The temperature of the room can be varied over the range 0 to -50°C, and maintained constant at any temperature within this range to within ±0.1C degrees.

4.1 Preparation of the Ice

The ice used in the experiments was made from water taken directly from the Ottawa distribution system. No attempt was made to remove impurities except to deaerate using an aspirator. This allowed ice over six inches thick to be formed before visible air bubbles began to appear in it.

The ice was made in either a cylindrical or rectangular tank, each of which was lined on the inside with plastic. The cylindrical tank was 65 cm in diameter and 60 cm deep; the rectangular one 60 x 90 cm and 25 cm deep. Freezing of the water was usually carried out with the temperature of the room at -10°C. The average rate of growth was about 0.1 cm/hr, and the temperature gradient in the ice decreased progressively from about 1/3°C/mm to about 1/10°C/mm.

Pressure due to expansion of the water on freezing was prevented by two methods. For one, an air filled rubber tube was submerged in the water. The air was kept at a constant pressure as the water froze by allowing it to be expelled from a tube kept at a fixed depth in an antifreeze solution. For the second method, a hole was kept open at the edge of the tank with a small heater.

The water was cooled until ice began to form on its surface. This ice was removed and freezing reinitiated by covering the surface with finely crushed ice. As a result, the crystallographic orientation at the surface varied randomly from grain to grain. A preferred orientation soon developed, however, because of the greater ease with which growth occurs perpendicular to the <0001> direction than parallel to it. Observation of 100 grains about 5 cm below the surface showed that 40% had their <0001> direction between 85° and 90° to the direction of growth; 29% between 75° and 85° and the remainder between 60° and 75°. The ice that formed was columnar-grained with random <0001> direction in the plane perpendicular to the direction of growth (i.e. type S2). A typical thin section cut parallel to the long direction of the grains and viewed with polarized light, is shown in the upper part of figure 6c.

The grain size gradually increased in the direction of growth. About 5 cm below the surface it was about 0.25 cm in

the plane perpendicular to the long direction of the columns, as determined by the linear intercept method (ASTM 1966); at 15 cm it was about 0.35 cm.

4.2 Preparation of the Specimens

The specimens used in the crack study were rectangular in shape, 5 x 10 cm in section and 25 cm long. They were cut so that the long direction of the columns was perpendicular to the 10 x 25 cm face. After removing the ice from the tank in which it was formed, the specimens were cut roughly to size with a band saw. At least 4 cm of the upper surface of the block was discarded so that the specimen did not include the initial random layer.

A special milling machine was developed for bringing the specimens to their final dimensions. The milling was done with a 7.5 cm diameter, 15 cm long spiral cutter of the type used for machining aluminium, in combination with a 20 cm diameter, 5 mm thick cutter. One face and one edge of each specimen were milled at the same time with this arrangement. The ends were machined with an end mill mounted in a lathe. Finished specimens were stored in kerosene to prevent sublimation in the dry atmosphere of the cold room. They were annealed at the test temperature for at least twenty-four hours prior to the application of the load.

4.3 Conduct of Experiments

were applied to the 5 x 10 cm ends of the specimens in a modified consolidometer manufactured by the Wykenham Farrance Co. This instrument, shown in figure 10 with a specimen in place, was of the lever type with a lever arm ratio of 20:1. It was modified by increasing the height of the lever support so that it could accept specimens 25 cm in length. The base upon which the specimens were placed was supported from the lever arm by two 1.8 cm diameter rods. This base was constrained to move vertically by a rod that was fixed to its bottom and which slid in a cilite bushing placed in the base of the consolidometer.

The load was applied to the specimens through steel plates, 1.25 cm thick, with surfaces ground to a mirror finish. Steel strips 3 mm thick were attached about the edge of the loading plates so as to provide an inner area just large enough to accept the end of the specimen. The purpose of the strips was to prevent the ice from sliding laterally, but it was found during tests that there was no tendency for this sliding to occur.

Strain was measured with an extensometer mounted onto collars clamped and frozen to the ice. The extensometer mounted on a specimen is shown in figure 11. The strain was transformed

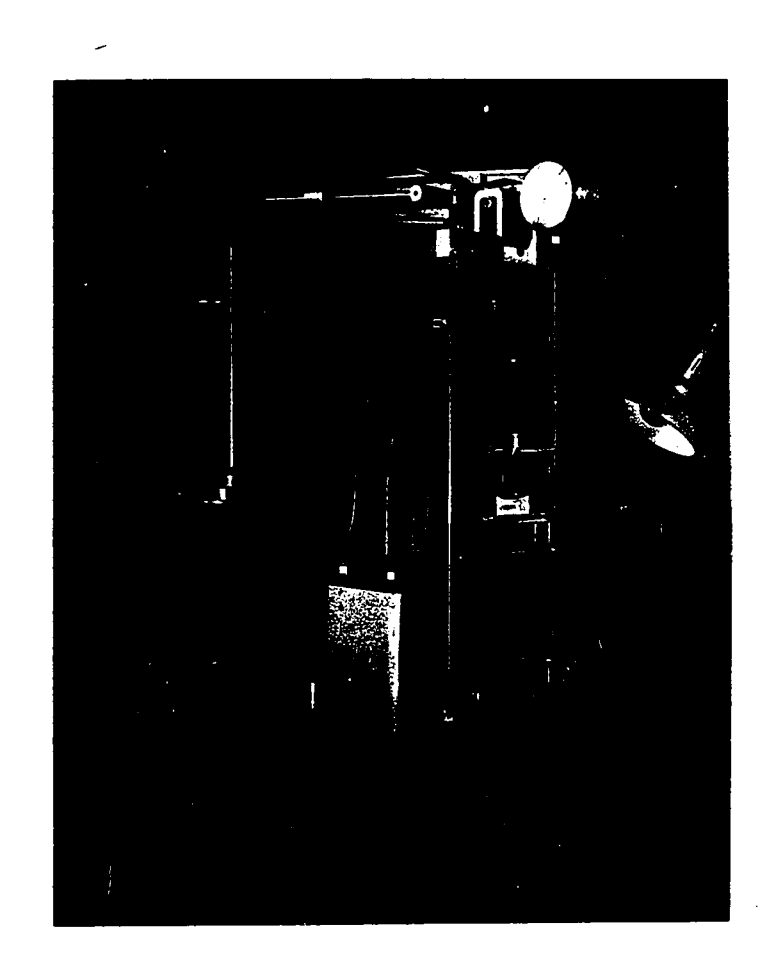


Figure 10

Loading frame with specimen and extensometer.

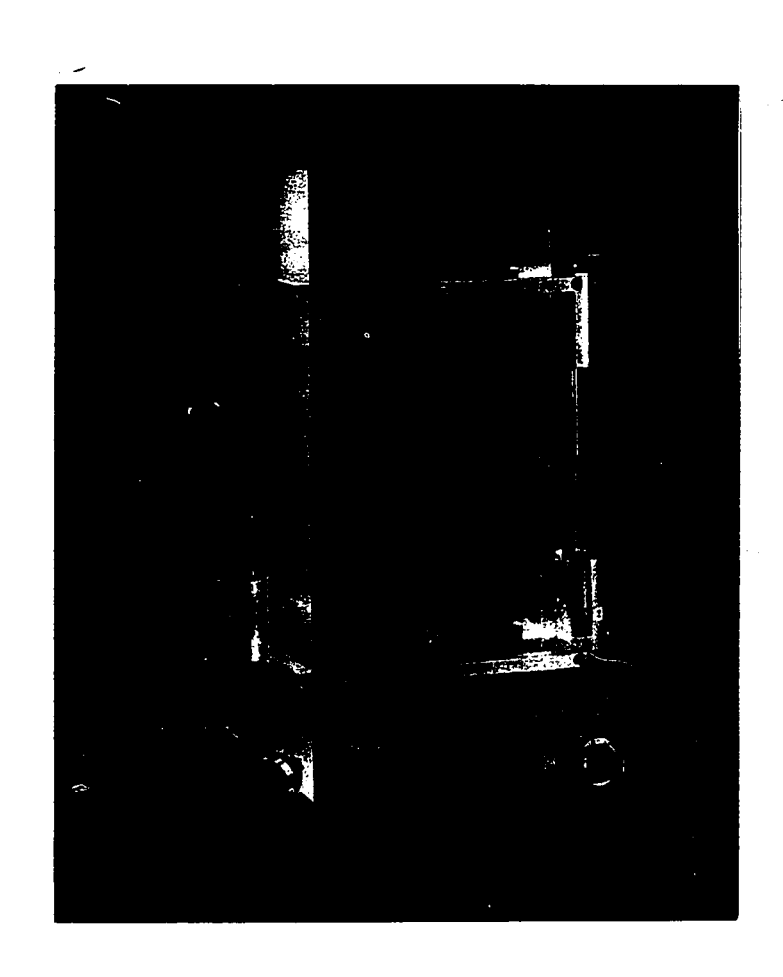


Figure 11
Extensometer mounted on a specimen.

into a voltage by the two linear differential transformers mounted so as to be at the centre of the two edges of the specimen. The extensometer was attached to the collars by four pivot screws that allowed rotation about axes in the centre plane of the specimen and perpendicular to its sides. With this arrangement the extensometer was relatively insensitive to any bending of the specimen that might occur during a creep test. It could measure displacements smaller than 10^{-4} cm.

The collars attached to the ice had knife edges that were clamped to the face of the specimen. A special rig was used to ensure that the collars were located correctly on the specimen so as to give an initial gauge length of 15 cm. After clamping in position, a small amount of water was placed with an eye dropper along the knife edges to freeze them to the specimen. This technique of measuring strains proved to be very satisfactory, and had an accuracy of better than 10^{-5} cm/cm.

After the collars were attached, a sheet of polyvinyl film (Saran wrap) was wrapped around the ice to prevent sublimation during a test. Saran wrap was found to be very suitable for this purpose because it tended to cling to the ice. The extensometer was then attached to the collars, the loading heads put in place and the specimen placed onto the supporting base of the loading frame. A ball and cone arrangement was placed

on top, and adjustments made so that the lever arm was in the proper position for beginning a test.

The weights used for applying the load were supported on a jack (see figure 10). The jack could be lowered so that the full load was applied to the specimen within a period of 2 seconds.

The lever system was calibrated using a Baldwin SR-4 load cell. This cell had been checked earlier on a Tinius Olsen Type U-CELOTRONIC testing machine, calibrated about every two years by the Tinius Olsen Co. The extensometers were calibrated with a TEN FIFTY CHECKMASTER manufactured by British Indicators Ltd.

Strains were recorded during the first part of the program on a Leeds and Northrup type G millivolt strip chart recorder. They were recorded on a Hewlett Packard 2010H data acquisition system in the latter part. The initial part of the load was still recorded on a strip chart recorder at this time because the most rapid rate of scanning of the logger was only 2 points per second.

The occurrence of cracks was observed visually. Cracks were readily seen when they formed in ice by using suitable lighting. The technique was to count the number of cracks that formed during given time intervals. The interval depended

upon the load and the stage of the test. For large stresses the time interval was usually one minute. For intermediate and small stresses longer intervals were used, and the location of counted cracks noted on the Saran wrap with a marking pencil. Each experiment yielded for a given load and temperature the time dependence of the strain and cracking activity. Six tests were conducted for each load condition, except for those at -31.0°C. In this case only four tests were carried out for each condition.

As described in Section 2.4.5, the cracks that formed were long and narrow, with their long direction in the long direction of the columns. Crack formation appeared to be uniform during the first part of the test for each condition of loading, except within about 4 cm of the ends of the specimen. Here, the constraints imposed by the loading plates caused a triangular section immediately adjacent to them to be almost free of cracks. The cracks were counted, therefore, only within the 15 cm gauge length.

Grain size was determined from thin sections cut from each face of the specimen, usually after the completion of a test. The sections were frozen to a glass plate and reduced in thickness to about 1 mm on a smooth brass surface kept at a temperature of about 4°C. They were then photographed with polarized light. The grain size was determined from the

photographs using the linear intercept method.

Observations were carried out at the average temperatures, \overline{T} , of -4.8°C, -9.5°C, -14.8°C and -31.0°C. The temperature of each test was within ± 0.3 C degrees of the associated average value.

5. TIME TO FORMATION OF FIRST CRACKS

For many solids, the time to failure in tension for a given temperature appears to have an exponential or power law dependence on the stress. These relationships are often found to provide a satisfactory fit to observations over several orders of magnitude of time. Considerable attention has been given to this behaviour in the Russian literature (e.g. Zhurkov and Sanfirova, 1958; Pines and Sirenko, 1959). Much of this work is reviewed by Bartenev and Zuyev (1968).

It was also observed that failure in tension often had the characteristics of a thermally activated process. For example, Zhurkov and Sanfirova assumed

$$t_f = t_o \exp \left(\frac{Q_f - \alpha\sigma}{kT}\right) = A(T) \exp \left(-B_{\alpha}\sigma\right)$$
 (24)

where t_0 , A and α are constants, and Q_f is the apparent activation energy for crack formation. The value of t_0 has been found to be approximately equal to the period associated with the natural frequency of vibration of atoms.

It was found in the present study that the time to formation of the first "large" crack (> 1 mm wide, 1 cm long) was a well defined event. Although the cracks formed during compression, their formation indicated that local tensile stresses

tending to be perpendicular to the applied stress, must have been induced. The time to formation of each of the first three large cracks was recorded for each test to determine if they were related in a meaningful way to stress and temperature. Preliminary results of this study for temperatures of -10.0°C and -31.0°C have been reported (Gold, 1967). Observations at average temperatures of -4.8°C, -14.8°C and -9.5°C have also been made and are presented herein.

5.1 Observations

The average logarithms of the time to formation, t_f , of the second large crack for $\overline{T} = -4.8^{\circ}C$, $-9.5^{\circ}C$, $-14.8^{\circ}C$ and -31.0°C are plotted against stress in figure 12. It can be seen that the logarithm of t_f appears to be almost linearly dependent on the stress, σ , for $\sigma \ge 8 \text{ kg/cm}^2$. The average time to formation deviates significantly from this dependence for $\sigma = 6 \text{ kg/cm}^2$. In some cases at $\overline{T} = -9.5^{\circ}\text{C}$ and $\sigma = 6 \text{ kg/cm}^2$, no second large crack formed in the time of the test, which was continued well beyond the time that would have been expected by linear extrapolation of the results for $\sigma \geqslant 8 \text{ kg/cm}^2$. total time of the test was used in these cases, and so the actual average value for $\sigma = 6 \text{ kg/cm}^2$ and $\overline{T} = -9.5^{\circ}\text{C}$ should be plotted at a larger time than is shown in figure 12. A deviation from the linear dependence has been observed for other materials (see Bartenev and Zuyev, p. 44), and is to be expected.

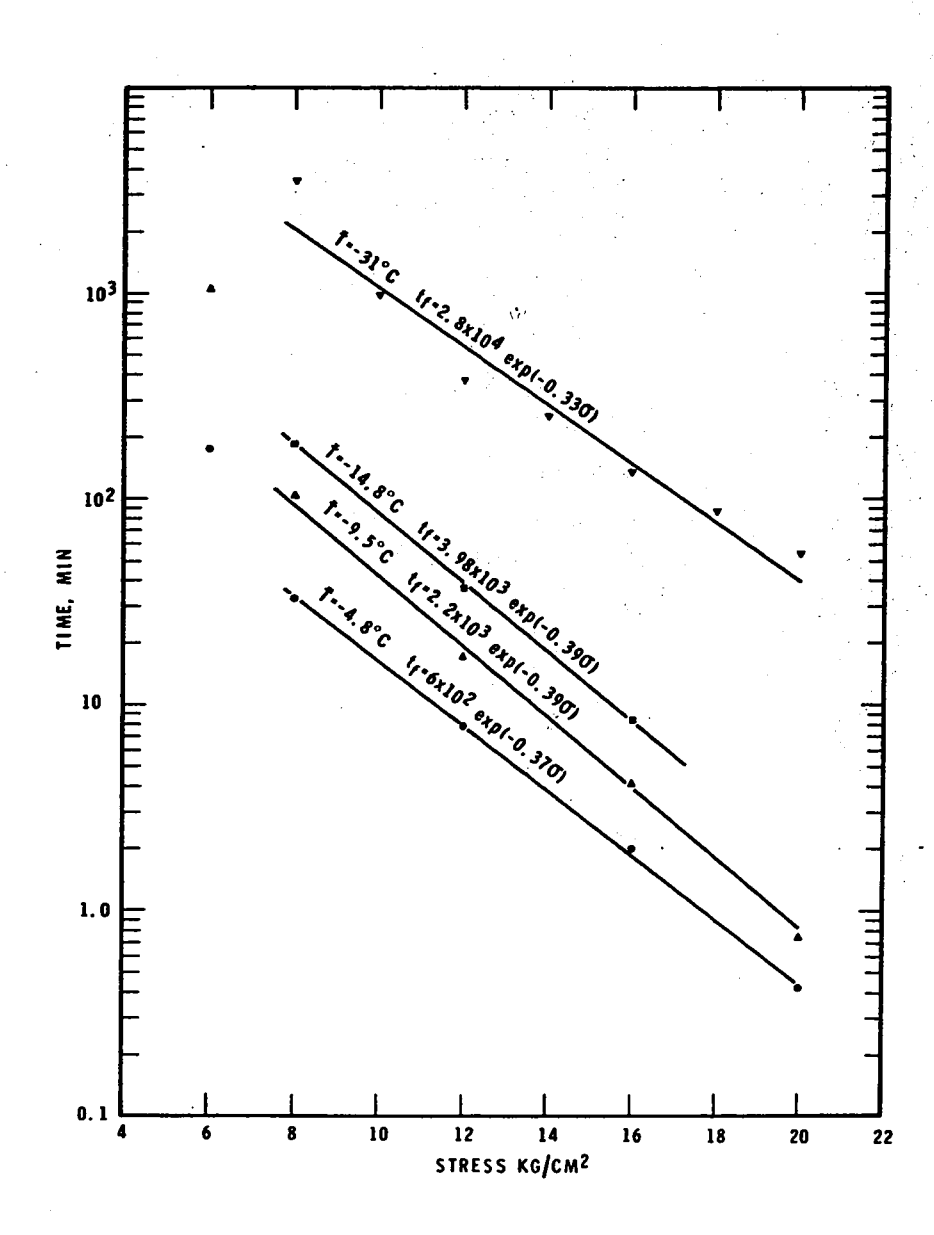


FIGURE 12 STRESS DEPENDENCE OF THE AVERAGE OF THE LOGARITHM OF THE TIME TO FORMATION OF SECOND LARGE CRACK

The observations for $\overline{T}=-31^{\circ}C$ appear to deviate significantly from a linear relationship. The results do not allow one to decide if this reflects the real behaviour, or the lack of sufficient number of observations.

Least squares fits were calculated for the observations in figure 12 for $\sigma \geqslant 8 \text{ kg/cm}^2$, and are shown along with their equations. The stress coefficient in equation (24), B_{α} , was found to be about 0.38 cm²/kg.

The time to formation of the first and third large crack had the same general dependence on the stress as for the second. It was considered that the average of the times to formation of the first three large cracks would yield a better correlation with stress, and this is shown in figure 13 along with the least squares fits for $\sigma \geqslant 8 \text{ kg/cm}^2$.

Values of A(T) obtained from the least squares fits given in figures 12 and 13 are plotted against $^1/_{\rm T}$ °K $^{-1}$ in figure 14. If equation (24) is valid, the results in figure 14 show that the apparent activation energy, ${\rm Q_f}$, decreases with decreasing temperature, and tends to a constant value for temperature lower than about -15°C

$$A(T) = t_0 \exp \left(\frac{Q_f}{kT}\right)$$
 (25)

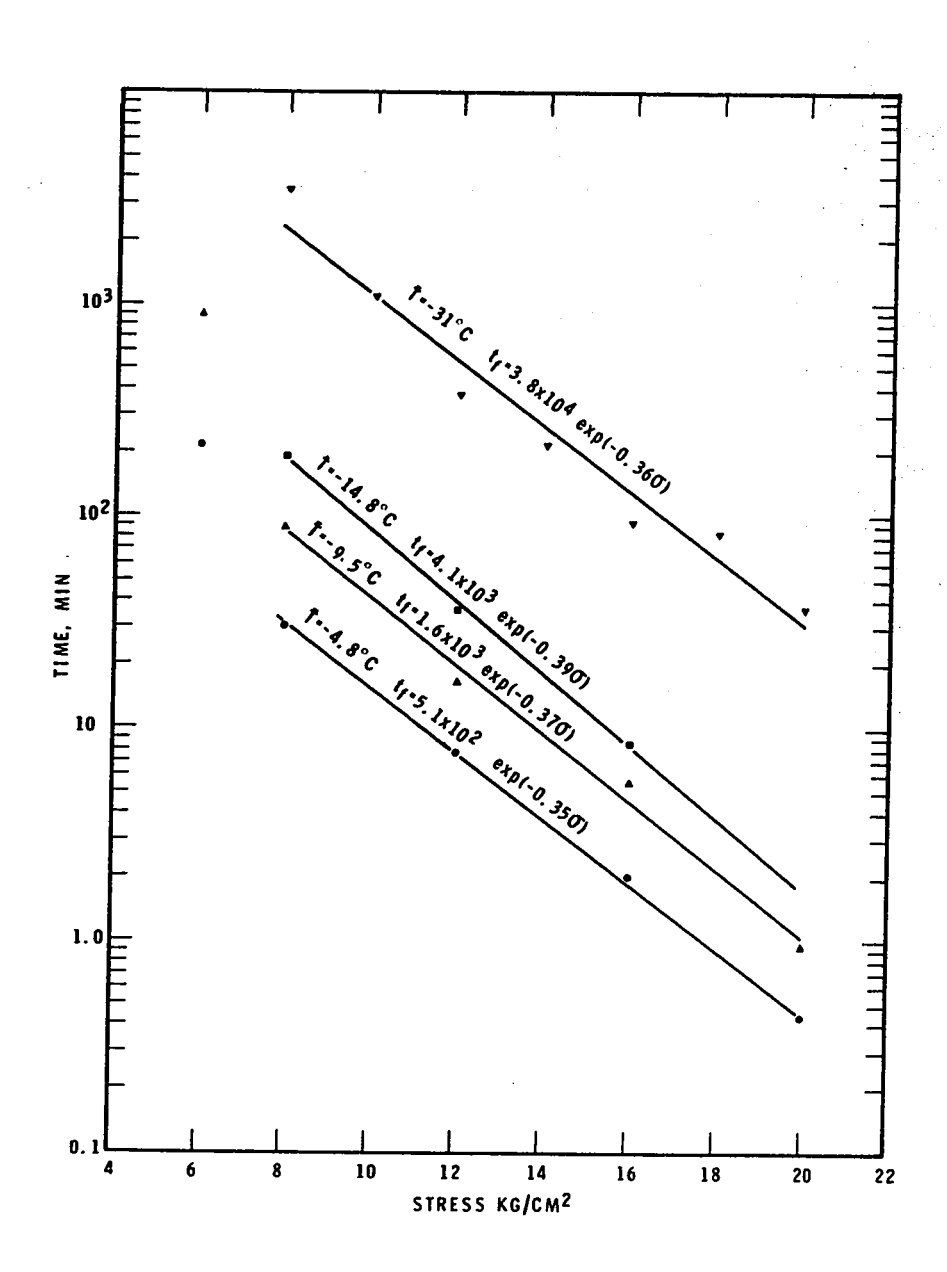


FIGURE 13
STRESS DEPENDENCE OF THE AVERAGE OF THE LOGARITHM OF THE TIMES TO FORMATION OF THE FIRST THREE LARGE CRACKS

The value of the apparent activation energy calculated from the results for the second large crack and temperature less than -15°C was 0.65 eV. Figure 14 shows that the apparent activation energy for the average of the first three large cracks tends to approach this value at lower temperatures.

5.2 <u>viscussion</u>

It is of interest to establish if the time to formation of the first large crack is consistent with crack nucleation by stress concentrations of the type associated with dislocation pile-ups. Let it be assumed that the criterion for nucleation is (Smith and Barnby, 1967, see Table V)

$$\tau_{e} \geqslant \left[\frac{\pi \gamma E}{4(1-v^{2})\ell}\right]^{\frac{1}{2}} \tag{26}$$

where tensor is the effective shear stress on a pile-up of length ℓ , and the remaining terms are as defined earlier (see p. 70).

Representative values of $\frac{E}{1-v^2}$ and the surface energy, γ , are:

$$\frac{E}{1-v^2} = 8.2 \times 10^{10} \frac{\text{dynes}}{\text{cm}^2}$$
 (Gold, 1958)

$$\gamma = 100 \text{ ergs/cm}^2$$
 (Hesstvedt, 1964).

Let the length of the pile-up, ℓ , for the minimum stress to cause crack initiation, be equal to the average grain diameter, d (0.30 cm). Substitution of these values into equation (26)

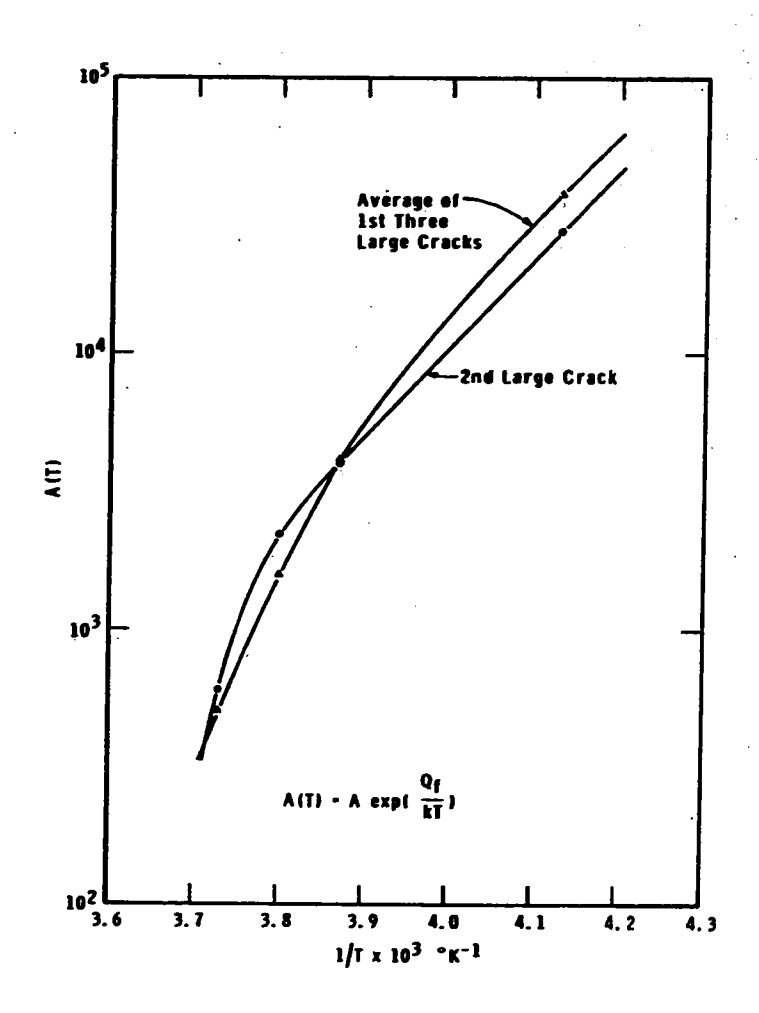


FIGURE 14
TEMPERATURE DEPENDENCE OF TIME TO FORMATION OF FIRST CRACKS

gives $\tau_e = 4.7 \text{ kg/cm}^2$ (4.6 x 10⁶ dynes/cm²). This estimate is in good agreement with the conditions associated with crack formation (i.e. applied compressive stress greater than about 6 kg/cm²).

Smith and Barnby give for the number of dislocations in the pile-up (see Table V)

$$n = \frac{\pi^2 \gamma}{2\tau_e b} \tag{27}$$

where b is the Burgers vector. Substitution into equation (27) of the value of τ_e obtained from equation (26), and b = 4.5 x 10^{-8} cm, gives n = 2,380. If it is assumed that the pile-up has the form shown in figure 15, this number of dislocations would give a displacement of nb = 1.07 x 10^{-4} cm. This would correspond to a strain of about 3.5 x 10^{-4} in the part of the grain to the right of the glide plane.

The average strain to the formation of the first crack for given temperature and stress is plotted in figure 16. It can be seen that, for applied stresses about equal to 6 kg/cm², this strain is considerably larger than 3.5×10^{-4} .

Equation (26) shows that as the effective shear stress on the pile-up increases, the length of the pile-up required for crack initiation decreases. Let the situation depicted in figure 15 represent one of the more extreme crack nucleating

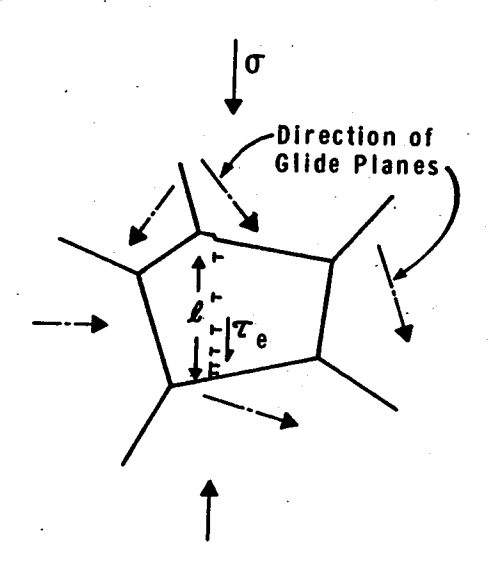


FIGURE 15 SIMPLE MODEL OF CRACK NUCLEATION BY A DISLOCATION PILE-UP IN A COLUMNAR-GRAIN OF SIZE d

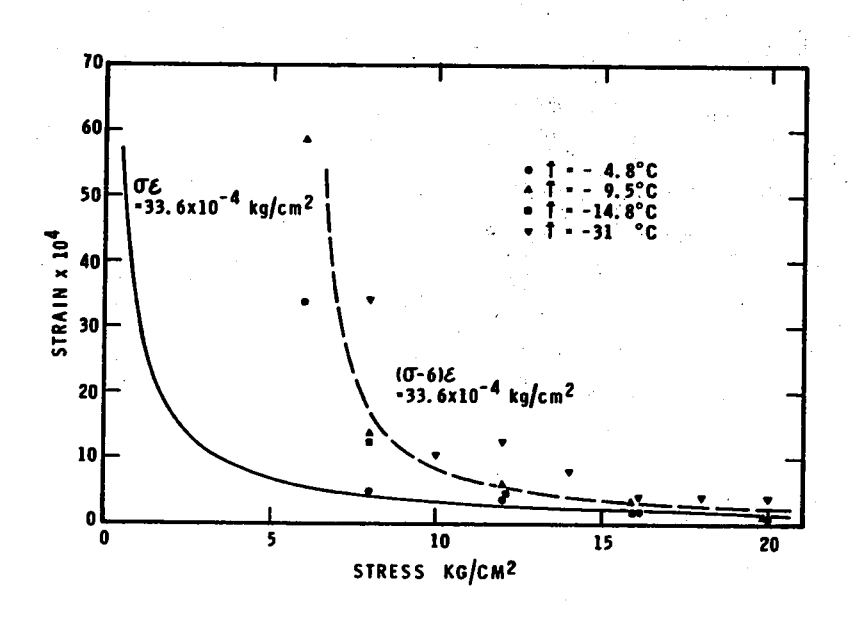


FIGURE 16
AVERAGE STRAIN TO THE FORMATION OF THE FIRST CRACK

conditions. Assume that the strain on the right hand side of the pile-up is £d, and on the left hand side is zero. The number of dislocations in the pile-up, therefore, is

$$n = \frac{\varepsilon d}{b} \tag{28}$$

The substitution of the expression for n given by equation (11) (i.e. $n = \frac{\pi(1-v)}{Gb} \tau_e \ell$) into equation (28) gives

$${}^{\tau}e^{\frac{\ell 2\pi(1-v^2)}{Eb}} = \frac{\varepsilon d}{b}$$

and the length of the pile-up associated with the effective shear stress $\boldsymbol{\tau}_{e}$ after strain ϵ is

$$\ell = \frac{\varepsilon d E}{\tau_e 2\pi (1 - v^2)}$$
 (29)

Substitution of this value for ℓ into equation (26) gives

$$\tau_{e} \varepsilon = \frac{\pi^{2} \gamma}{2d} \tag{30}$$

Equation (30) indicates that at the nucleating site the product of the effective shear stress and the strain to the formation of the first crack should be a constant. Let τ_e be equal to $\sigma/2$, where σ is the applied stress. Substitution of $\gamma=100$ ergs/cm² and d=0.30 cm in equation (30) gives

$$\sigma \varepsilon \simeq 3,300 \text{ dynes/cm}^2 = 33.6 \times 10^{-4} \text{ kg/cm}^2$$
 (31)

Equation (31) is plotted in figure 16. It can be seen that the plotted curve underestimates the strain to the formation of the first crack for stresses less than about 16 kg/cm 2 .

It was pointed out in Section 2.4.5 that new modes of deformation were observed to develop and operate in previously undeformed columnar-grained ice in the strain range of 0.01 to 0.25%. Figure 16 shows that the strain to the formation of the first cracks lies in this range. This suggests that the deviation of the observations from the theoretical prediction is due to the development and operation of these modes (e.g. multiple slip and climb of dislocations out of their glide plane).

As climb would involve diffusion, its effect would become more significant for given temperature the longer it takes to deform the specimen to the strain necessary for crack initiation. This is consistent with the results shown in figure 16, where it can be seen that, in general, the longer the time taken for the formation of the first crack, the greater is the deviation from equation (31). The observations show that when the stress is less than about 6 kg/cm^2 , the operating modes of deformation are sufficient to prevent the occurrence of the conditions necessary for crack formation (e.g. equation 30).

If the formation of the first cleavage crack is dependent on the strain for stress greater than about 6 kg/cm², it should be possible to fit the observations with a polynomial in $(\sigma$ -6). The expression

$$(\sigma-6)\varepsilon = 33.6 \times 10^{-4} \text{ kg/cm}^2$$

is plotted in figure 16, and it can be seen to provide a good fit to the observations.

Even if it is proven that crack initiation is associated with dislocation pile-ups, the stress condition at the site of the crack will still be a matter of considerable speculation. In addition to the stress associated with the initiating pile-up, there can be stresses due to neighboring pile-ups and incompatibility of strains of adjacent grains. The formation of voids during compressive creep indicates that these stresses can be tensile over a significant area perpendicular to the applied stress.

According to the Griffith criterion, a crack nucleus in ice must be about 0.5 cm wide to propagate under a uniform tensile stress of 6 kg/cm². The cracks formed for compressive stress of 6 kg/cm² had widths considerably smaller than 0.5 cm. This indicates that the stresses responsible for them must have been local in character (i.e. they are not Griffith cracks, but probably involve stress fields in addition to that associated with the initiating pile-up as discussed in the previous paragraph).

Let it be assumed that a crack of width 2c is formed by the running together of n freely slipping edge dislocations. Bullough (1964) has shown that if the contribution of the shear stress, τ_e , and of the transverse tensile stress, are neglected, the width of the dislocation crack is given by

$$2c = \frac{E \quad n^2 b^2}{16\pi (1-v^2)\gamma}$$
 (32)

If nb = 1.07 x 10⁻⁴ cm, $\frac{E}{1-v^2}$ = 8.2 x 10¹⁰ dynes/cm² and γ = 100 ergs/cm², then equation (32) gives 2c = 0.187 cm. This is in good agreement with size of the first "large" crack (i.e. \simeq 1 mm). The contribution of a shear stress and any transverse tensile stress would increase the crack width.

The foregoing discussion has shown that the formation of the first large cracks was consistent with models of crack initiation by dislocation pile-ups. It was pointed out in Section 3.2 that criteria for crack nucleation based on dislocation theory do not involve the crack width. The question can be asked, therefore, if crack initiation was a thermally activated process in the sense that the crack nucleus grew to a critical size by the breaking of molecular bonds by thermal fluctuations.

Figure 16 shows that for stresses greater than 10 $\rm kg/cm^2$, the strain to the formation of the first crack was equal to

 5×10^{-4} to within a factor of about 2. The time to formation of the first crack, therefore, can be expressed approximately by

$$t_{f} = \frac{\varepsilon}{\frac{\varepsilon}{\epsilon}} = \frac{5 \times 10^{-4}}{\frac{\varepsilon}{\epsilon}}$$
 (33)

where $\vec{\xi}$ was the average strain rate during the first 5 x 10^{-4} strain. It will be seen from the information presented in Section 6 that this average strain rate was about equal to the strain rate at a strain of 2.5×10^{-4} . This indicates that the temperature and stress dependence of the time to formation of the first cracks was due mainly to the exponential dependence of the strain rate on these quantities. conclusion is supported by the approximate equality of the apparent activation energy for crack formation and for creep of polycrystalline ice (see Table IV). It is of interest, also, that Krausz (1970) found from strain relaxation experiments that the activation volume for ice should be between 0.4 x 10^{-20} cm³ and 9 x 10^{-20} cm³. The value obtained for α in equation (24) from the observations on the time to formation of the first cracks, was about 1.4 x 10^{-20} cm³. These arguments indicate that the observed crack formation in ice was not a thermally activated process in the sense assumed by Zurkov and Sanfirova with respect to equation (24), but the dominant role played by the strain rate made it appear to be so.

5.3 Conclusions

Crack formation occurred in type S2 ice during creep under a uniaxial compressive stress when the stress exceeded about 6 kg/cm². The first cracks formed at a strain less than about 10^{-3} for stress equal to or greater than 10 kg/cm^2 , and their time to formation depended exponentially on the stress. The time to formation of the first cracks also appeared to depend exponentially on $^{1}/_{\text{T}}$, but the apparent activation energy decreased with decreasing temperature, tending to a constant value for temperature less than about 258°K (-15°C). The apparent exponential dependence of time to formation on stress and temperature is considered to be due to the dependence of the strain rate on these quantities.

The formation of the first large cracks (> 0.1 cm wide) was consistent with dislocation models of initiation. Most of the energy required for their formation must have come from stress fields close to the site of the crack. The observations indicated that the behaviour deviated from that predicted by simple dislocation models, and the deviation became more significant the lower the stress and the temperature. It is considered that this deviation was due to the contribution of other modes of deformation, including the climb of dislocations out of their glide plane.

6. CRACKING ACTIVITY DURING CREEP

Little information is available on the stress and strain dependence of the number of cracks that form during the deformation of materials subject to cleavage crack formation. Hahn et al (1959) observed the strain dependence of the crack density developed during the plastic deformation of steel.

McMahon (1964), Kaechele (1967) and Kaechele and Tetelman (1969) have made similar observations for polycrystalline iron. Williams (1968) presented information on the crack density developed during creep of an aluminium -20% zinc alloy.

These studies were carried out on granular materials.

Crack densities were determined from the surface trace of the crack, made visible by polishing and etching. This introduced the difficult problem of determining the three dimensional characteristics of the crack distribution from surface observations only. Kaechele (1967) presented a theoretical discussion of this problem. The situation for columnar-grained ice is considerably simpler. Not only does its transparency allow observations to be made in the interior, but the symmetry causes the cracking activity to be two dimensional rather than three.

6.1 Results of Observations on Crack Formation

The total number of cracks formed up to the time of each

count was determined for each test, and divided by the area of observation to obtain the crack density. A plot was made of crack density vs time, and a line drawn through the points. These plots were used to calculate the average crack density vs time for each stress and temperature condition. The observations and average curve for $\sigma = 12 \text{ kg/cm}^2$ and $\overline{T} = -9.5^{\circ}\text{C}$ are shown in figure 17 as an example. Average crack densities for $\overline{T} = -4.8^{\circ}\text{C}$, -9.5°C , -14.8°C and -31.0°C are presented in figures 18 (a,b,c,d) respectively.

The discussion concerning crack initiation and time to formation of the first cracks indicated that the cracking activity should be more directly related to strain than to time. Crack densities for each test, N (\$\epsilon\$, \$\sigma\$, \$\To\$), were plotted against creep strain. The average crack density for given strain was calculated for each condition from these curves, and these are presented in figures 19 (a,b,c,d). It can be seen that the initiation and development of the cracking activity occurs over the same range of strain for all stress and temperature conditions. The standard deviations presented with each curve show the extent to which the behaviour was reproducible for given conditions.

The average cracking rate (number of new cracks per cm² per unit strain) is plotted against the strain in figures 20 (a,b) for $\overline{T} = -9.5^{\circ}\text{C}$ and -31.0°C . These curves were obtained

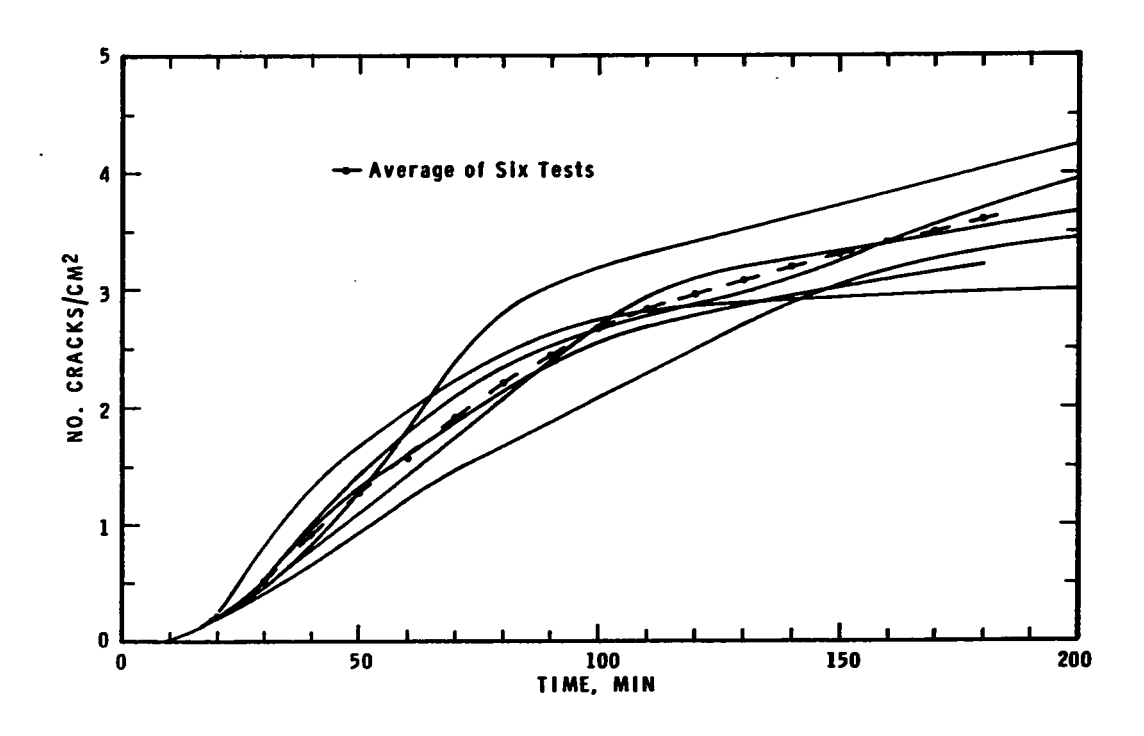


FIGURE 17 TIME DEPENDENCE OF THE CRACK DENSITY FOR σ = 12 Kg/cm² 2 2 = -9.5°C

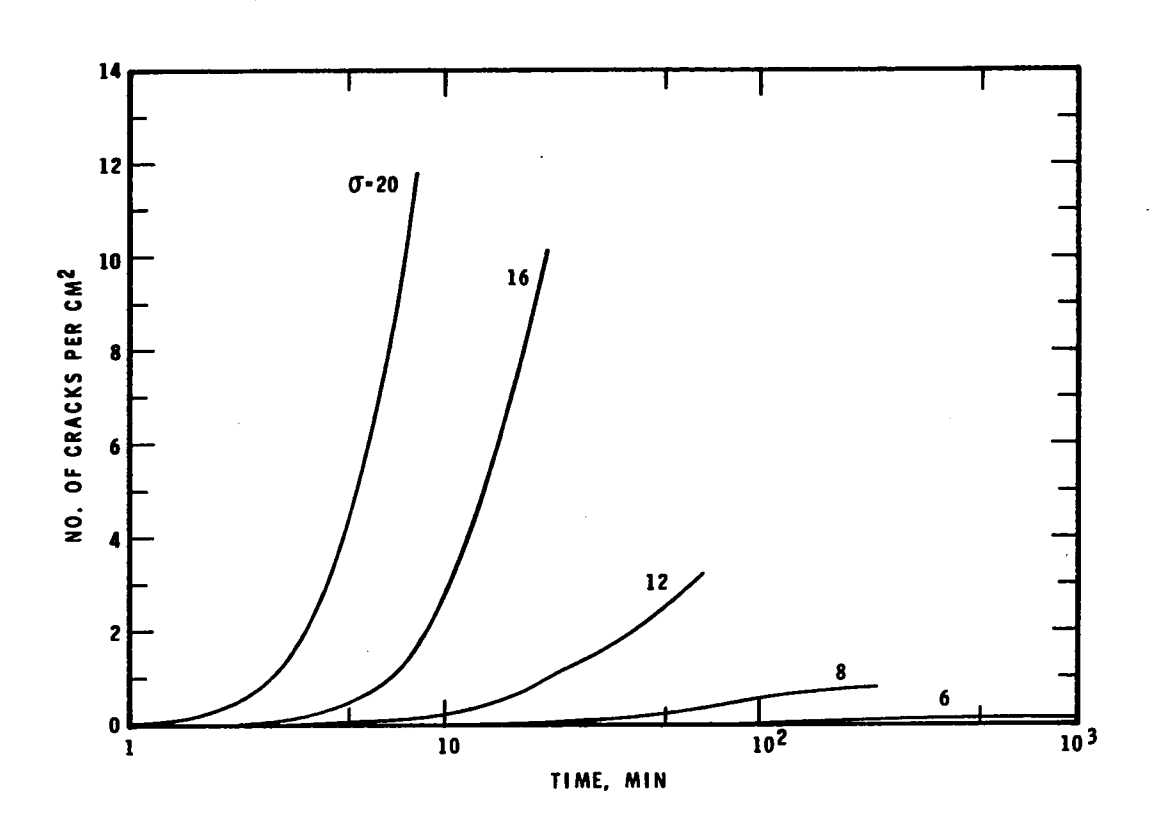


FIGURE 18a time dependence of crack density for compressive stress $\sigma \, \text{Kg/cm}^2$ t- -4.8°C

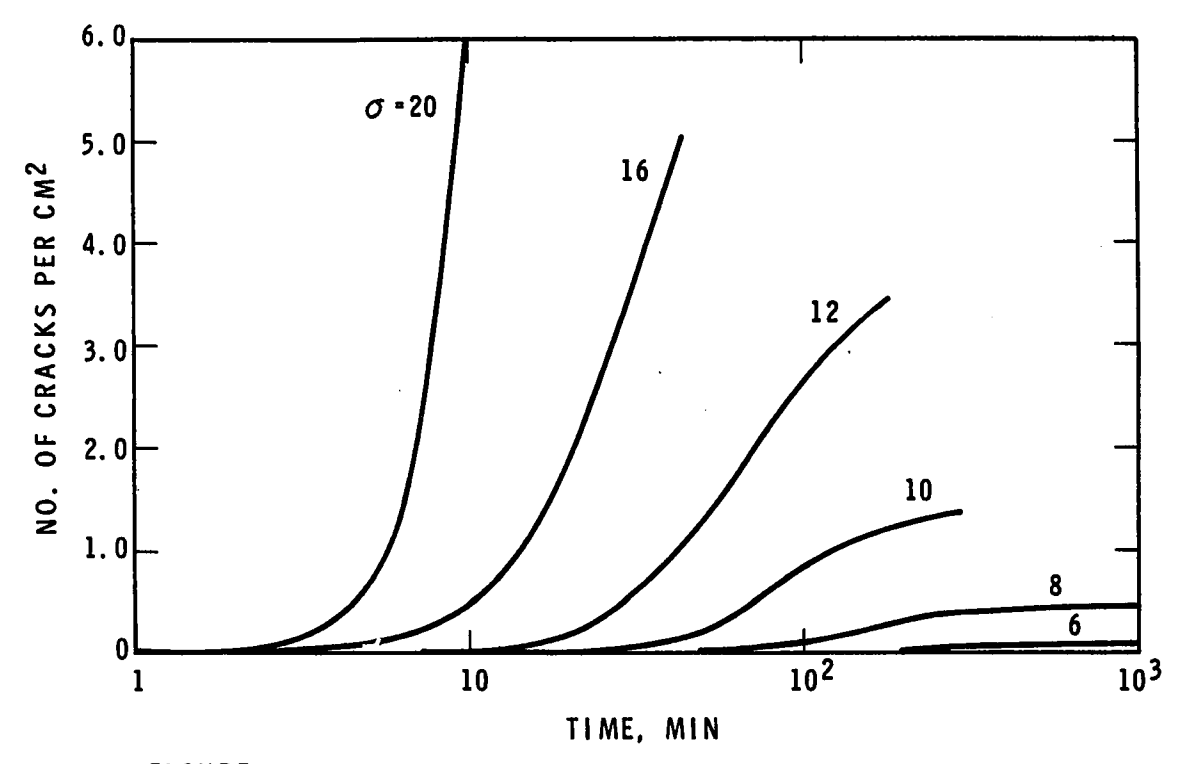


FIGURE 18b

TIME DEPENDENCE OF CRACK DENSITY FOR COMPRESSIVE STRESS σ KG/CM² \bar{T} = -9.5°C

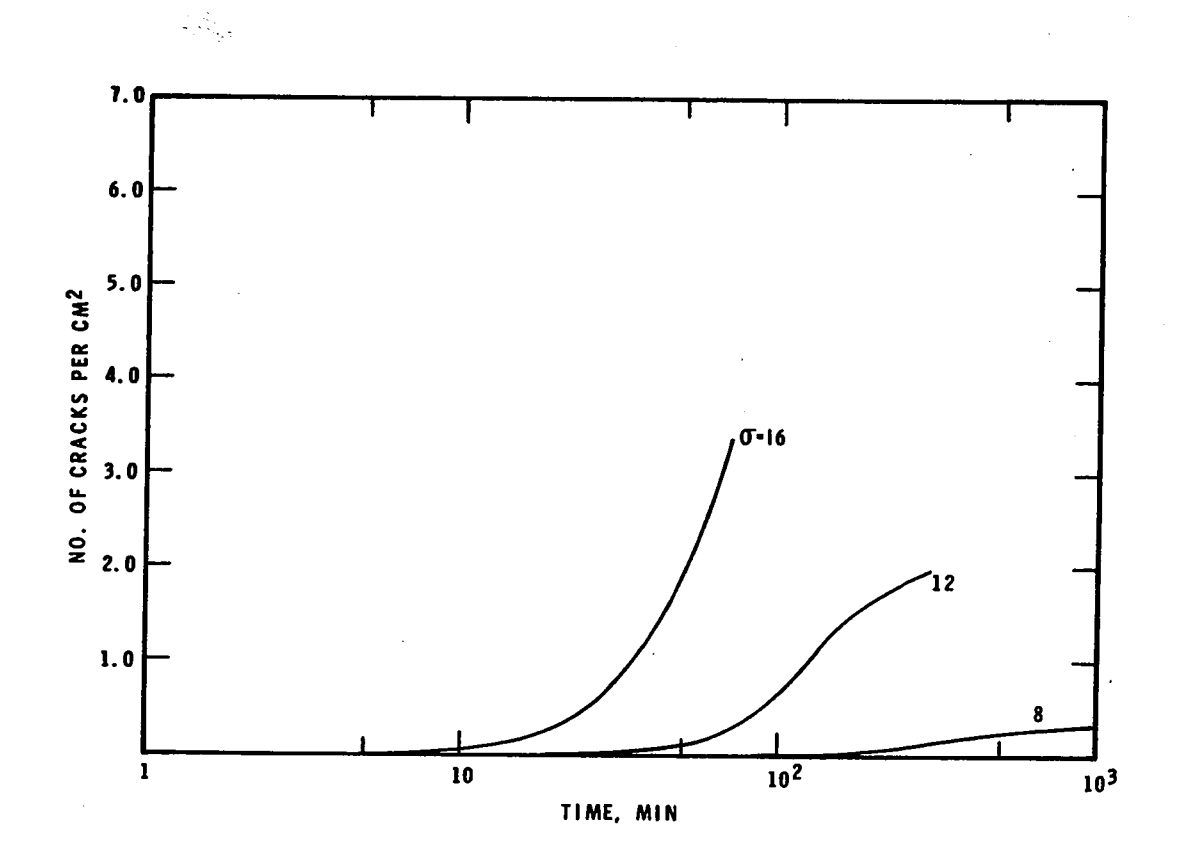


FIGURE 18c TIME DEPENDENCE OF CRACK DENSITY FOR COMPRESSIVE STRESS σ Kg/cm² 2 $^{-14.8^{\circ}C}$

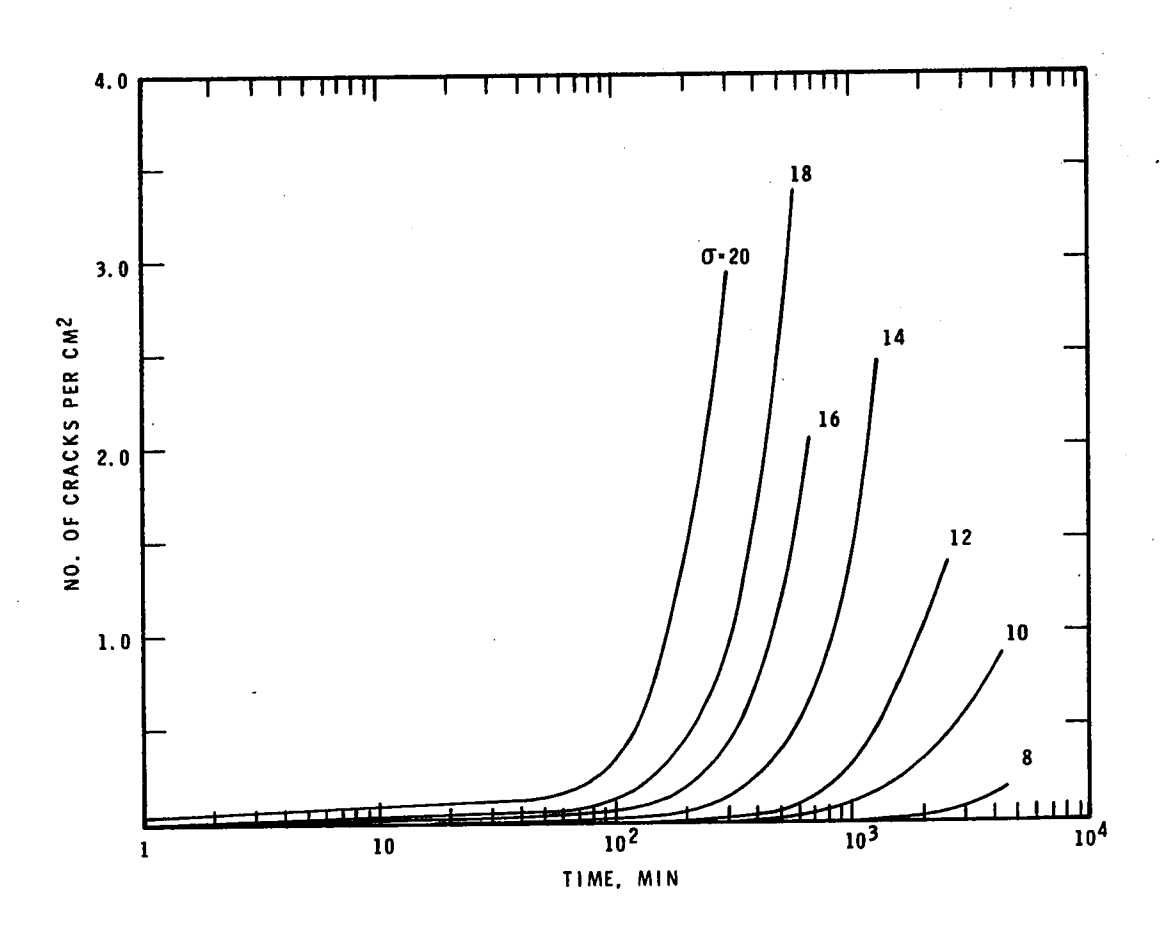


FIGURE 18d TIME DEPENDENCE OF CRACK DENSITY FOR COMPRESSIVE STRESS σ Kg/Cm² T- -31°C

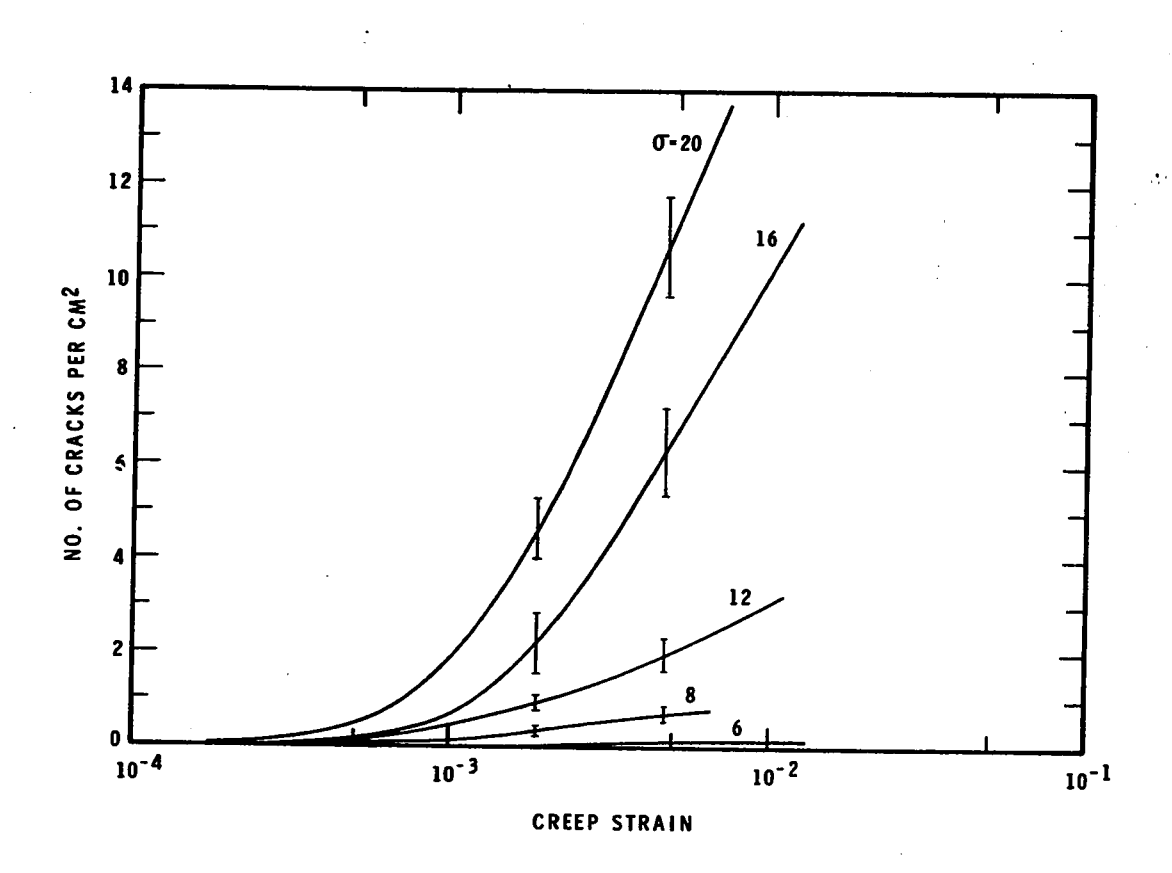


FIGURE 19a STRAIN DEPENDENCE OF CRACK DENSITY FOR COMPRESSIVE STRESS σ kg/cm² $\bar{\tau}$ --4.8°C. The Height of the vertical bars is twice the standard deviation in the observations

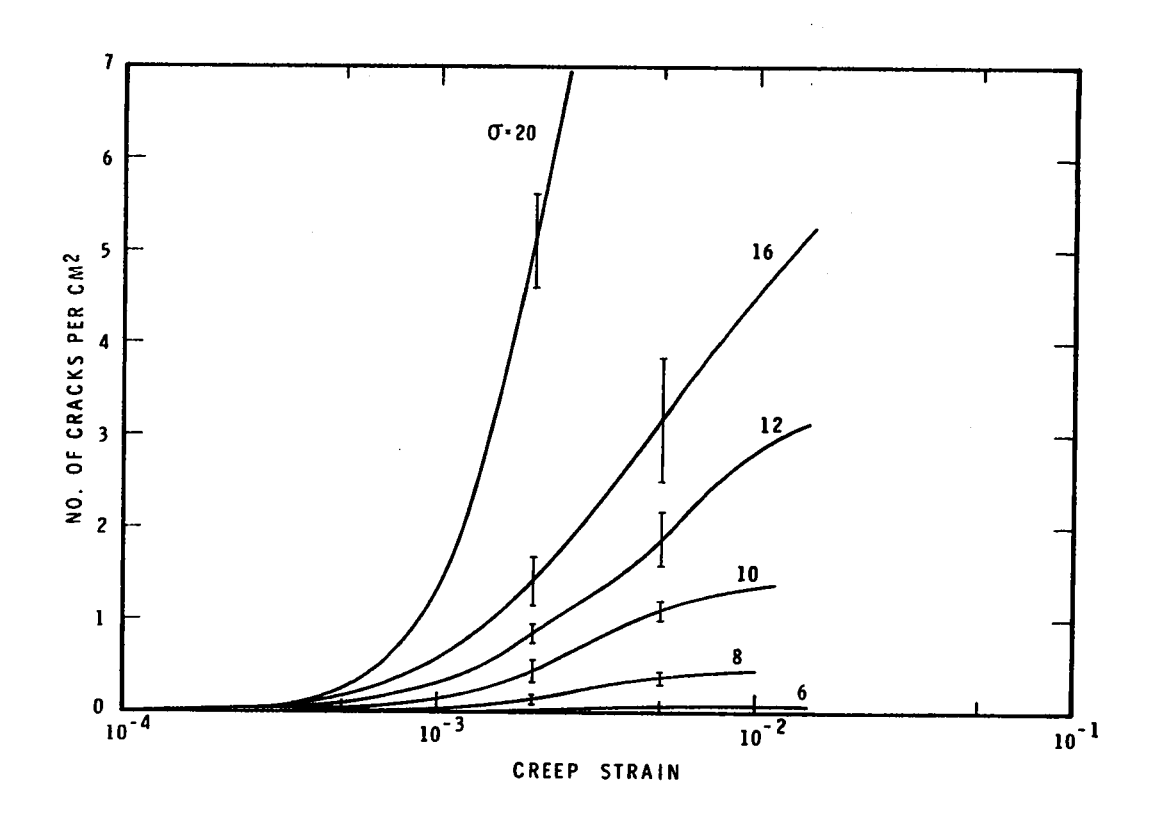


FIGURE 19b STRAIN DEPENDENCE OF CRACK DENSITY FOR COMPRESSIVE STRESS σ kg/cm² Tr -9.5"C. The height of the vertical bars is twice the standard deviation in the observations.

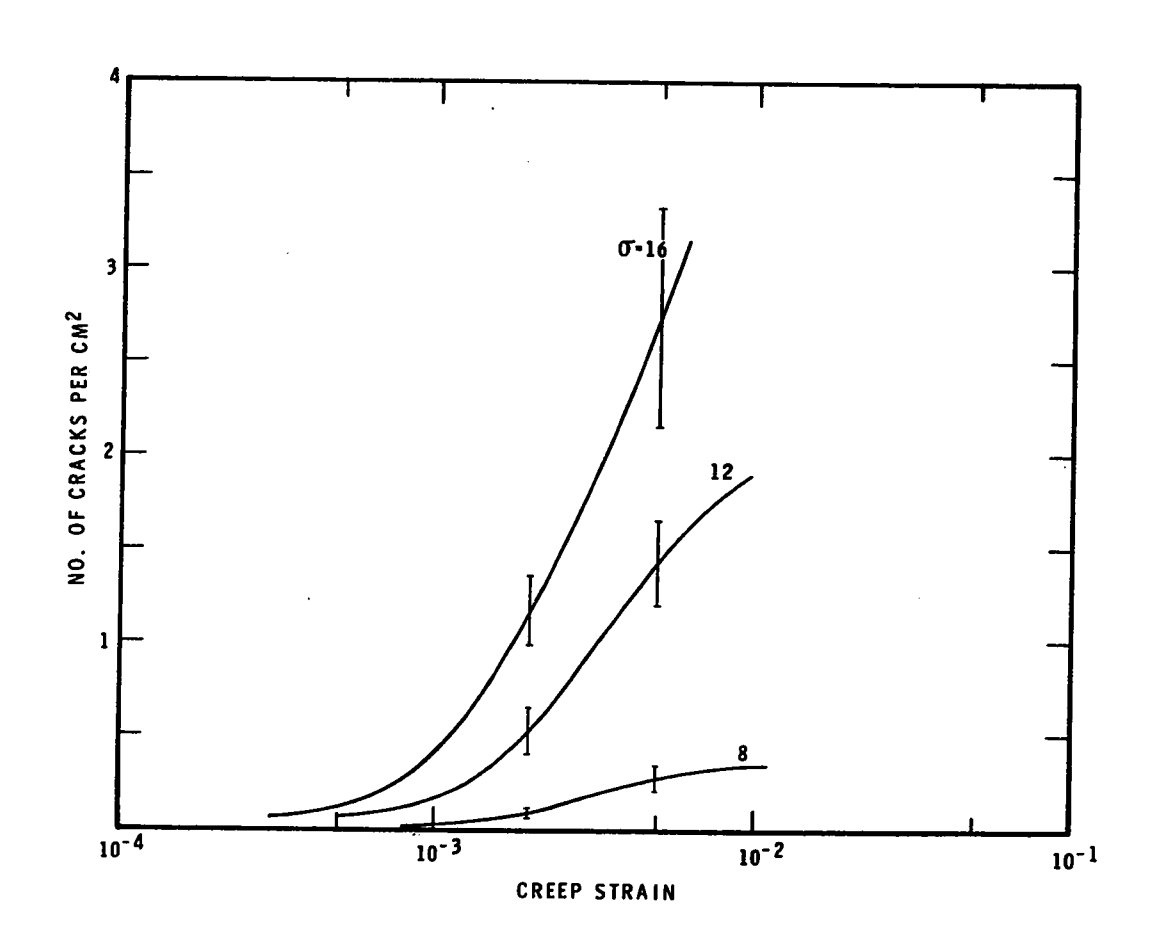


FIGURE 19c STRAIN DEPENDENCE OF CRACK DENSITY FOR COMPRESSIVE STRESS σ Kg/cm² $\bar{\tau}$ - -14.8°C. The Height of the vertical bars is twice the standard deviation in the observations.

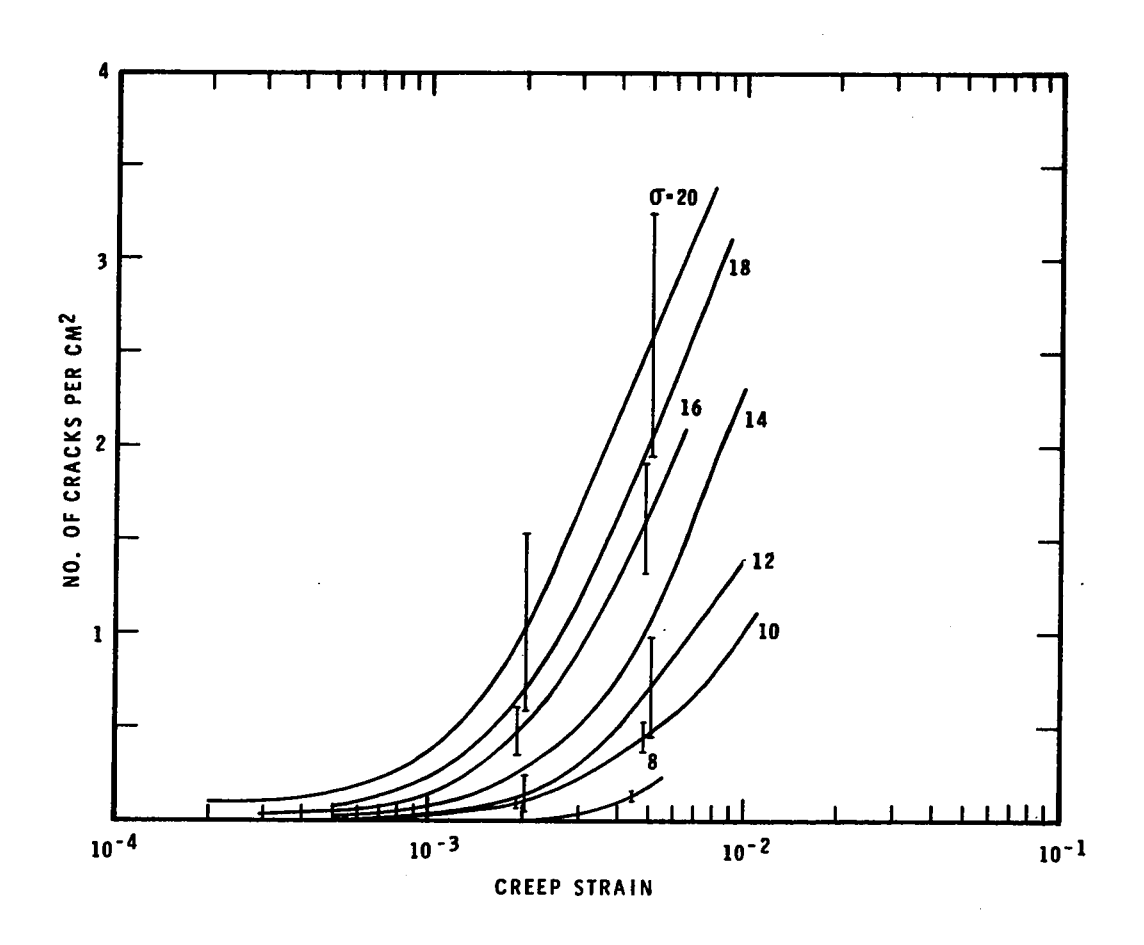


FIGURE 19d STRAIN DEPENDENCE OF CRACK DENSITY FOR COMPRESSIVE STRESS σ Kg/cm² $^{+}$ -31°C. The Height of the vertical bars is twice the standard deviation in the observations.

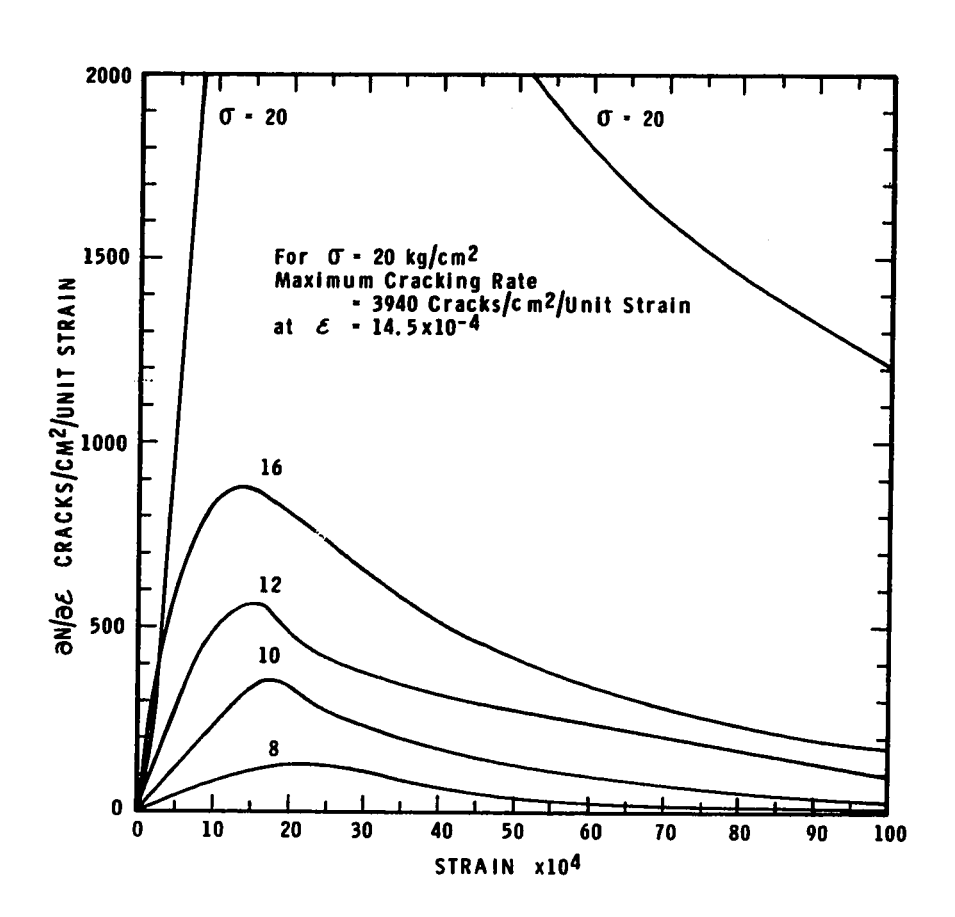


FIGURE 20a STRAIN DEPENDENCE OF CRACKING RATE FOR GIVEN STRESS OT, KG/CM2 \bar{T} = -9.5°C

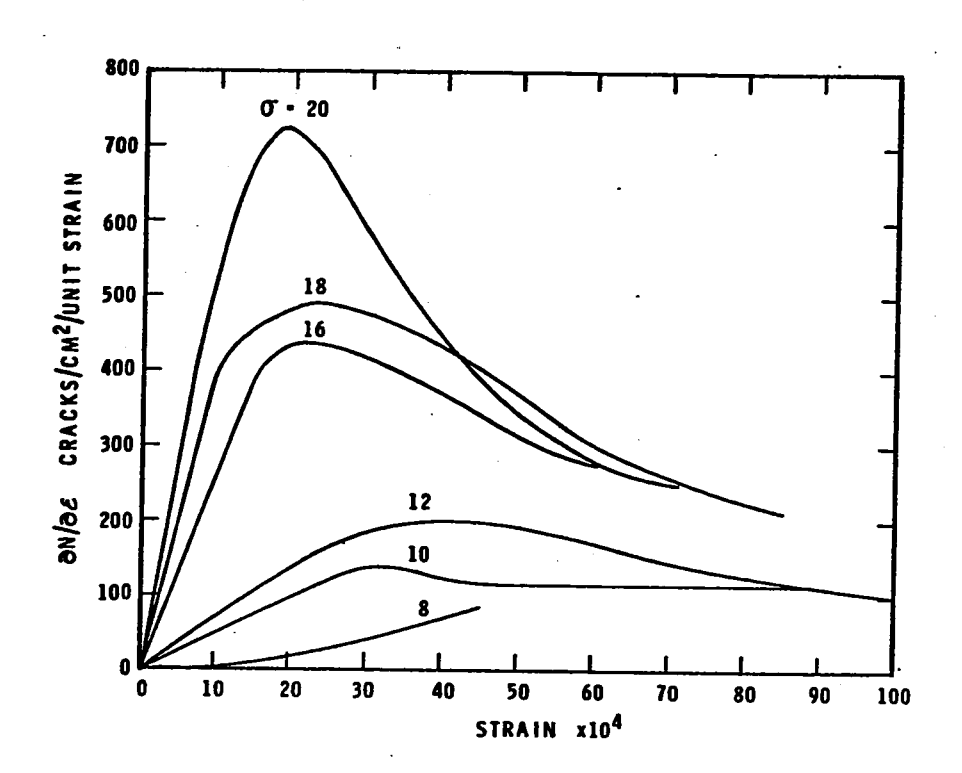


FIGURE 20b STRAIN DEPENDENCE OF CRACKING RATE FOR STRESS σ , Kg/cm² $^{-31}^{\circ}$ C

from the average crack density vs strain curves by determining the change in the density for change in strain of 5×10^{-4} , dividing the difference by the change in strain, and plotting the result at the midpoint of the range. A smooth curve was drawn through the plotted points. It can be seen that there is a maximum in the cracking rate within the creep strain range of 10×10^{-4} to 25×10^{-4} for $\overline{T} = -9.5^{\circ}\text{C}$.

The average cracking rate for each temperature is plotted against the strain in figures 21 (a,b,c) for stresses of 8, 12 and 16 kg/cm² respectively. These figures show that the maximum average cracking rate for each stress decreased with decreasing temperature. Figures 19 (a,b,c,d) show the same dependence for the average crack density. Figures 21 (a,b) indicate that for stresses of 8 and 12 kg/cm², there was a tendency for the maximum in the cracking rate to shift to larger strain with decreasing temperature. This tendency was not present for a stress of 16 kg/cm².

The results for $\overline{T}\geqslant -15^{\circ}C$ show that for stress less than about 10 kg/cm², the cracking rate tended to zero for strain larger than about 10^{-2} . This tendency was not so apparent for $\overline{T}=-31.0^{\circ}C$. It was appreciated after the completion of the testing that the characteristics of the cracking activity for $\overline{T}=-31.0^{\circ}C$, and $\sigma\leqslant 12$ kg/cm², appeared to be different from those for higher temperatures, (see figure 20b). The cracking

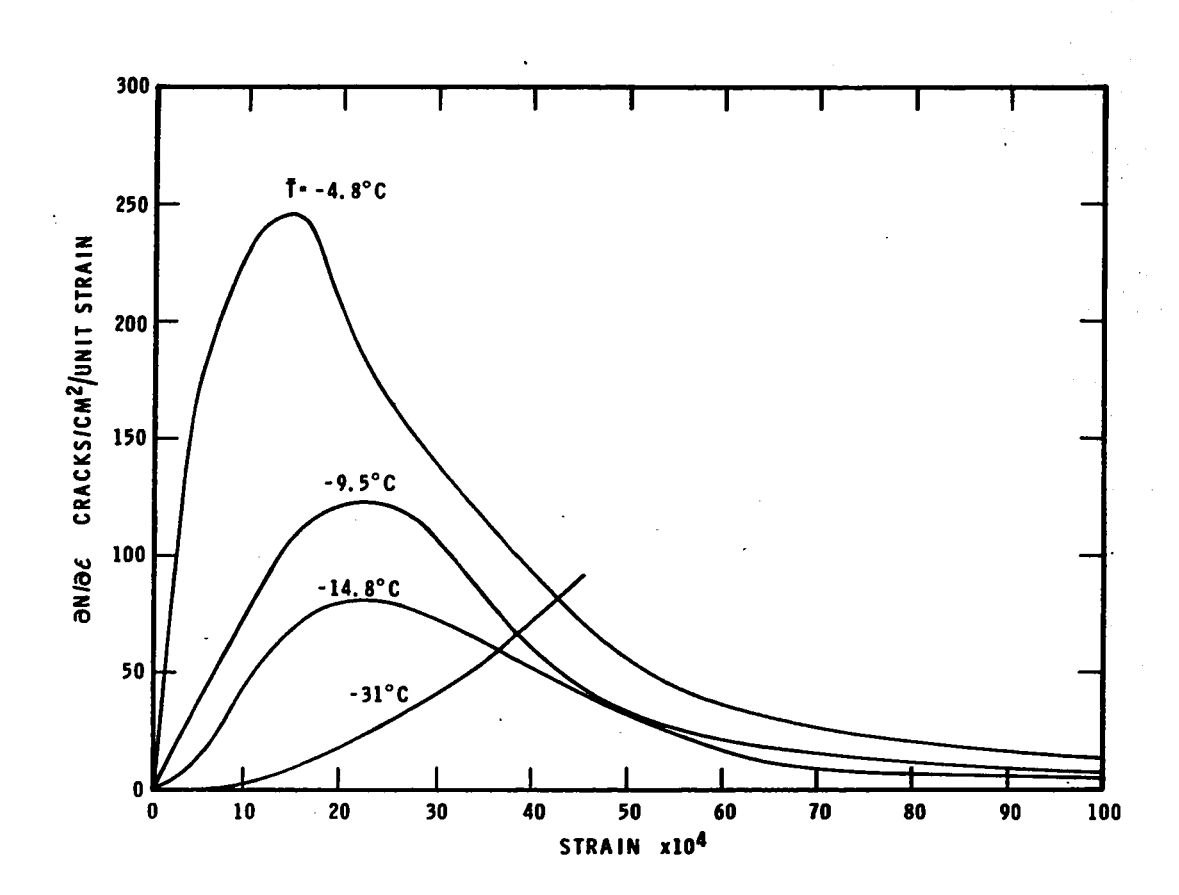


FIGURE 21a STRAIN DEPENDENCE OF THE AVERAGE RATE OF CRACK FORMATION $\partial N/\!\!\!/\partial \mathcal{E}$ $\sigma\text{-8}$ KG/C m^2

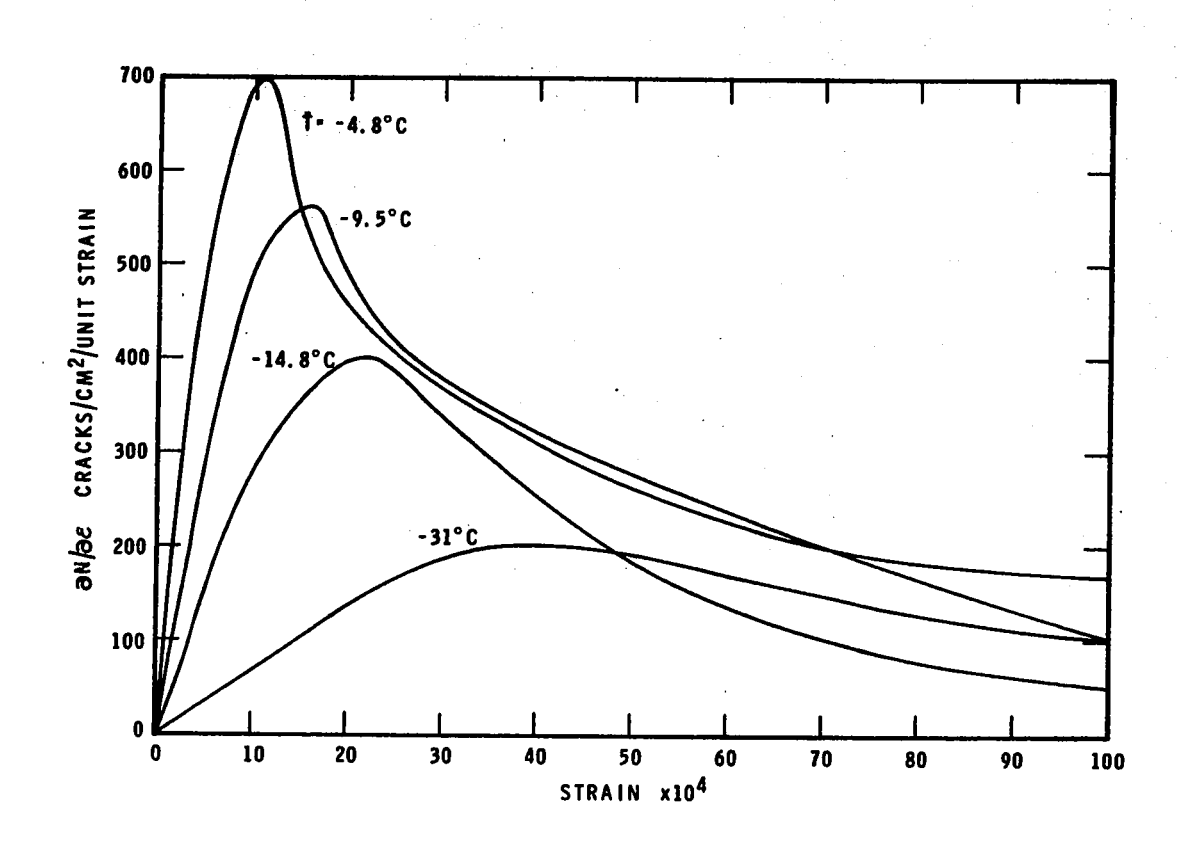


FIGURE 21b STRAIN DEPENDENCE OF THE AVERAGE RATE OF CRACK FORMATION $\frac{\partial N}{\partial \mathcal{E}}$ $\sigma\text{-12 kg/cm}^2$

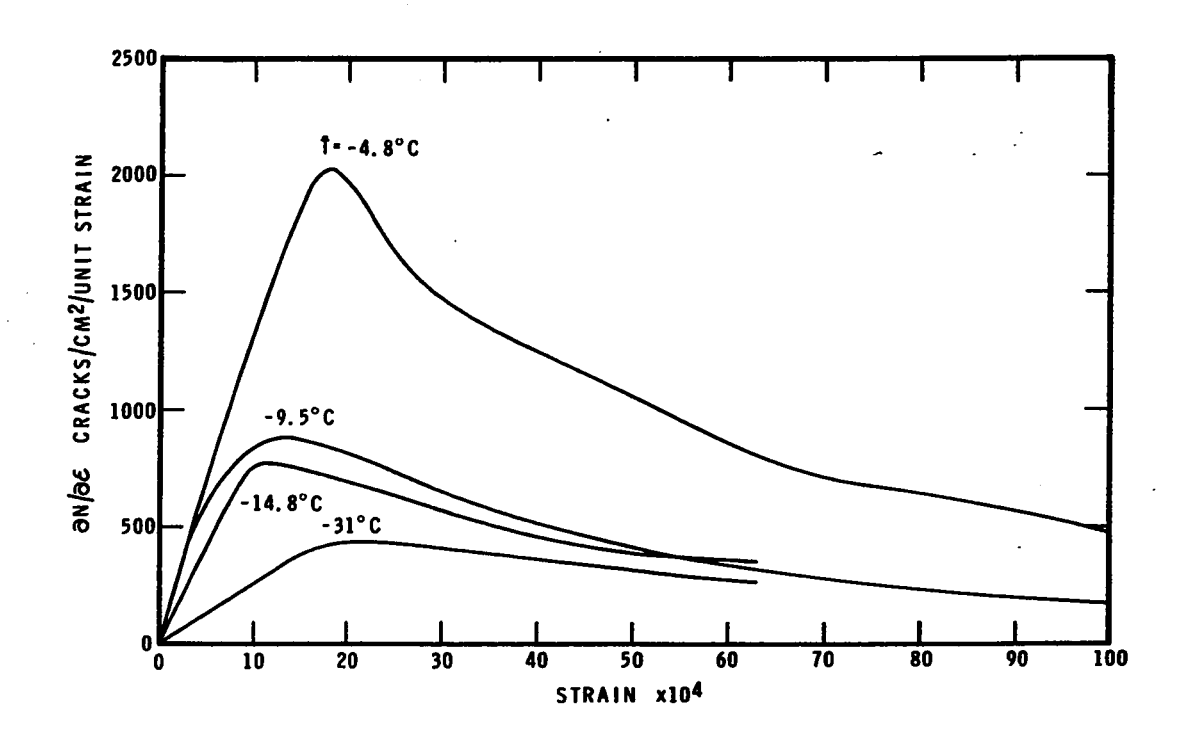


FIGURE 21c STRAIN DEPENDENCE OF THE AVERAGE RATE OF CRACK FORMATION, $\partial n/\!\!/\!\!/\partial \mathcal{E}$ σ = 16 kg/cm²

rate for $\overline{T}=-31.0^{\circ}\text{C}$ and $\sigma=8~\text{kg/cm}^2$, for example, was larger than would have been anticipated from the results at higher stress and temperature. This particular inconsistency may be due to the smallness in the number of cracks that formed for this test condition, and the corresponding decrease in statistical significance. Although each of these tests was run for about three and one half days, it can be seen from figures 19 (d) and 21 (a) that the cracking rate had not reached its maximum value. The cracking behaviour for $\overline{T}=-31.0^{\circ}\text{C}$ will be considered further in the discussion in Section 6.3.

For stress \geqslant 12 kg/cm² for all temperatures, it was clear from the nature of the cracking activity, and from the fact that the deformation progressed directly from the primary to the tertiary stage of creep, that the rate of cracking would have remained significant even if the deformation had been continued beyond a strain of 10^{-2} (see figures 19, a,b,c,d).

It should be pointed out that when the crack density exceeded about 3 per cm², it became increasingly difficult to record all cracking events. This was particularly the case for the larger loads. A true record of the cracking rate in a specimen containing many cracks was beyond the capability of visual methods. It is considered that the observations for densities less than 3 per cm² are a good record of the cracking activity. Observations at larger densities most certainly

underestimate the cracking activity, but do give a good qualitative picture of it.

The stress dependence of the average crack density for a strain of 20×10^{-4} is shown for the four test temperatures in figure 22. This figure confirms the conclusion drawn from the observations of the time to formation of the first cracks, that significant cracking activity does not occur until the compressive stress exceeds about 6 kg/cm². Figure 22 indicates also a tendency for the critical stress for crack formation to increase with decreasing temperature.

If it is assumed that the stress dependence of the crack density has the form

$$N = A(\sigma - C)^{n}$$
 (34)

where A, C and n are constants, then a log N vs log (σ -C) plot of the curves in figure 22 gives

$$n \approx 3.3$$
 for $C = 0$

$$n \simeq 1.7$$
 for $C = 6$.

These plots were reasonably linear over the whole range of stress to 20 kg/cm² for C = 6, and over the range $10 \le \sigma \le 20$ for C = 0. The foregoing indicates the degree to which the cracking activity depends upon the stress.

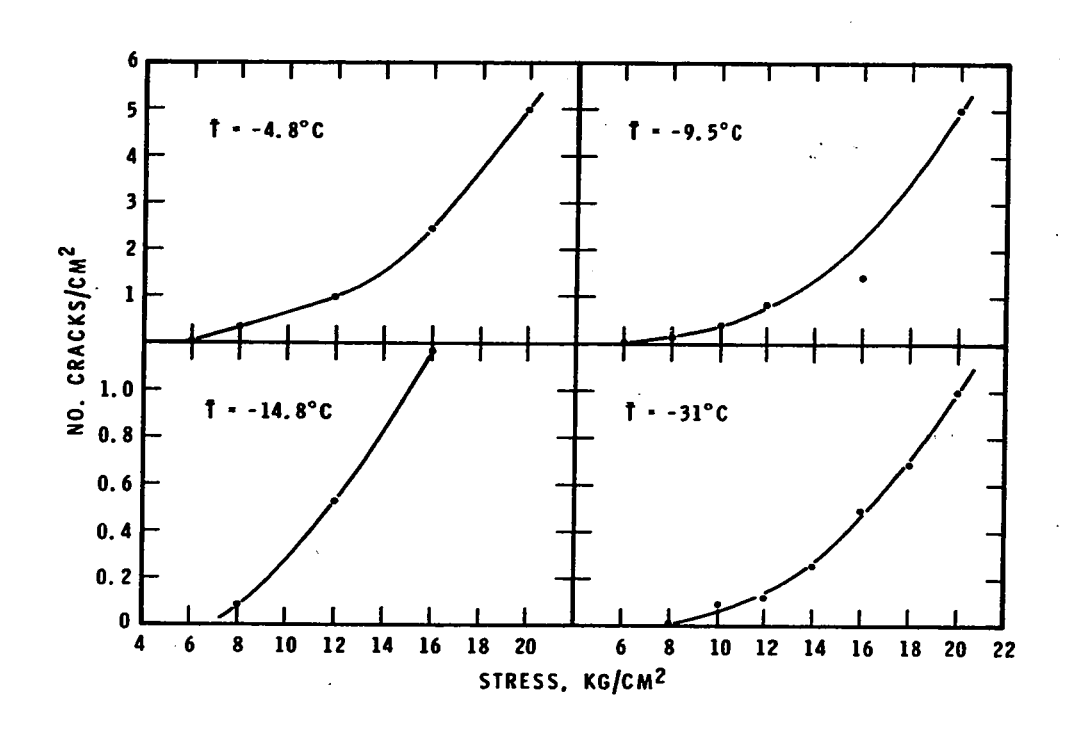


FIGURE 22 STRESS DEPENDENCE OF CRACK DENSITY AT STRAIN OF $20 \text{x} 10^{-4}$

Several tests were run at stresses less than 6 kg/cm² to determine if cracks would form. Cracks did form in some cases for stresses of 4 and 5 kg/cm², but these were few and small. They tended to heal with continued deformation, or collapse into several spherical voids. It is of interest, and of some significance, that the strain to formation of these cracks was about the same as that associated with the maximum cracking rate at higher stress (i.e. what would appear to be the most severe strain condition for crack formation).

The temperature dependence of the average crack density at various strains is presented in figure 23 for stresses of 8, 12, 16 and 20 kg/cm². This figure shows clearly the marked decrease in the crack density with decreasing temperature. The results for $\sigma = 8$ kg/cm² are particularly interesting because they indicate that the crack density at this stress tends to a limiting value with further decrease in temperature. Maximum values for the average crack density for this stress and $\overline{T} = -4.8$ °C, -9.5°C and -14.8°C were estimated from figure 19 by simple extension of the curves to a strain of about 2×10^{-2} , and are also plotted in figure 23.

If the stress was sufficiently high, cracks would form in the ice as the load was applied. These cracks were usually small and associated with the grain boundaries. There was

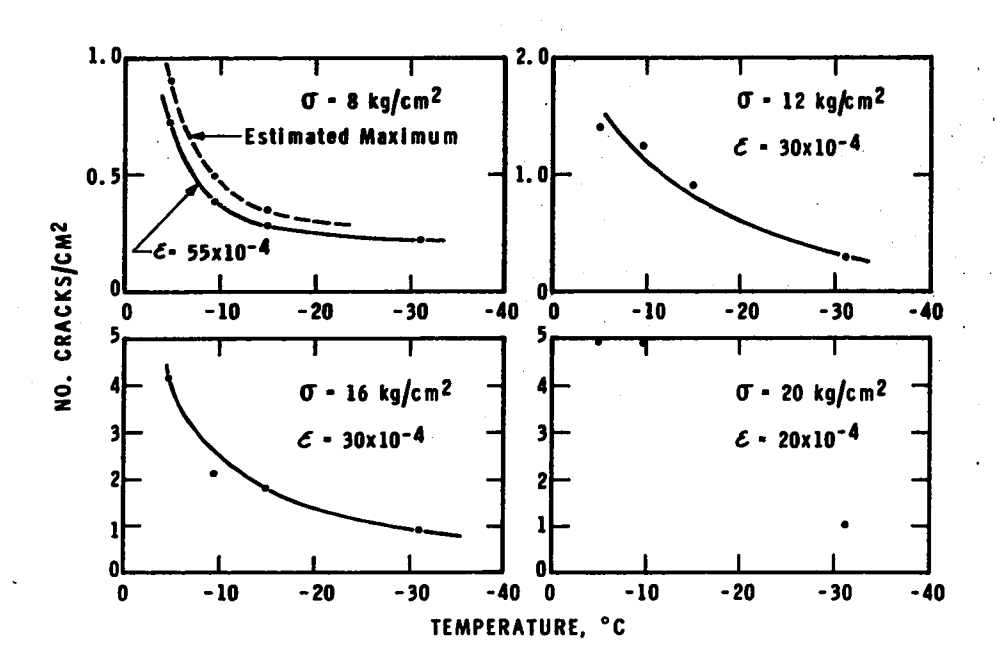


FIGURE 23
TEMPERATURE DEPENDENCE OF CRACK DENSITY FOR GIVEN STRESS AND STRAIN

always a quiescent period following their formation and prior to the cracking activity that has been described. The stress dependence of this initial crack density is shown in figure 24. It can be seen that with decreasing temperature, the initial crack density decreases and the stress required to cause these cracks to appear, increases.

The cracks formed on the application of the load were subtracted from the total crack count when calculating the crack densities shown in figures 18 and 19. It will be shown in Section 7.4 that this initial cracking activity may be an integral part of the subsequent activity. Subtraction of it, however, did not affect the calculation of the average rates of cracking, and resulted in a downward displacement of the curves in figures 18 and 19 of less than 5% of the maximum observed density for stresses \$ 16 kg/cm².

6.2 Creep Behaviour

The average creep curve for each set of conditions was obtained by calculating the arithmetic mean of the associated tests. In all cases, the initial elastic strain was subtracted from the recorded strain. The average creep rates were calculated from the creep curves by determining the change in strain over appropriate consecutive changes in time. These creep rates were plotted against the strain corresponding to the time at the midpoint of the time interval. A smooth line was

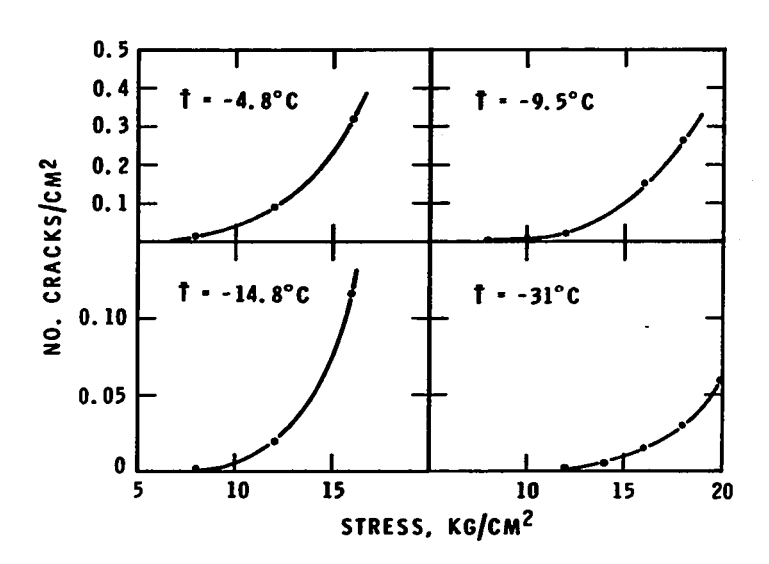


FIGURE 24
STRESS DEPENDENCE OF INITIAL CRACK DENSITY

drawn through each set of plotted points, and these are presented in figures 25 (a,b,c,d).

The creep rates corresponding to these curves are listed in Table VII. For each stress and temperature the calculated creep rate was subtracted from the creep rate as given by the respective curve at the corresponding strain. These differences were squared and summed, and the sum divided by the number of calculated creep rates. The square root of this number was taken as a measure of the goodness of fit of the curves to the creep rates, and is presented in the Table as the root mean square deviation (R.M.S. dev.).

It can be seen that for stresses less than about 12 kg/cm², the strain rate had a maximum between the strain of 10×10^{-4} to 20×10^{-4} . This was about the same range as for the maximum in the cracking rates. This maximum tended to larger strain with increasing stress. With continued deformation the strain rate approached the constant value associated with the secondary creep stage.

For a stress of 12 kg/cm² or greater, the creep rate continuously increased with strain, showing that the primary stage of creep passed directly to the tertiary stage. It is of interest that for σ = 12 kg/cm² and \overline{T} = -31.0°C, there was evidence of the maximum and an apparent secondary stage prior to the onset of the tertiary stage. This feature disappeared

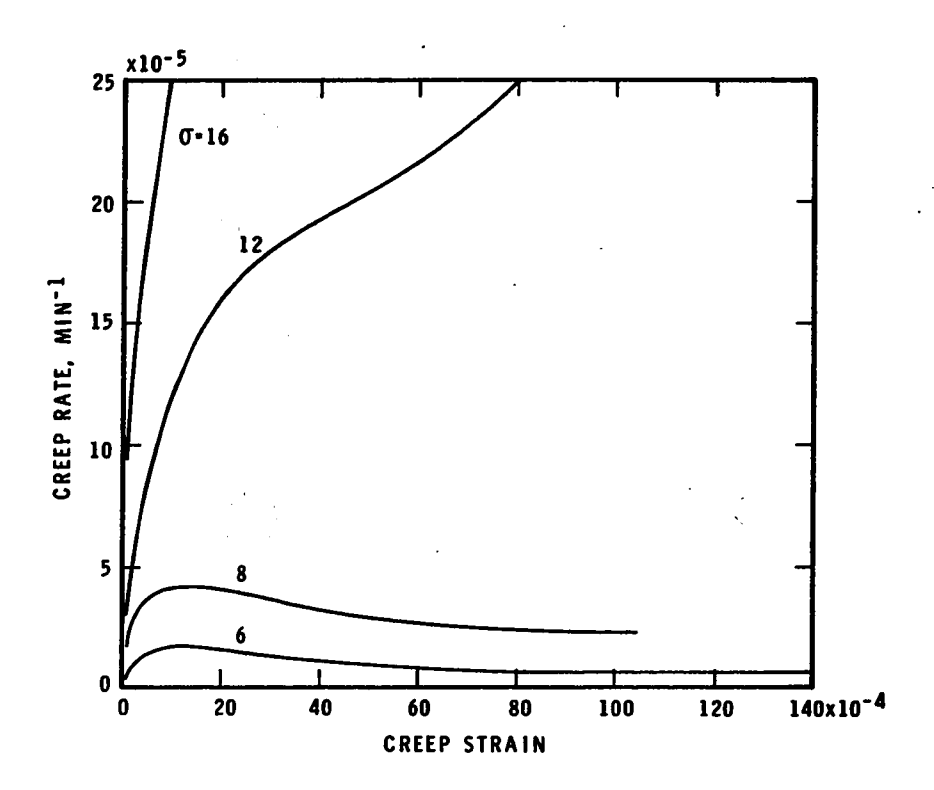


FIGURE 25a STRAIN DEPENDENCE OF THE AVERAGE CREEP RATE FOR GIVEN STRESS $\sigma.$ \tilde{T} = -4.8°C

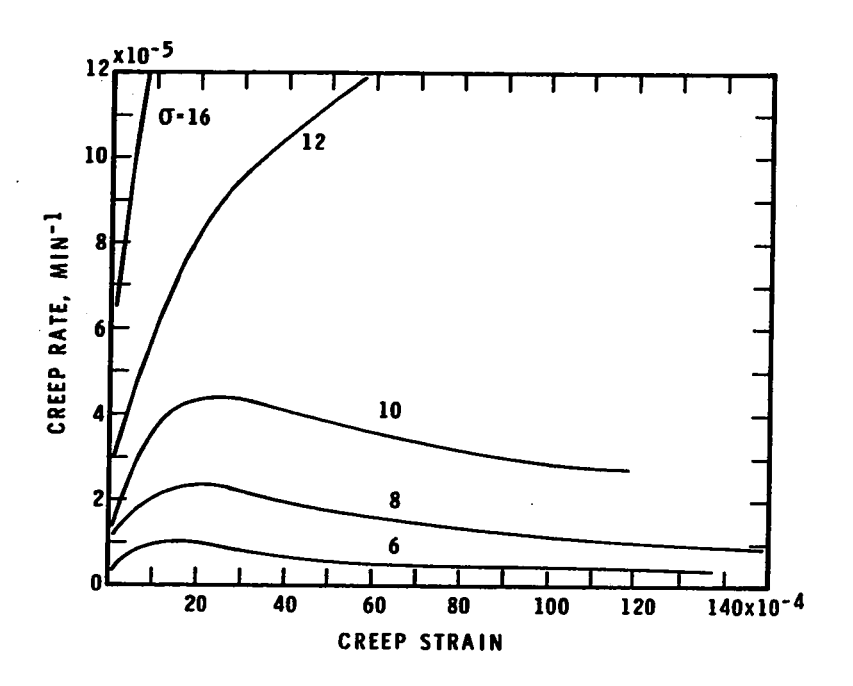


FIGURE 25b STRAIN DEPENDENCE OF AVERAGE CREEP RATE FOR GIVEN STRESS. T = -9.5°C

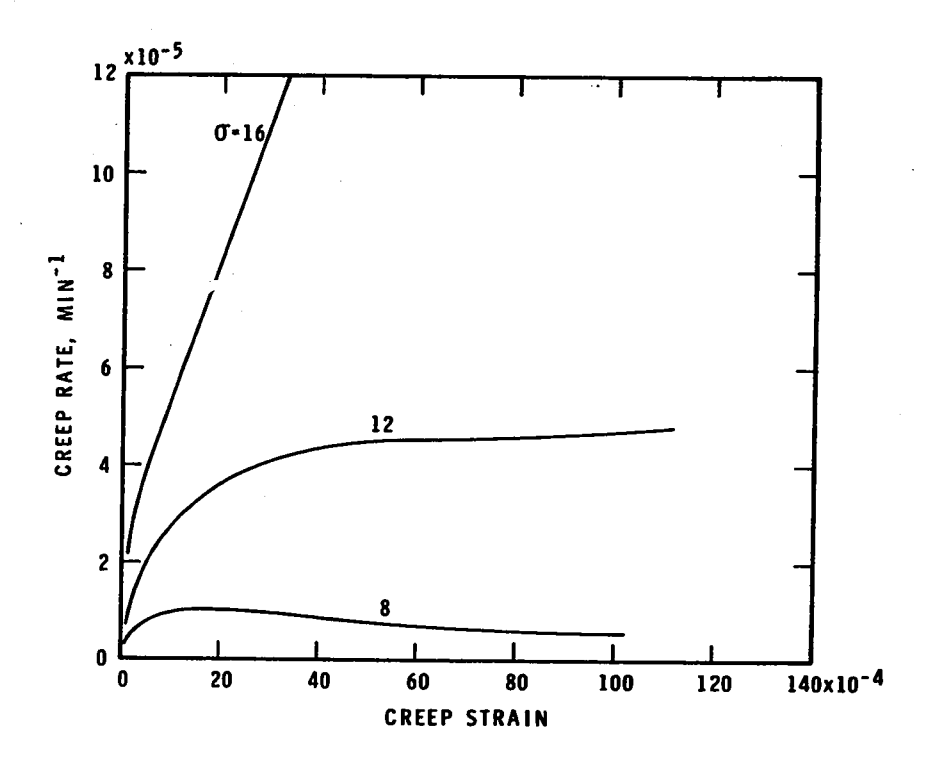


FIGURE 25c STRAIN DEPENDENCE OF THE AVERAGE CREEP RATE FOR GIVEN STRESS 0. \dot{T} = -14.8°C

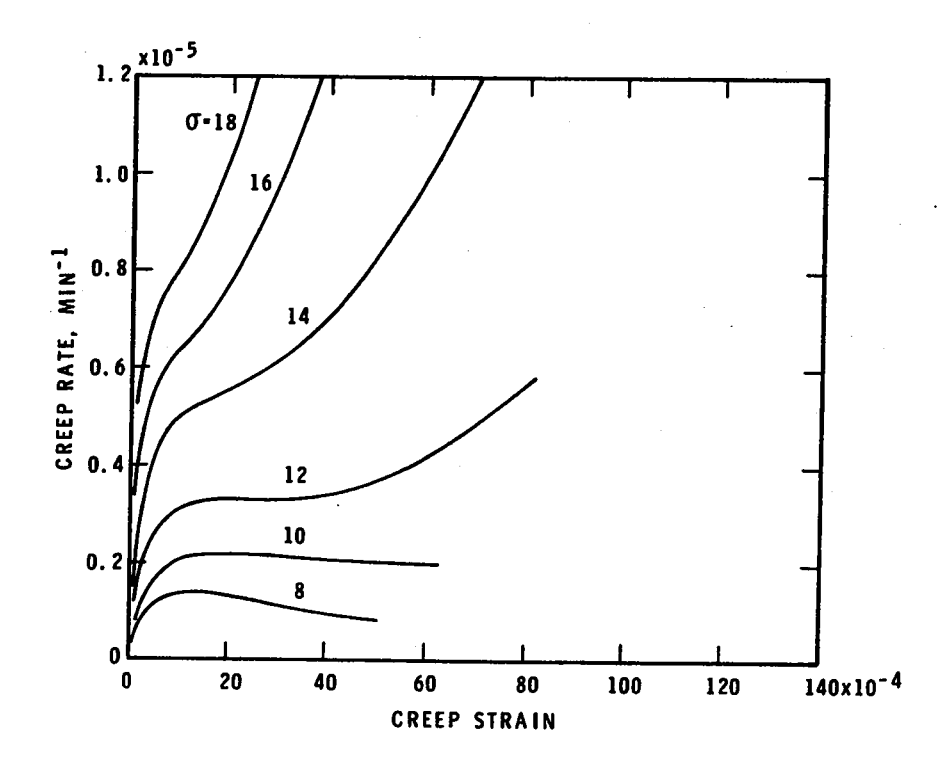
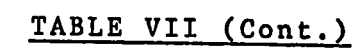


FIGURE 25d STRAIN DEPENDENCE OF THE AVERAGE CREEP RATE FOR GIVEN STRESS $\sigma.$ $\,$ † - -31°C

TABLE VII
Strain Dependence of the Strain Rate

| | | | T | = -4.8 | °C | | Strai | n rate | x104 m1 | n-1 | | | • |
|--------------------|-------------------------|-------------------------|----------------------------------|----------------------------------|----------------------------------|-------------------------|----------------------------------|----------------------------------|----------------------------------|-------------------------|-------------------------|-------------------------|-------------------------|
| Stress | Strain x10 ⁴ | | | | | | | | | | | D M C | |
| kg/cm ² | 5 | 10 | 15 | 20 | 30 | 40 | 50 | 60 | 70 | 80 | 90 | 100 | R.M.S. dev. |
| 6 | 0.142 | 0.171 | 0.171 | 0.156 | 0.132 | 0.111 | 0.095 | 0.084 | 0.077 | 0.073 | 0.070 | 0,067 | 0 004 |
| 8 | 0.360 | 0.405 | 0.414 | 0.408 | 0.363 | 0.320 | 0.289 | 0.268 | 0.250 | 0.237 | 0.232 | 0.007 | 0.004 |
| 12 16 | 1.85 | 1.18 | 1.42 | 1.59 | 1.81 | 1.93 | 2.05 | 2.16 | 2.31 | 2.50 | 2.71 | 2.94 | 0.01 |
| 10 | 1.05 | 2.55 | 3.17 | 3.75 | 4.94 | 6.11 | 7.28 | 8.45 | 9.61 | 10.80 | 11.97 | 13.12 | 0.19 |
| | | | | | · | | | | <u> </u> | | | | |
| | | | T | = -9.5 | °C | | Strai | n rate | ×104 | <u> </u> | | | |
| 6 | 0.076 | 0.095 | T 0.098 | = -9.5 0.092 | | 0.067 | | | | 0.045 | 0.042 | | |
| 8 | 0.156 | 0.200 | 0.098 | 0.092 0.235 | °C 0.079 0.216 | 0.067 0.193 | Strai 0.057 0.172 | 0.051 | 0.048 | 0.045 0.131 | 0.042 | 0.040 | 0.002 |
| 8 10 | 0.156 0.259 | 0.200 | 0.098 0.225 0.405 | 0.092 0.235 0.430 | 0.079 0.216 0.431 | 0.193 | 0.057 0.172 0.382 | | | 0.045 0.131 0.317 | 0.042 0.123 0.299 | 0.040 0.117 | 0.002 0.007 |
| 8 10 12 | 0.156 0.259 0.423 | 0.200 0.351 0.595 | 0.098 0.225 0.405 0.725 | 0.092 0.235 0.430 0.822 | 0.079 0.216 0.431 0.953 | 0.193 0.407 1.050 | 0.057 0.172 0.382 1.125 | 0.051 0.154 0.358 1.190 | 0.048 0.141 0.336 1.255 | 0.131 0.317 1.320 | 0.123 0.299 1.387 | 0.040 | 0.002 |
| 8 10 | 0.156 0.259 | 0.200 | 0.098 0.225 0.405 | 0.092 0.235 0.430 | 0.079 0.216 0.431 | 0.193 | 0.057 0.172 0.382 | 0.051 0.154 0.358 | 0.048 0.141 0.336 | 0.131 0.317 | 0.123 | 0.040 0.117 0.284 | 0.002 0.007 0.017 |



| Stress kg/cm ² | $\overline{T} = -14.8$ °C Strain rate x10 ⁵ | | | | | | | | | | | | |
|------------------------------|--|-------------------------|----------------------------------|----------------------------------|----------------------------------|-------------------------|----------------------------------|-------------------------|------------------|-------|-------|--------|-------------------------|
| | Strain XIU | | | | | | | | | | | R.M.S. | |
| | 5 | 10 | 15 | 20 | 30 | 40 | 50 | 60 | 70 | 80 | 90 | 100 | dev. |
| 8 12 | 0.758 1.92 | 0.933 | 1.013 3.21 | 1.033 | 0.972 | 0.858 | 0.766 4.47 | 0.698 | 0.650 | 0.613 | 0.585 | 0.558 | 0.02 |
| 16 | 3.95 | 5.40 | 6.83 | 8.28 | 11.14 | 14.00 | 16.83 | 19.70 | 4.55 | 4.57 | 4.60 | 4.68 | 0.08 0.29 |
| | | | Ŧ | = -31. | 0°C | | Strai | n rate | ×10 ⁵ | | | | |
| | | | | = -31. | 0°c | | Strai | n rate | ×10 ⁵ | | | • | |
| 8 | 0.113 | 0.133 | 0.137 | 0.130 | 0.111 | 0.096 | 0.084 | n rate | x10 ⁵ | | · | | 0.004 |
| 10 | 0.163 | 0.204 | 0.137 0.214 | 0.130 0.216 | 0.111 | 0.206 | 0.084 | 0.199 | 0.198 | 0.198 | 0.198 | 0.198 | 0.004 |
| 10 12 | 0.163 | 0.204 | 0.137 0.214 0.328 | 0.130 0.216 0.332 | 0.111 0.212 0.330 | 0.206 | 0.084 0.201 0.369 | 0.199 0.420 | 0.198 0.487 | 0.566 | | | 0.004 0.004 0.014 |
| 10 | 0.163 | 0.204 0.309 0.500 | 0.137 0.214 0.328 0.528 | 0.130 0.216 0.332 0.552 | 0.111 0.212 0.330 0.620 | 0.206 0.340 0.721 | 0.084 0.201 0.369 0.853 | 0.199 0.420 1.011 | 0.198 | | 0.198 | | 0.004 0.014 0.009 |
| 10 12 14 | 0.163 0.261 0.425 | 0.204 | 0.137 0.214 0.328 | 0.130 0.216 0.332 | 0.111 0.212 0.330 | 0.206 | 0.084 0.201 0.369 | 0.199 0.420 | 0.198 0.487 | 0.566 | | | 0.004 |

for this stress with increasing temperature, indicating that the direct transition from the primary to the tertiary stage occurred for smaller stress the higher the temperature.

The temperature and stress dependence of the creep rate is often assumed to have the following form (Jonas, 1969; Jonas et al, 1969).

$$\dot{\varepsilon} = \phi_{s} \exp \left[\frac{-\Delta H_{o}}{kT} \right] \exp \left[\frac{\alpha (\tau - \tau_{b})}{kT} \right]$$
 (35)

where

 φ_{8} is a factor that depends upon the state of the structure, ΔH_{0} is the activation enthalpy when no effective stress is acting, α is the activation volume, and $\tau - \tau_{b}$ the effective shear stress acting in the glide plane.

It was pointed out in Section 2.4.5 that the back stress, τ_b , is probably equal to about 90% of the resolved shear stress for polycrystalline ice. Equation (35) is similar to equation (3), with $\frac{Q}{R} = \frac{\Delta H_0}{k}$ and $\phi_s \exp\left[\frac{\alpha (\tau - \tau_b)}{kT}\right] = C \tau_y^n$.

The logarithm of the steady state creep rate is plotted against $^1/T^0K^{-1}$ in figure 26 for a test carried out under a stress of 3 kg/cm². The test was continuous, and the same specimen was used to determine the creep rate at temperatures of -5°C, -10°C, -15°C, -20°C and -35°C. By the end of the test the specimen had been deformed about 3%. It can be seen that

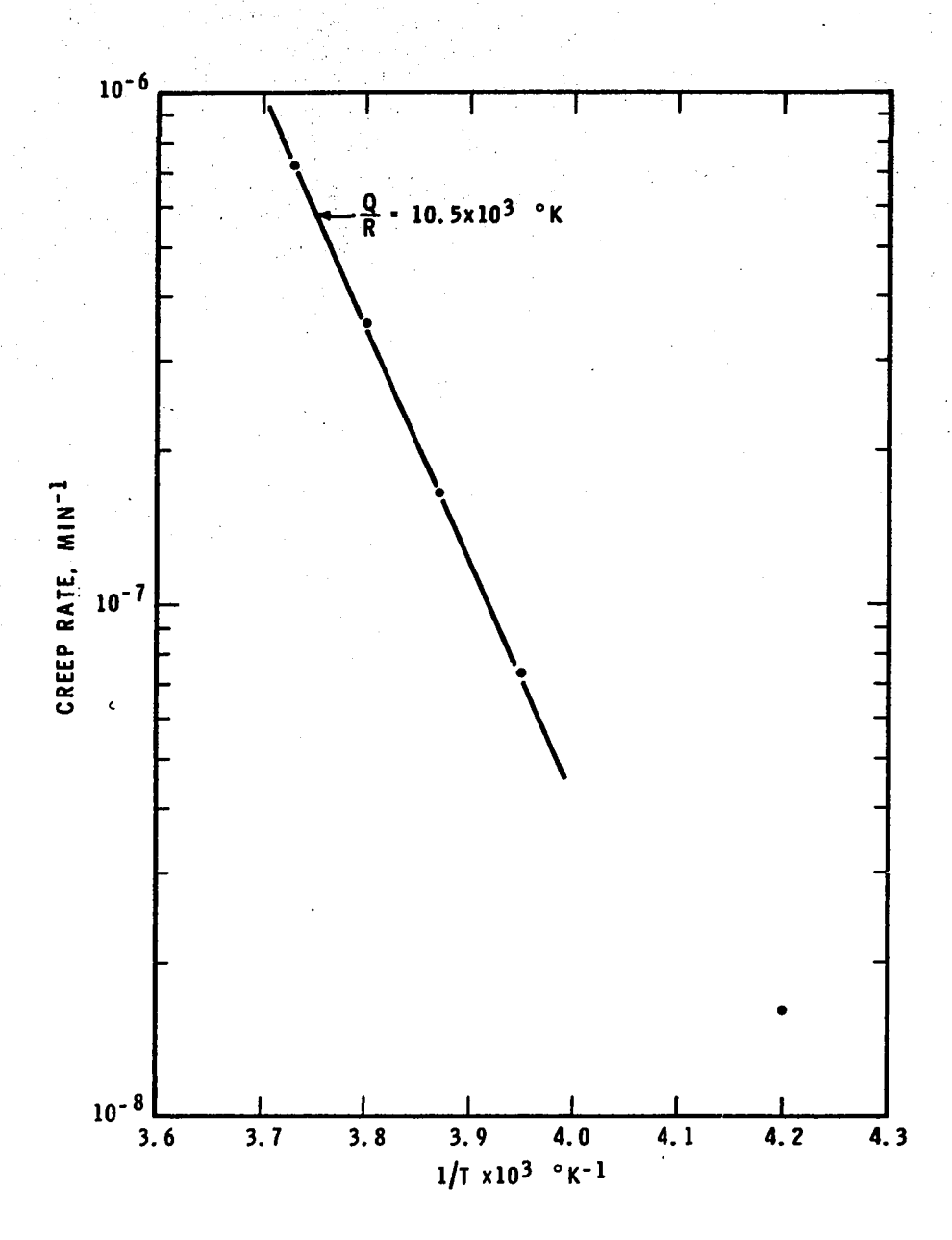


FIGURE 26 TEMPERATURE DEPENDENCE OF THE STEADY STATE CREEP RATE σ - 3 $\mbox{Kg/cm}^2$

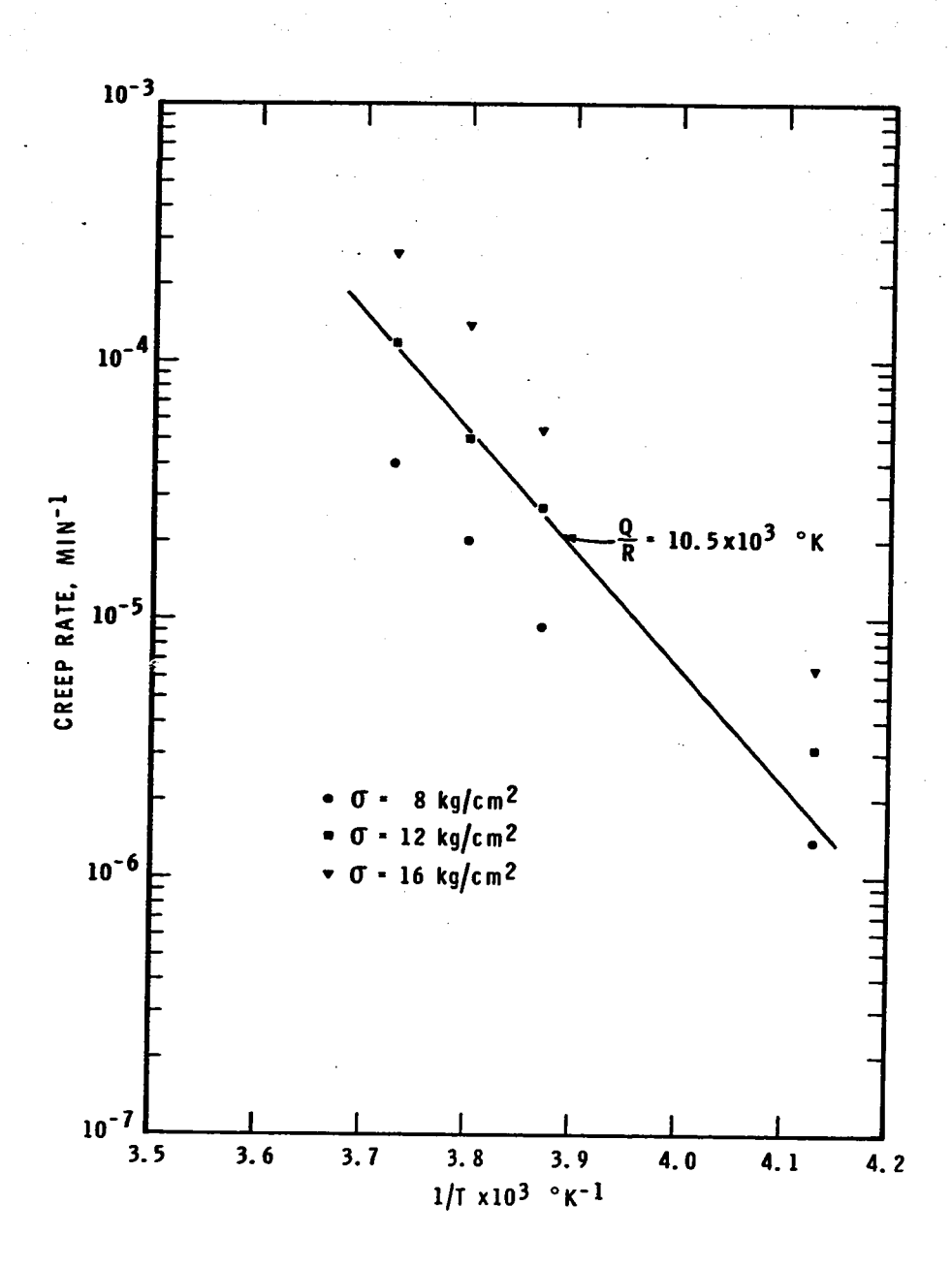
a straight line with a slope $Q/R = 10.5 \times 10^{30} K$ is a good fit to the observations for temperature higher than -20°C. The result obtained at -35°C deviates appreciably from this line in a direction that indicates a decrease in the apparent activation energy. Observations at -10°C were made after the observations at -35°C.

The logarithm of the average strain rates at strains of 10^{-3} and 5×10^{-3} are plotted against $^{1}/T^{0}K^{-1}$ in figure 27 (a,b) for the stresses 8, 12 and 16 kg/cm². Lines having a slope of Q/R = 10.5×10^{30} K are drawn through the points. It can be seen that these lines are a reasonably good fit to the results for temperature higher than -15° C, and that the strain rates at -31.0° C deviate significantly in the same direction as for $\sigma = 3$ kg/cm². The observations plotted in figure 27 show that the apparent activation energy during the transient creep stage was relatively constant.

By rearranging equation (35), the following expression for a "temperature corrected" strain rate is obtained:

$$\dot{\varepsilon} \exp\left[\frac{Q}{RT}\right] = \phi_{s} \exp\left[\frac{\alpha(\tau - \tau_{b})}{kT}\right]$$
 (36)

The average strain rates were modified by this temperature correction using $Q/R = 10.5 \times 10^{30} K$. The results are plotted in figures 28 (a,b,c) for the stresses 8, 12 and 16 kg/cm².



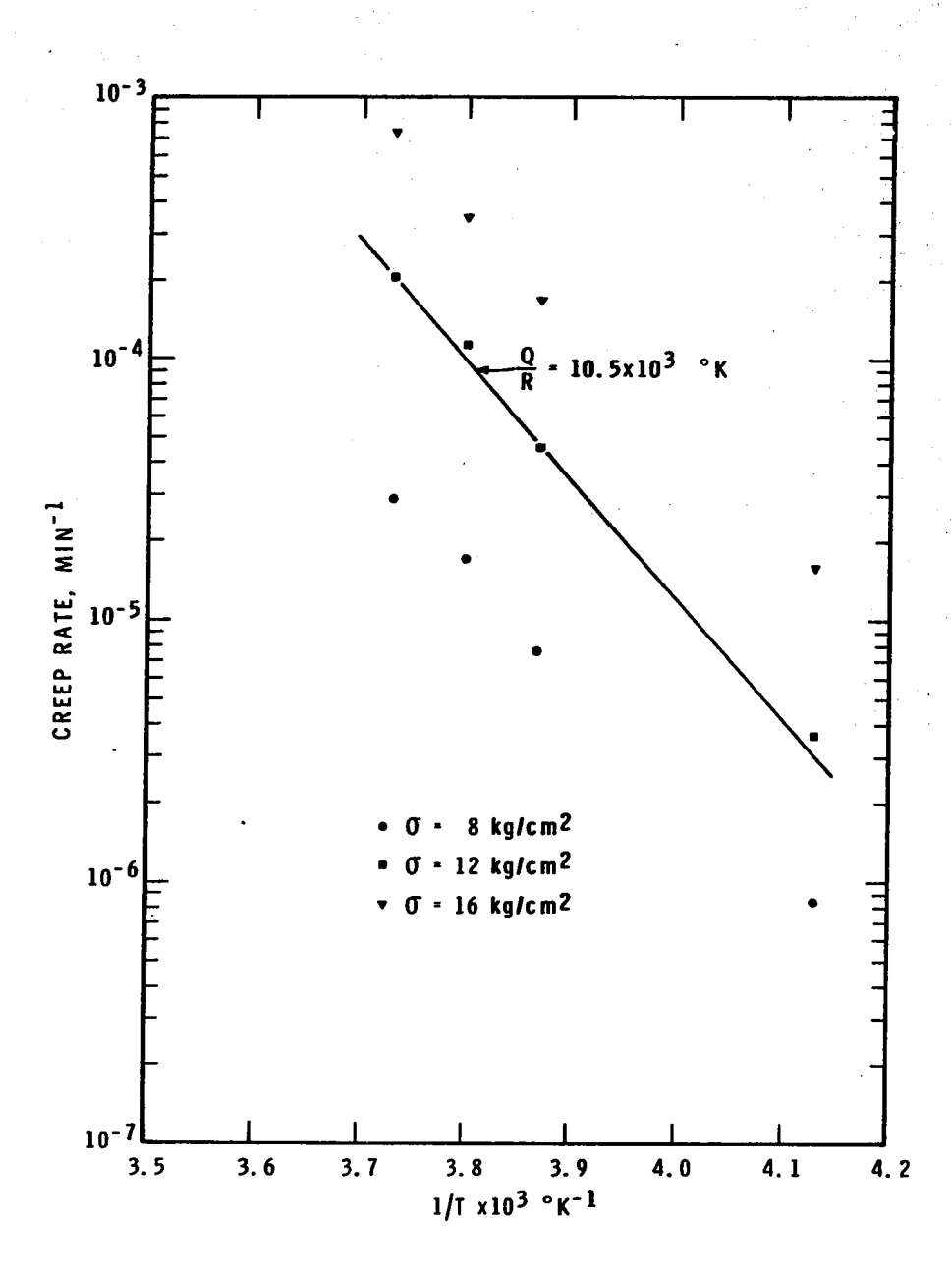


FIGURE 27b
TEMPERATURE DEPENDENCE OF THE CREEP RATE AT STRAIN = 5x10⁻³

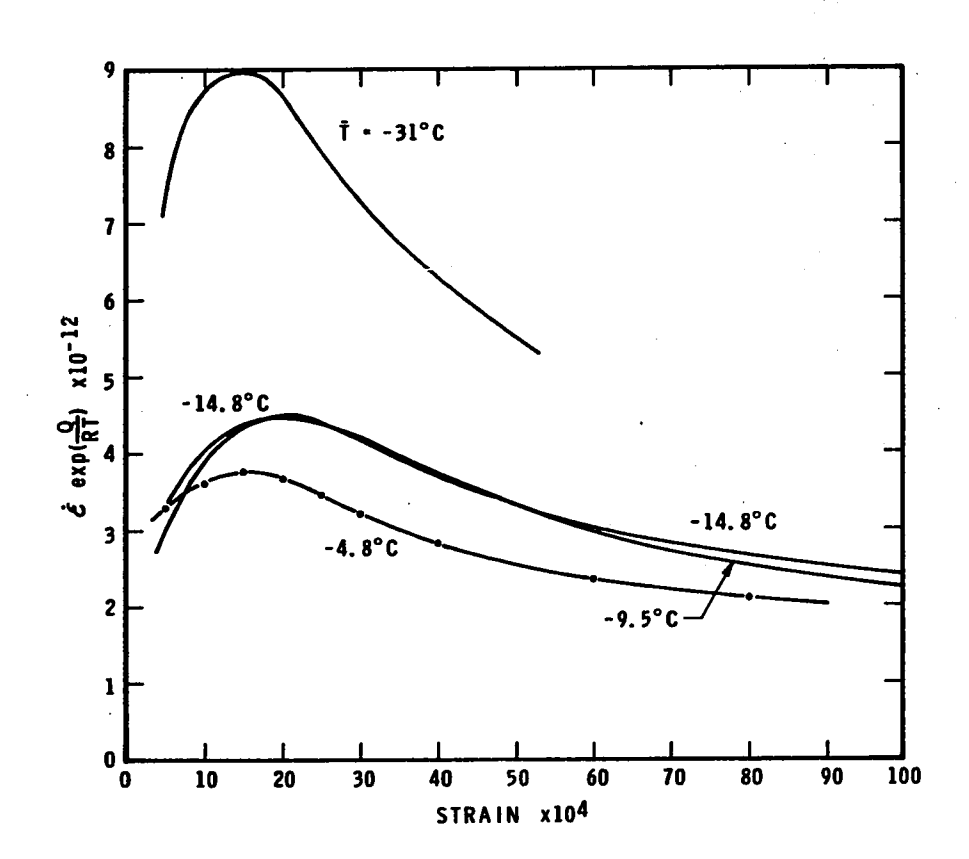


FIGURE 28a
THE STRAIN DEPENDENCE OF THE TEMPERATURE-CORRECTED STRAIN RATE. Ø - 8 KG/CM² Q/R - 10.5×10³ °K

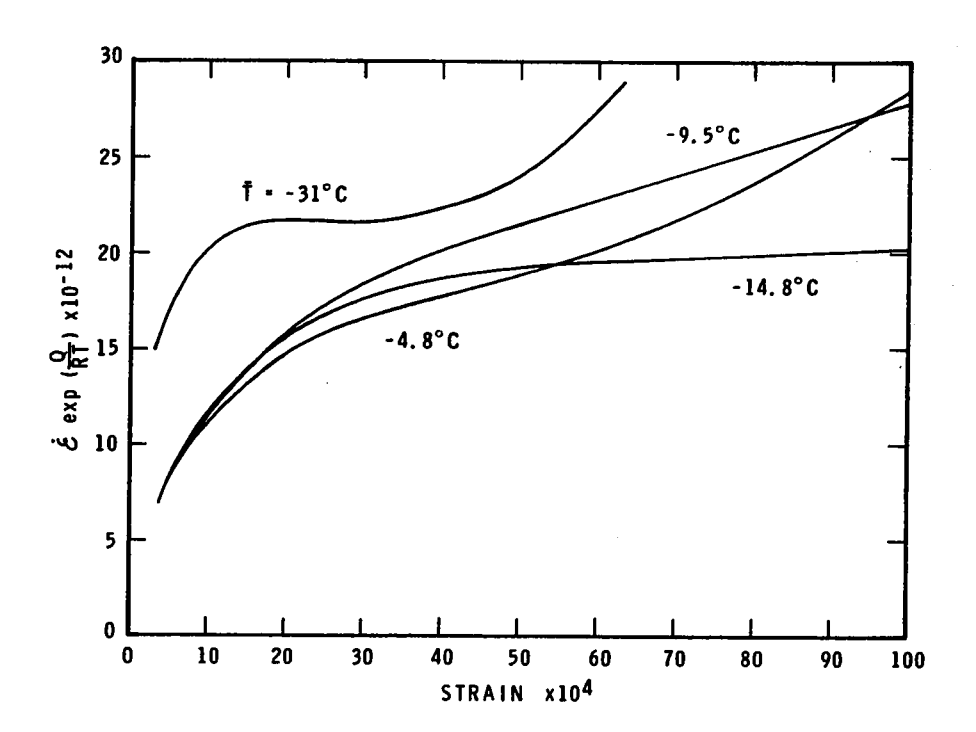


FIGURE 28b STRAIN DEPENDENCE OF THE TEMPERATURE-CORRECTED STRAIN RATE. σ - 12 kg/cm² Q/R - 10.5×10³ °K

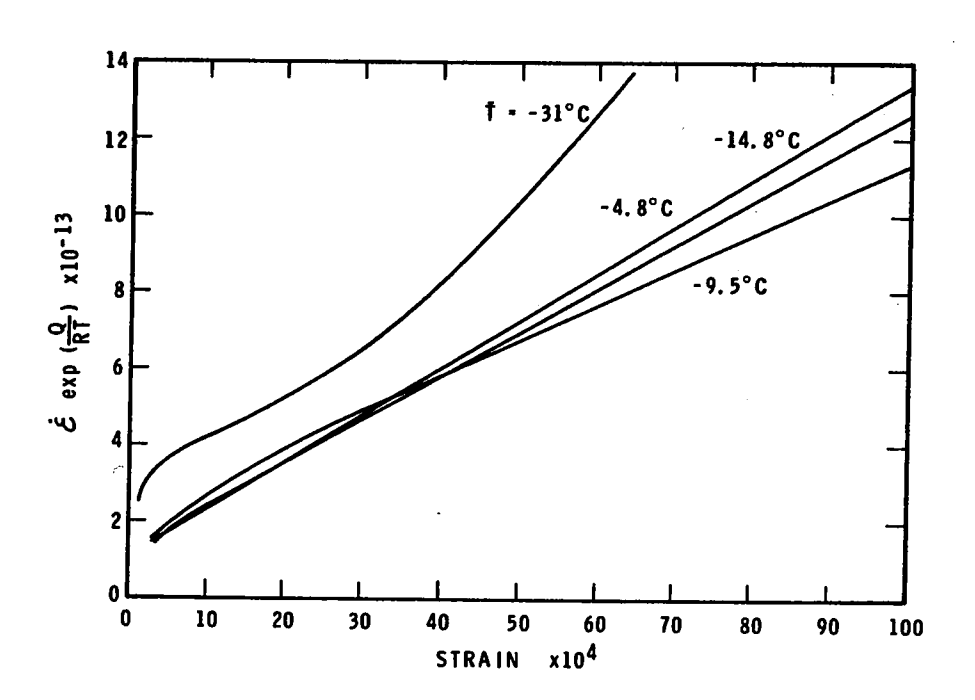


FIGURE 28c STRAIN DEPENDENCE OF THE TEMPERATURE-CORRECTED STRAIN RATE. σ = 16 kg/cm² Q/R = 10.5 x 10³ °K

Figure 28 does bring out clearly the nature of the change in the creep behaviour that occurred over the stress range of 8 to 16 kg/cm². The development of a secondary creep stage is clearly evident at 8 kg/cm². For a stress of 12 kg/cm², the secondary stage is suppressed and the tertiary stage initiated before the strain exceeds 10^{-2} . The tertiary stage is initiated at a strain of less than 5×10^{-4} for a stress of 16 kg/cm^2 .

The position of the curves for $\overline{T}=-31.0\,^{\circ}\text{C}$ clearly indicates that the apparent activation energy must be smaller at this temperature. It can also be seen more clearly in figure 28 that the curves for $\sigma=12$ and $16~\text{kg/cm}^2$ have characteristics that would be associated with lower stresses at higher temperatures (e.g. the curve for $\sigma=16~\text{kg/cm}^2$ and $\overline{T}=-31.0\,^{\circ}\text{C}$ is similar in shape to those for $\sigma=12~\text{kg/cm}^2$ and $\overline{T}\geqslant14.8\,^{\circ}\text{C}$; the curve for $\overline{T}=-31.0\,^{\circ}\text{C}$ and $\sigma=12~\text{kg/cm}^2$ actually has a short secondary creep stage).

The stress dependence of the temperature corrected strain rate at $\varepsilon = 10^{-2}$ is shown in figure 29. It can be seen that for $3 \leqslant \sigma \leqslant 10 \text{ kg/cm}^2$, this dependence has the form given by equation(3), i.e.

$$\dot{\epsilon} \exp \left[\frac{Q}{RT} \right] = C\sigma^n = \phi_s \exp \left[\frac{\alpha(\tau - \tau_b)}{kT} \right]$$
 (37)

where C is a constant. The line drawn through the points has

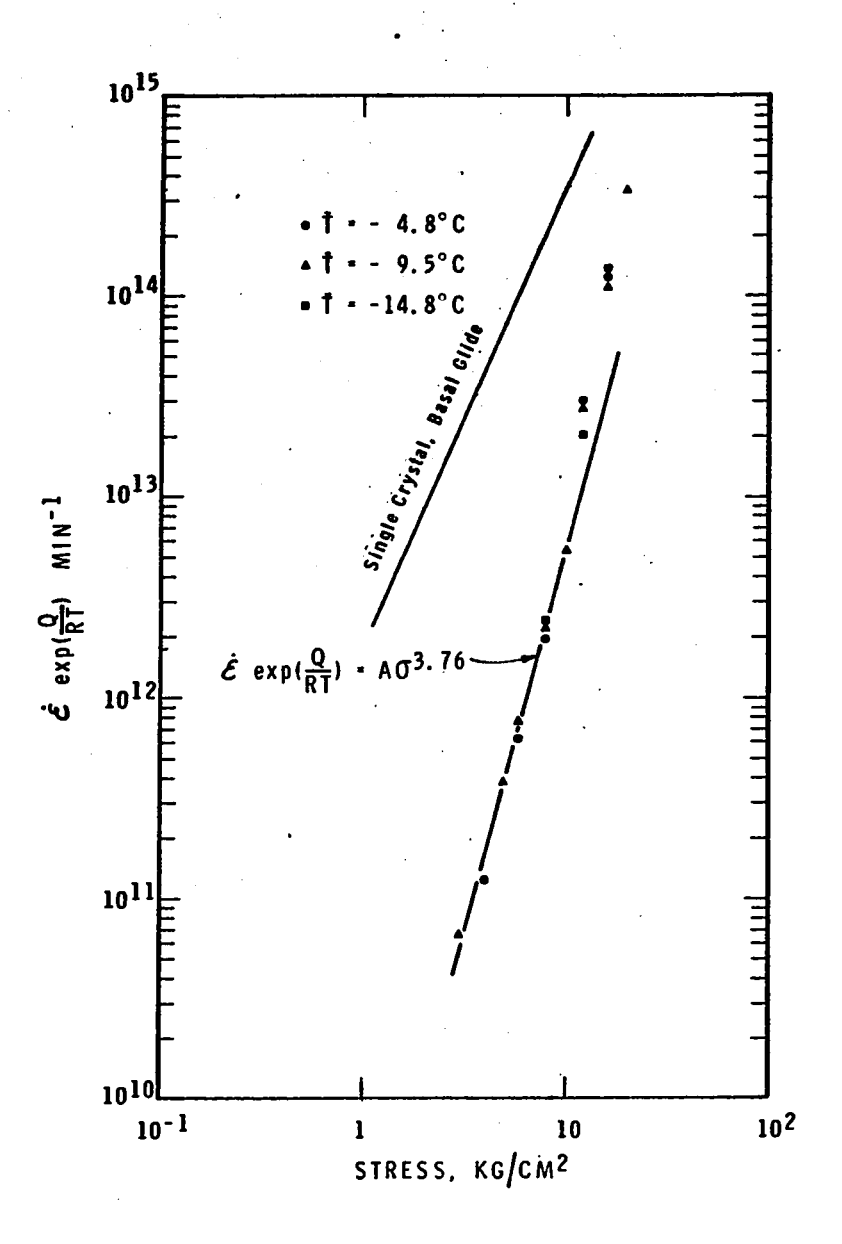


FIGURE 29 THE STRESS DEPENDENCE OF $\dot{\mathcal{E}}$ exp($\frac{Q}{RT}$), Q/R = 10.5×10³ K $\dot{\mathcal{E}}$ = 10⁻²

a slope, n, equal to 3.76. This value for the exponent of the stress is in good agreement with that obtained by Steinemann for granular type T1 ice (see figure 2).

Figure 29 shows how the creep rates for $\sigma > 10 \text{ kg/cm}^2$ diverge from what would be predicted from the results for $\sigma \le 10 \text{ kg/cm}^2$. The line drawn through the observations in figure 3 for single crystals oriented for basal glide, is reproduced and extended in figure 29. The results for type S2 columnar-grained ice converge more rapidly to the single crystal results with increasing stress above 10 kg/cm² than for below it. This indicates the greater extent to which the constraints between grains were broken down during the first 10^{-2} of the creep strain when the stress exceeded 10 kg/cm^2 .

6.3 Discussion

Cracking activity is a factor that has not been taken into consideration in studies of the deformation behaviour of ice. It is clear from the results of the present work, however, that it was closely associated with the development of the failure condition for type S2 ice during creep under uniaxial compressive loads greater than 10 kg/cm^2 . When the stress exceeded 10 kg/cm^2 , the cracking activity was directly responsible for the onset of the tertiary stage of creep before the strain exceeded 0.25%.

Prior to the onset of tertiary creep, the cracking activity was usually distributed relatively uniformly throughout the specimen. The marked transition that occurred in the creep behaviour over the stress range of 10 to 12 kg/cm2, suggests that for a given stress there may be a critical crack density which, if exceeded, allows tertiary creep to begin. An estimate was made of the crack density at the transition from the secondary or primary stage of creep to the tertiary, from the average strain dependence of the creep rate and crack density. The observations showed that a crack density of 1.4 cracks/cm² could develop for $\sigma \leq 10 \text{ kg/cm}^2$ without the tertiary stage being initiated. The rate of change of the creep rate changed from negative to positive within the first 40 x 10^{-4} strain for $\sigma = 12 \text{ kg/cm}^2$, when the crack density was about 1.6 cracks/cm2. When the stress was equal to or greater than 16 kg/cm², tertiary creep was established before the crack density exceeded about 0.5 crack/cm².

The tertiary stage was often clearly associated with non-uniform cracking activity. This is illustrated in figure 30, which is a photograph of a specimen deformed 2.3% by a stress of 20 kg/cm². Note how crack formation has tended to concentrate in zones approximately parallel to the planes of maximum shear, as pointed out in Section 2.5.

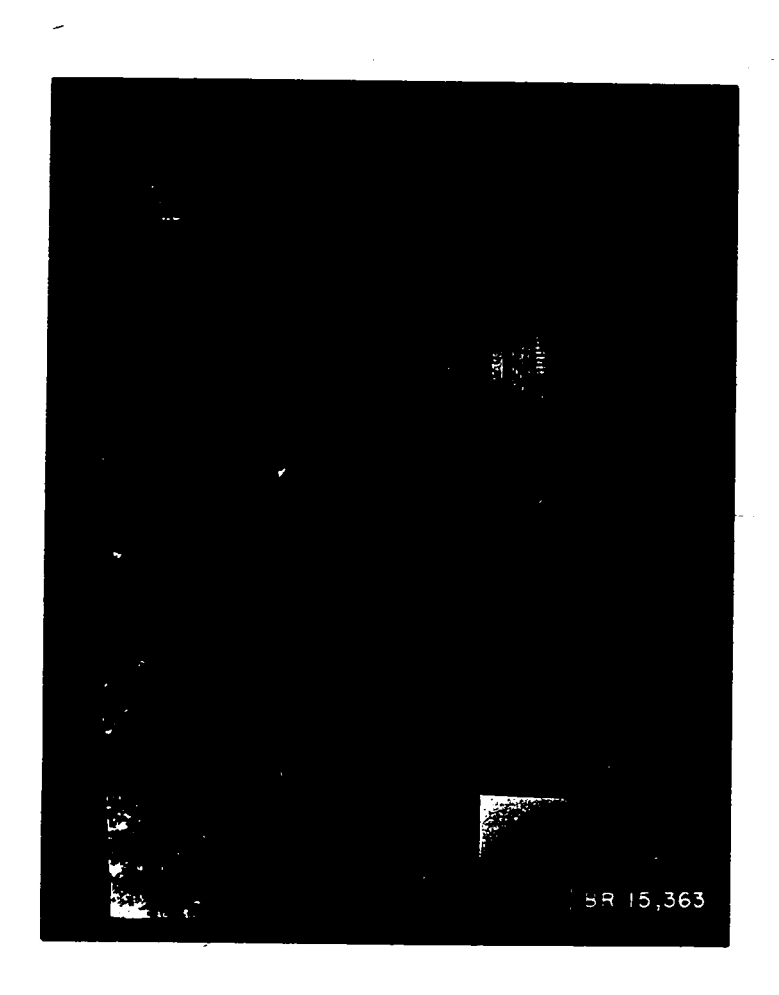


Figure 30

Fault zones formed in type S2 ice; $\sigma = 20 \text{ kg/cm}^2$; $\varepsilon = 2.3\% \text{ T} = -9.8^{\circ}\text{C}$.

Displacements at the edges of the specimens showed that a significant proportion of the creep in the tertiary stage occurred within the zones of greatest cracking activity. The strain, therefore, must be non-uniform once these faulted zones are formed. This raises the question of the validity of the usual methods of determining strain and relating it to the stress when this condition has been established. For example, the strain rates in faulted zones would be larger than the specimen average shown in figure 28 for stresses greater than or equal to 12 kg/cm². This implies that in these zones the strain rate was even closer to that for the single crystal than indicated by this figure.

The formation of a crack in ice was a visual indication of the establishment of the stress and energy conditions required for its nucleation. As each specimen was prepared in the same way, it would be expected that the number of potential crack nucleating sites should have been about the same for each test. The vertical bars in figure 19 indicate the variation that did occur between specimens. What the observations provided, therefore, was a reasonable record of the stress, strain, time and temperature dependence of the crack nucleating condition for type S2 ice subjected to uniaxial compression.

One of the results that is difficult to explain is the strong temperature dependence of the crack density (see figure

23). Consider the criterion for crack initiation given by equation (30) (i.e. $\tau_e \varepsilon = \frac{\pi^2 \gamma}{2d}$). Temperature affects this relationship through its effect on the surface energy, γ , and the strain, ε , required to produce the necessary length of dislocation pile-up (i.e. the necessary number of dislocations in the pile-up). The temperature dependence of γ is not sufficient to explain the temperature dependence of the crack density shown in figure 23. The number of dislocations in a pile-up should increase with decreasing temperature, and this would cause the crack density for a given strain to also increase with decreasing temperature. It must be concluded that the temperature dependence observed was due to other factors that affect the occurrence and size of stress concentrations (e.g. the number of dislocations in pile-ups and the shear stress acting on them).

The increase that was observed in the apparent activation energy with increase in temperature, indicates that a deformation process with a larger activation energy became more significant at the higher temperatures (Sherby and Burke, 1967). As the apparent activation energy tended to that for self-diffusion with decrease in temperature, it is considered that the deformation at the lower temperatures was determined mainly by diffusion controlled processes such as dislocation climb. Results of studies on single crystals indicate that such processes control their deformation for temperatures up to at

least -10°C (see Table III). This suggests that the increase in the apparent activation energy for polycrystalline ice for temperatures above -31°C is due to processes associated with the presence of grain boundaries.

Various modes of deformation and recovery can contribute to the ability of grains to conform to the change in shape of their neighbors. The relative importance of these modes depends upon both the temperature and the stress (Sherby and Burke, 1967). For example, for high temperatures (temperature greater than one-half the melting temperature) and low stresses ($\sigma < 1 \text{ kg/cm}^2$), diffusion can provide for ice the degrees of freedom necessary for the arbitrary change in shape of the grains (Nabarro-Herring creep). As the stress is increased, slip becomes more important than diffusion in bringing about this change in shape. The movement of dislocations in their glide planes, however, provides only two degrees of freedom for easy slip for type S2 ice. For the geometry of the specimen and load used in the present study, only one of these would be effective (see p. 58). As this would result in discontinuities in the strain at the grain boundaries, processes such as grain boundary sliding, grain boundary migration, multiple slip, etc., must operate to provide the extra degrees of freedom required for coherency.

No visual evidence of grain boundary sliding was observed in the present experiments. Significant grain boundary sliding would have been difficult because of the width of the grains and the associated greater probability of irregularly shaped boundary regions. There was often extensive deformation in the immediate vicinity of the boundaries, as can be seen in figures 4, 5 and 6. Although there was no visual evidence of sliding in this study, indirect evidence does indicate that the tendency would have been there, and that it would have probably provided stress relief in the vicinity of stress concentrations. Considerable evidence was observed of grain boundary migration when the strain exceeded about 5 x 10⁻⁴.

If processes such as grain boundary migration and grain boundary sliding make a significant contribution to maintaining coherency in the boundary regions, it would have the effect of reducing the contribution that would otherwise have been required by diffusion processes within the grain (e.g. dislocation climb, cross-slip). The increase in strain rate that would be produced would mean that the time required for a given strain would be correspondingly smaller than if self-diffusion processes were acting alone. This can be appreciated by referring to figure 26 and visualizing the difference that would exist between the line drawn with a slope $\frac{Q}{R} = 10.5 \times 10^{30} K$, and one with a slope $\frac{Q}{R} = 8 \times 10^{30} K$ passing through the point at

 $^{1}/_{T} = 4.2 \times 10^{-30} \mathrm{K}^{-1}$. This latter line would give the strain rates that would have been expected if the process (or processes) with an apparent activation energy of 0.61 eV (16 kcal/mole) was controlling at the higher temperatures. Both of the foregoing factors would cause the number of dislocations in a pile-up for a given strain to increase with increasing temperature (i.e. there would be a decreasing need for dislocations to climb out of their glide planes, and a smaller time for climb than would have been available if the lower temperature process or processes still controlled the deformation).

The foregoing suggestion is supported by a conclusion reached by Krausz (1968) from a study of strain relaxation in ice at -10°C. Krausz concluded that, at this temperature, it is improbable that cross-slip or climb have a significant effect on the plastic deformation. It is also supported by observations by the author on the temperature dependence of the Young's modulus of type S2 ice (Gold, 1958). These observations indicated that the grain boundary regions have a viscous nature for temperatures greater than -40°C. When this type of ice was stressed perpendicularly to the long direction of the grains, Young's modulus was considerably more temperature dependent than for single crystals stressed parallel or perpendicularly to the basal plane. The modulus became equal

to that for single crystals at -40°C. It was suggested that the greater temperature dependence of Young's modulus for polycrystalline ice was due to relaxation in the grain boundary regions.

If the suggested changes in the modes of deformation do occur for ice, it would explain the observed stress, strain and temperature dependence of the crack density and cracking The greater cracking rate at higher temperatures would be due not only to the greater stress concentrations associated with pile-ups (i.e. larger number of dislocations for given strain), but also to the larger stresses that would probably be imposed on grains with their basal planes tending to be parallel or perpendicular to the applied stress. This would occur because of the greater stress relaxation that would occur for grains oriented for easy glide. The boundary regions would become more rigid with decreasing temperature, and there would be greater opportunity for accommodation between grains to occur by cross-slip and climb of dislocations out of regions of stress concentration. Not only would this reduce the number of crack nucleating sites and, therefore, the rate of cracking and crack density, but also cause the load to be carried more uniformly by the structure. The tendency for the crack density for given stress and strain to become independent of temperature at the lower temperatures (see figure 23) indicates that

the relative contribution of the various modes becomes effectively constant for this condition. The argument that has been presented suggests that the apparent success of the theory of thermally activated processes in correlating phenomena associated with crack formation, may, in some cases, be due to the temperature dependence of other processes associated with the deformation rather than thermally activated crack nucleation, as pointed out in Section 5.2.

Decreasing the stress for a given temperature and strain, or decreasing the temperature for a given stress and strain, increases the time available for dislocations to move out of regions of stress concentration. This could explain the shift in the maximum in the cracking rate to larger strains with decreasing stress and temperature, as greater strains would be required to establish the crack nucleating condition. For stresses greater than 12 kg/cm², this effect would probably be removed by the onset of tertiary creep.

If the cracking activity is determined in the way that has been described, it will be particularly difficult to establish rigorously the correct model for the effect of stress. Nucleation depends on the probability of having the required relative grain orientations at a particular site. Whether or not a crack will be produced at such potential sites will depend upon the possibility of modes of deformation and recovery

maintaining the stress below the level required for nucleation (e.g. grain boundary migration, diffusion processes). A discussion of the influence of stress, therefore, would require a knowledge of how the contribution of the various modes depends on temperature, time, strain and stress.

In summary, it is considered that the formation of a crack marks the site of a stress concentration of sufficient size to cause nucleation. The number of sites available for crack nucleation depends on the relative contribution to the strain and internal stress of the various modes of deformation and recovery. These modes have different temperature dependencies, and so their relative contribution changes with temperature. For temperature above about -30°C, most of the adjustment that must take place in the grain boundary region to maintain coherency, does so by grain boundary sliding and migration. This allows larger pile-ups of dislocations in grains for given strain, and also larger stresses to develop on grains whose basal planes tend to be parallel or perpendicular to the applied stress. As a result, there will be a corresponding increase in the number of sites at which cracks will form.

As the temperature decreases, grain boundary processes, such as sliding and migration, become less significant and modes of deformation involving diffusion within the grain make

a relatively greater contribution to maintaining coherency.

This implies that there would be greater opportunity for dislocations to climb out of regions of high stress concentration, and thereby reduce the probability of crack formation.

When the crack density reaches a critical value for a given stress, the structure becomes unstable, and tertiary creep develops, often through the formation of a fault zone in which the cracking activity tends to concentrate. This transition occurs at smaller stresses with increasing temperature because of the greater cracking activity associated with this condition.

7. STATISTICS OF THE CRACKING ACTIVITY IN ICE

When a solid is subjected to plastic deformation, energy is stored in it due, for example, to the creation of dislocations and formation of dislocation pile-ups. The way in which the work done on the solid is transformed and stored in a given region by the various modes of deformation will depend significantly on the characteristics of the grains in the immediate vicinity, and their relative orientation. For many conditions of interest, the energy that is stored is fixed spatially, and there is little tendency for it to flow from one region to another. It is clear that some energy must flow because of the forces tending to bring about statistical equilibrium. If the interaction between regions is sufficiently weak, however, they can be considered independent in the statistical sense (e.g. see Landau and Lifshitz, 1958, p. 8).

The initiation of a mode of deformation in a solid will probably have a significant effect in the immediate vicinity in which it occurs, but need not significantly affect other regions if they are statistically independent. This can be the case when yield or flow occurs uniformly throughout a specimen. The initiation of a mode of deformation, however, may induce an instability that can propagate through the specimen, as in the formation of a Lüders band. Fracture is also an instability of this type. During fracture, the energy flow

is highly localized in the unstable region at the tip of the propagating crack.

The observations have shown that type S2 ice can be broken down by the formation of non-propagating cleavage cracks until it is unable to sustain the load. The onset of this instability is associated with the tertiary stage of creep, continuous cracking activity and, in some cases, the formation of a fault plane. Crack formation can take place, however, without inducing an unstable condition, as shown by the existence of the secondary creep stage in the compressive stress range of 6 to 10 kg/cm², and the associated drop-off in cracking activity. This indicates that for certain conditions of load and strain, type S2 ice may be made up of statistically independent regions as far as crack formation is concerned. A series of observations was undertaken to determine if this was the case.

7.1 Spatial Distribution of Cracks

Attention has been given to the spatial distribution of random events taking place within a given area (e.g. Feller, 1957, p. 149). If the area can be divided into non-overlapping independent regions of equal area, the probability of finding exactly k events in any one region is given by the Poisson

distribution

$$p(k, \lambda) = \frac{e^{-\lambda} \lambda^{k}}{|k|}$$
 (38)

where λ is the expected or average number of random events per region.

Three sets of specimens were deformed under a constant compressive stress of 10 kg/cm² to strains of 15 x 10⁻⁴, 25 x 10⁻⁴ and 50 x 10⁻⁴ respectively. Each specimen was subsequently cut so as to expose the middle plane perpendicular to the long direction of the columns. This surface was polished by slight melting. A lucite sheet on which was scribed a 10 x 15 cm grid with 1 cm spacing between the lines, was placed on it. The number of cracks intersecting the surface within the central area of each specimen was counted for each one centimeter square area of the grid.

Imagine the grid as being 15 rows and 10 columns of one centimeter squares, with the columns parallel to the edge of each specimen. In Table VIII is listed the average total number of cracks formed in each column of squares for each set of experiments, along with the average and standard deviation for the inner 8 columns. The grid is sketched at the bottom of the Table to show how it was placed on the specimens. Column 1 is adjacent to one edge of the specimen and column 10 to the second edge.

TABLE VIII

Strain dependence of average number of cracks per specimen in 1 x 15cm columns at midplane of Type S2 ice.

| Strain | No. of Specimens | COLUMNS | | | | | | | Average | | | | |
|-----------------------|---------------------|---------|-------|-------|-------|-------|-------|-------|---------|-------|------|----------------------|--------------------|
| | | 1 | 2 | 3 | 4 | 5 | 6 | 7 | 8 | 9 | 10 | Columns 2-9 incl. | Standard deviation |
| 15 x 10 - 4 | 21 | 3.05 | 4.14 | 5.09 | 5.52 | 4.28 | 4.90 | 4.43 | 4.52 | 3.52 | 2.09 | 4.55 | 0.58 |
| 25 x 10 ⁻⁴ | 20 | 6.60 | 10.00 | 11.40 | 10.00 | 11.10 | 11.75 | 12.00 | 10.70 | 8.95 | 2.90 | 10.73 | 0.97 |
| 50 x 10 ⁻⁴ | 10 | 11.00 | 15.70 | 19.20 | 19.40 | 18.10 | 17.50 | 21.10 | 18.60 | 14.00 | 7.50 | 17.90° | 2.09 |

| | 1 | <u>.</u> | <u></u> | C | OL | UM | NS - | 3 | -: | 10 |
|------------------|---|----------|---------|---------------|----------|-----|---------|---|----------|----------|
| I | | | L | | L | L | | | | |
| | 4 | | L | - | ŀ | ├- | ┞ | - | H | |
| SPECIMEN | | | | - | \vdash | | H | - | - | |
| | | | | | | | | | | |
| | _ | | L | <u> </u> | L | _ | L | L | | L |
| <u>~</u> | - | | - | \vdash | - | ┝ | ┝ | ┝ | - | |
| 캀 | | | | | | | | H | | |
| - } | | | | | | | | | | |
| ביחק ב ביחק ב | 4 | - | - | - | L | H | H | _ | | |
| ╬ | 1 | | - | - | | - | - | H | \vdash | \vdash |
| | | | | | | | | | | |
| | | | | | | | | | | |
| | | | | | | . , | | | | |

It can be seen in Table VIII that the average number of cracks in columns 1 and 10 are considerably more than one standard deviation smaller than the average number for columns 2 to 9 inclusive. This edge effect appears to extend to columns 2 and 9 also, particularly at the higher strain. It was decided, therefore, that only the cracks counted in columns 3 to 8 inclusive would be used for the study of the spatial distribution. The analysis was also limited to rows 3 to 12 inclusive so as to use observations only from the central area of each specimen. It was also decided to use for the analysis the number of cracks in non-overlapping square areas 2 x 2 cm in order to obtain a wider distribution in the number of cracks per area. The total area of observation per specimen was 60 cm².

In Table IX are listed for each set of experiments the number of squares containing exactly k cracks. If a crack occurred at the boundary between two squares, it was assigned to that square in which the greater portion of it lay. Also given in the Table is the expected value for the number of cracks per 4 cm², λ , and the theoretically determined number of squares containing exactly k cracks. The χ^2 test was used as a measure of the goodness of fit of the Poisson distribution to the observations. The calculated and relevant theoretical values of χ^2 are given in the Table. χ^2_{95} (7) is the theoretical

TABLE IX

Spatial Distribution of Cracking Activity per Area 4 cm² $\sigma = 10 kg/cm^2 \quad \text{Temp.} = -10 \, ^{\circ}\text{C}$

| k s k | ε = 1 λ = 1 | 5 x 10 ⁻⁴ | | $\varepsilon = 25 \times 10^{-4}$ $\lambda = 2.963$ | | | | | $\varepsilon = 50 \times 10^{-4}$ $\lambda = 5.245$ | | |
|-------------|---|----------------------|-------------------------|---|-------------|-----------------------------|-----------------------|-------------------------|---|--------------------------|---|
| Number | Number Obs. f | of Squares Theor. Fi | \frac{(f_1-F_1)^2}{F_1} | Num Obs f | <u>ber</u> | of So | luares Theor. F | \frac{(f_1-F_1)^2}{F_1} | Number Obs. f | of Squares Theor. F | $\frac{(f_{\underline{1}}-F_{\underline{1}})^2}{F_{\underline{1}}}$ |
| 0 | 100 109 | 85.0 111.6 | 2.65 | 33 53 | . • | 15.5 45.9 | | 19.74 | 3 5 } 16 | 0.8 | 2.5 x 10 ⁻³ |
| 3 4 | 50 33 14 | 73.0 32.1 10.5 | 7.24 | 53 51 47 | | 67.8 66.9 49.8 | | 3.23 3.78 | 27 | 10.9) | 3.37 |
| 5 | 7 1 23 | 2.8 | 7.06 | 28 19 | | 29.4 14.7 | | 0.16 0.07 1.26 | 21 22 16 | 24.8 26.0 22.8 | 0.58 0.61 2.03 |
| 7 8 9 | 1) | | | 6 4 3 | 16 | 6.0 | 10.0 | 3.60 | 20 16 5 | 17.0 11.2 6.5 | 0.53 2.05 0.35 |
| ≥10 | | | · | 3 | | | 10.0 | 3.00 | 7 | 6.9 | 2.9×10^{-3} |
| Tot. | 315 | 315.0 | | 300 . | | 300.0 | • , | | 150 | 150.0 | , |
| Σ i | (f ₁ -F ₁) ² F ₁ | | 17.04 | | | | | 32.94 | | · | 9.52 |
| | $\chi^2_{99.5}(3) = 12.84$ | | | | | $\chi^2_{99.5}$ (6) = 18.55 | | | | $\chi^2_{95}(7) = 14.07$ | |

 $F_i = \sum_{k=1}^{\infty} \frac{\exp(-\lambda)\lambda^k}{\lfloor k \rfloor}$

value for 7 degrees of freedom that has a 5% probability of being exceeded in a random sample of a Poisson distribution.

The observations presented in Table IX show that according to the χ^2 test, the hypothesis that the cracking activity has a Poisson spatial distribution would have to be rejected for $\varepsilon = 15 \times 10^{-4}$ and 25 x 10^{-4} , but is acceptable for $\varepsilon = 50 \times 10^{-4}$. For $\varepsilon = 15 \times 10^{-4}$ and particularly for $\varepsilon = 25 \times 10^{-4}$, there are more squares with no cracks than expected theoretically. Similarly, there are less squares with two cracks. This does indicate the possibility that the formation of a crack is not a truly independent event, i.e. the formation of one crack in a region lowers the probability of a crack being formed subsequently in adjacent regions. As the occurrence of a crack depends upon the relative crystallographic orientation of the grains in the region in which it occurs, the lack of complete independence may also be due to crystallographic orientation not being truly random. This could explain the tendency for the number of squares with more than four cracks to exceed that predicted by the Poisson distribution for $\varepsilon = 15 \times 10^{-4}$ and 25 x 10⁻⁴.

The Poisson distribution tends to the normal distribution with increasing λ . The hypothesis that the results for ϵ = 50 x 10⁻⁴ have a normal distribution was tested, and the result is shown in Table X. It can be seen from the Table that

TABLE X

Spatial distribution of cracking activity per area 4cm^2 , $\sigma = 10\text{kg/cm}^2$, $\epsilon = 50 \times 10^{-4}$, Temp. = -10°C.

$$F_i = \sum_{i=1}^{L} f_i \left\{ \frac{1}{S\sqrt{2\pi}} \exp \left[-\frac{1}{2} \left(\frac{k-u}{S} \right)^2 \right] \right\} = 5.245 \text{ cracks/sq.}$$

| Number | N 1 | | | | | |
|---------------------------------|---|------------------------------------|-----------------------------|--|--|--|
| of cracks k | Observed f | of Squares Theoretical Fi | $\frac{(f_i - F_i)^2}{F_i}$ | | | |
| 0 | 3 5 8 | 3.0 10.9 | 0.77 | | | |
| 2 3 | 8 | 10.5 | 0.59 | | | |
| 4 | 27 | 15.8 | 7.92 | | | |
| 4 | 21 | 20.6 | 0.01 | | | |
| 6 | 22 | 23.0 | 0.04 | | | |
| 7 | 16 | 22.1 | 1.68 | | | |
| 8 | 20 16 | 18.4 | 0.14 | | | |
| 9 10 11 12 13 14 | 1 1 1 2 1 1 2 1 1 2 1 1 2 1 1 1 1 1 1 1 | 13.1 8.1 4.3 2.0 0.8 0.2 0.1 | 0.64 | | | |
| Total | 150 | 150.0 | 12.62 | | | |
| $\chi_{95}^2(7) = 14.07$ | | | | | | |

the value calculated for χ^2 is less than the 5% critical value, and so the hypothesis cannot be rejected. This result, along with those shown in Table IX, indicates that the initial cracking activity has a spatial distribution that is approximately Poisson, and that it tends to a normal one with increasing strain.

The spatial crack distribution was also observed for a series of experiments with $\sigma=8$ kg/cm² and $\epsilon=400$ x 10^{-4} . It was analyzed in the same manner as the observations for $\sigma=10$ kg/cm², and the results are presented in Table XI. The χ^2 test again shows that the hypothesis that the cracking activity has a spatial Poisson distribution must be rejected.

It was observed during these experiments that many of the cracks that formed were unstable, and collapsed into sheets of cavities with continued deformation. Cavities were also observed to form in sheets which, with increasing strain, became indistinguishable from collapsed cracks. These phenomena may be responsible for some error in the observed distribution, although care was taken to prevent this from occurring. This set of observations did demonstrate that cavity formation might influence the crack distribution by causing stress relief in regions which would otherwise have contained cracks. It also demonstrated clearly that for a compressive stress of 8 kg/cm², type S2 ice exhibits the type of ductile behaviour

TABLE XI

Spatial distribution of cracking activity per area 4 cm², $\sigma = 8kg/cm^2$, $\varepsilon = 400 \times 10^{-4}$, Temp. = -10°C

$$\mathbf{F}_{\mathbf{i}} = \sum_{\mathbf{i}} \mathbf{f}_{\mathbf{i}} \frac{\exp(-\lambda)\lambda^{k}}{\lfloor \underline{k} \rfloor}$$

 $\lambda = 2.496$

| Number | Number | | | | | |
|-----------------------------|------------------|-------------------------------|-----------------------------|--|--|--|
| of cracks k | Observed f | Theoretical ^F i | $\frac{(f_1 - F_1)^2}{F_1}$ | | | |
| 00 | 20 | 8.6 | 15.10 | | | |
| 1 | 21 | 21.5 | 0.01 | | | |
| 2 | 14 | 26.9 | 6.18 | | | |
| 3 | 22 | 22.4 | 0.01 | | | |
| 44 | 12 | 14.0 | 0.29 | | | |
| 5 6 7 ≥ 8 | 7 5 3 1 | 6.9 2.9 1.1 } | 1.67 | | | |
| Total | 105 | 105.0 | 23.26 | | | |
| $\chi^2_{99.5}$ (4) = 14.86 | | | | | | |

that is associated with cavity formation and creep fracture in other materials.

Some observations were carried out on the spatial distribution of cavities formed during compressive creep for $\sigma = 5 \text{ kg/cm}^2$. The distribution again appeared to be approximately Poisson, but difficulties were experienced in making an accurate count. The principal difficulty was to establish whether sheets or collections of cavities were single or multiple "events". It was considered that more attention would have to be given to developing techniques of defining the extent of a single cavitating event before a meaningful statistical analysis could be undertaken.

If the size of the sub-areas into which the area of observation for the study of the spatial distribution of cracks is increased, it would be expected that the distribution in the number of cracks per sub-area would tend to become normal. The total number of cracks within the 60 cm² observation area was determined for each specimen in the set of experiments carried out at $\varepsilon = 15 \times 10^{-4}$, 25×10^{-4} and 50×10^{-4} . The average number of cracks, λ , the variance, s, and the percentage of specimens with number of cracks less than or equal to a given number, k, was calculated for each set. These percentages were plotted against the normalized abscissa, $\frac{k-\lambda}{s}$, on normal probability paper, and are shown in

figure 31. Shown also is the normal distribution. It can be seen that this distribution is a good fit to the observations. This shows that the distribution in crack densities obtained for given conditions of load, strain and temperature, can be assumed to be normal.

The study of the spatial distribution showed that the size of the area used for the observations of the cracking activity reported in Section 6, was large enough to provide a reasonable sample of the crack density. It can be appreciated that if the specimens had been only 2 to 6 cm in width, the usual size for studies of the deformation behaviour of ice, the results would have been significantly affected by size effects. This would have been the case, in particular, for the results on the cracking activity.

7.2 Crack Orientation

The initiation of a crack in type S2 ice depends not only on the crystallographic orientation of the grain in which it forms, but also on the relative orientation of surrounding grains. It was clear from the observations that the conditions required for crack initiation could be achieved in several ways, but the probability of a crack occurring in a given plane decreased with decreasing angle between the compressive stress and the perpendicular to that plane.

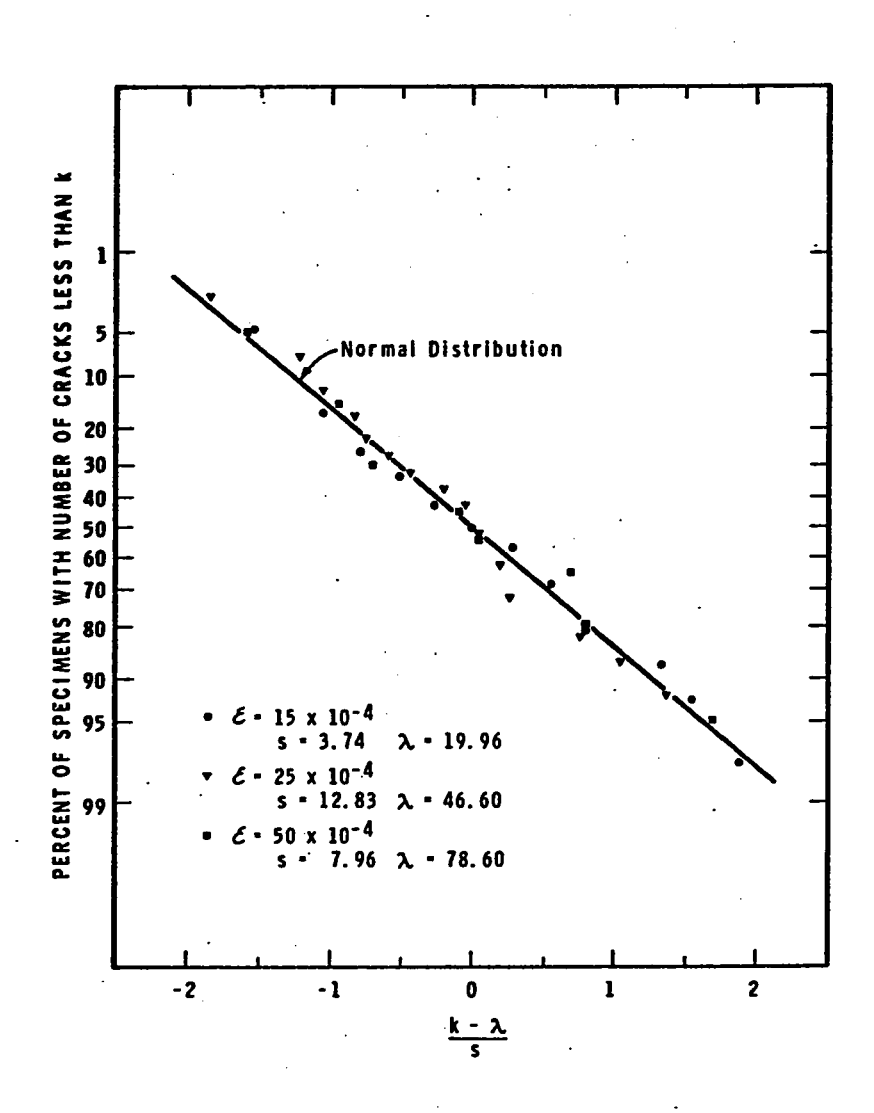


FIGURE 31 NORMALIZED PLOT OF PERCENTAGE OF SPECIMENS WITH NUMBER OF CRACKS IN OBSERVATION AREA LESS THAN OR EQUAL TO k FOR GIVEN STRAIN ε . OBSERVATION AREA - 60 cm²

The simplest assumption that could be made about the distribution in the angles between the applied stress and the perpendicular to the plane of the cracks, was that it was normal about the direction perpendicular to the stress (i.e. the most probable direction of crack propagation was parallel to the compressive stress). Observations were made on the angle, θ , between the stress and the plane of the crack, θ being measured in the plane perpendicular to the long direction of the grains. In Table XII is presented the number of cracks that formed in consecutive intervals of 2.5°. Because of the way in which the ice and specimens were prepared, it could be assumed that the probability of a crack forming in the 2.5° interval centred on $\boldsymbol{\theta}_{\boldsymbol{i}},$ was equal to that for the interval centred on $-\theta_{i}$. The observations in corresponding intervals were grouped, therefore, and presented as forming in the range centred on $\pm \theta_{i}$.

The theoretical normal distribution obtained using the mean $(\overline{\theta}=0)$ and variance of the observed distribution, is also presented in the Table. Application of the χ^2 test shows that the assumption that the observed distribution was normal cannot be rejected. About 25% of the observed cracks were at grain boundaries, 42% in the basal plane, 20% perpendicular to the basal plane, and the remainder were irregular.

TABLE XII

Angular Distribution of Cracks

Assumed $F_i = \frac{\sum f_1(2.5)}{S\sqrt{2\pi}} \exp \left[-\frac{1}{2}\left(\frac{\theta i}{S}\right)^2\right]$ where f_i and F_i are the observed and calculated number of cracks, respectively, in 2.5° range centred on θi °.

| <u></u> | | · | |
|--|---|---|---|
| degrees | f _i | F ₁ | $\frac{(f_{i} - F_{i})^{2}}{F_{i}}$ |
| ± 1.25 ± 3.75 ± 6.25 ± 8.75 ±11.25 ±13.75 ±16.25 ±18.75 ±21.25 ±23.75 ±26.25 ±28.75 ±31.25 ±33.75 ±46.25 ±43.75 ±46.25 ±48.75 ±51.25 ±53.75 ±56.25 ±58.75 | 58 43 38 48 52 35 19 29 29 28 31 29 12 17 12 8 6 14 6 12 10 3 15 14 | 44 43.2 42.6 41.6 39.6 38.2 36.0 33.0 31.2 28.6 26.0 23.6 21.0 18.6 16.2 14.2 12.0 10.2 8.6 16.2 14.2 12.0 10.2 13.2 13.2 13.2 | 4.45 - 0.50 0.99 3.99 0.27 5.24 0.48 0.16 0.01 .96 1.24 3.85 .01 1.09 .55 - 1.23 0.11 |
| Total | 566 | 566 | 21.77 |
| 0 = 0 | S = 25.65 | ° χ^2_{95} (1 | 1.8) = 28.87 |

7.3 Crack Widths

The width of a crack is a measure of the amount of energy in the region available for its propagation. It should also be a measure of the amount of damage that it has done to the structure. For deformation in tension, the width is particularly important because the cracks cause a reduction in effective cross-sectional area and, if sufficiently large, will propagate as Griffith cracks. Some observations were made on crack widths to obtain information concerning the characteristics of their distribution. These observations provided additional insight concerning the crack forming process.

Measurements were made with a microscope of the width of the cracks formed during strains of 2×10^{-4} , 4×10^{-4} , 7×10^{-4} and 15×10^{-4} , under a compressive stress of 12 kg/cm^2 . The measurements for the first three strains were made on the same specimens, the cracks being marked in an appropriate way during deformation. A second set of specimens was used for cracks formed during a strain of 15×10^{-4} . All the cracks that could be seen were measured and grouped in intervals of 0.01 cm. The observations were carried out at -10° C.

The observed distribution in the crack widths for given strains is shown in figure 32. Given also is the total number

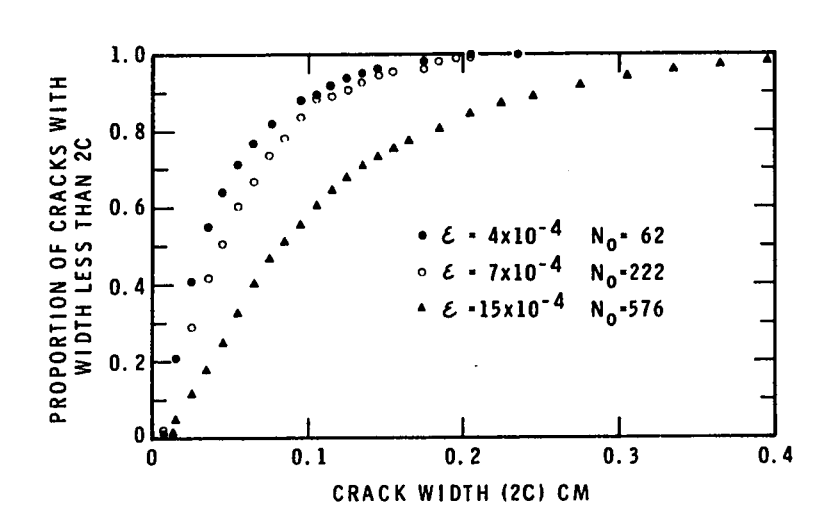


FIGURE 32 DISTRIBUTION IN THE CRACK WIDTHS FOR GIVEN STRAINS, σ - 12 kg/cm²

of cracks measured for each range of strain. It can be seen that the minimum crack width was about 0.01 cm. Cracks of width of 0.005 cm were readily seen with the lighting system used, but it was possible that some of the very small cracks disappeared when specimens were prepared for observation after removal of the load. It is considered that the observations were a true measure of the distribution for crack widths greater than 0.01 cm.

The distribution according to width for the cracking activity in the strain ranges 0 to 2×10^{-4} , 2×10^{-4} to 4×10^{-4} , 4×10^{-4} to 7×10^{-4} , and 7×10^{-4} to 15×10^{-4} , is shown in figure 33. The observations made with the set of specimens strained to 15×10^{-4} were adjusted, using the strain dependence of the average crack density presented in figure 19 (b), so as to conform with the set strained to 7×10^{-4} . Figure 33 shows the abrupt decrease in cracks observed for widths less than 0.01 cm. No cracks were seen with widths less than 0.005 cm.

The probability distributions were determined for the observations presented in figure 33. These distributions were plotted against the logarithm of the crack width on normal probability paper, and are presented in figure 34. A straight line was drawn through the points corresponding to the range 7×10^{-4} to 15×10^{-4} , and lines parallel to this through the

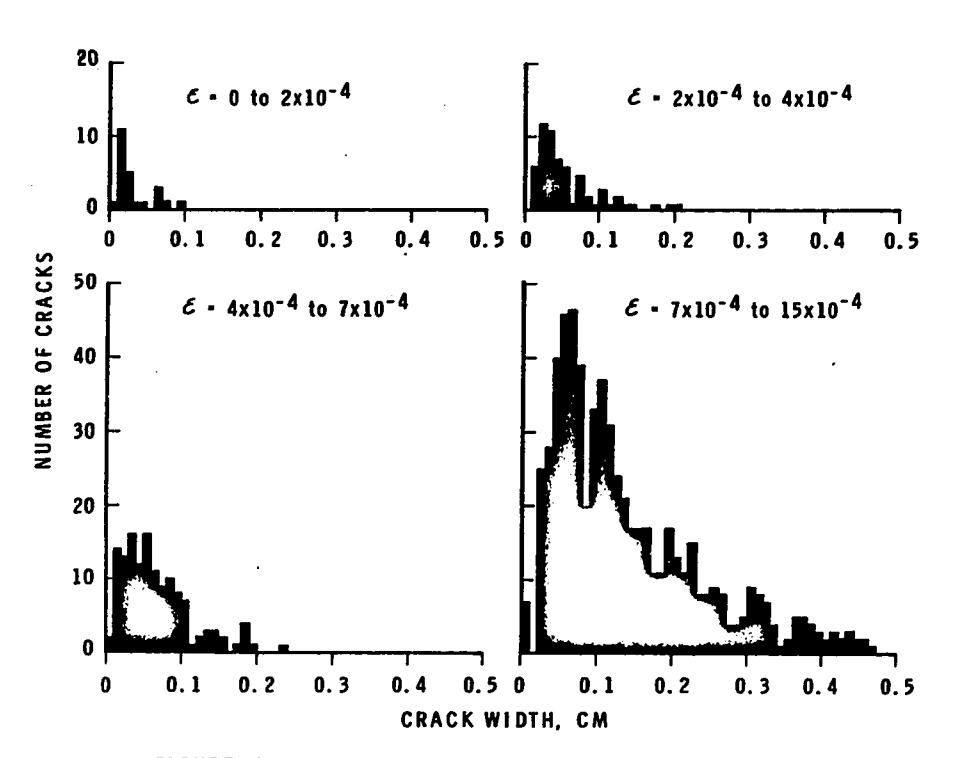


FIGURE 33
DISTRIBUTION ACCORDING TO WIDTH OF CRACKS FORMED IN INDICATED RANGE OF STRAIN

other three sets of points. It can be seen that these lines are a reasonably good fit to the observations, particularly for the strain ranges of 2×10^{-4} to 4×10^{-4} and 7×10^{-4} to 15×10^{-4} . There is appreciable scatter for the range 0 to 2×10^{-4} , which could be attributed to the small number of observations for this range. There is also a shift in the observations for the strain range of 4×10^{-4} to 7×10^{-4} , which could also be attributed to a statistical fluctuation.

The results shown in figure 34 indicate that the crack widths have a log-normal distribution of the form

$$p(c/\epsilon) = \frac{1}{\ln \sigma' \sqrt{2\pi}} \exp \left[-\frac{1}{2} \left(\frac{\ln 2c - \ln 2c_o}{\ln \sigma'} \right)^2 \right]$$
 (39)

where $p(c/\epsilon)$ is the probability density function at strain ϵ for cracks of width 2c, and c and σ' are constants.

It is particularly significant that the logarithmic standard deviation appears to be independent of the strain in the present study. Its value was found to be lno' = 0.820.

Figure 34 shows that the mean value for the distribution, $\ln 2c_0$, increased with strain. The values for $2c_0$ from this figure are presented in figure 35 with the corresponding range of strain. It can be seen that for the range of strain covered, $2c_0$ increased with ϵ at a rate that, at least initially, was less than linear.

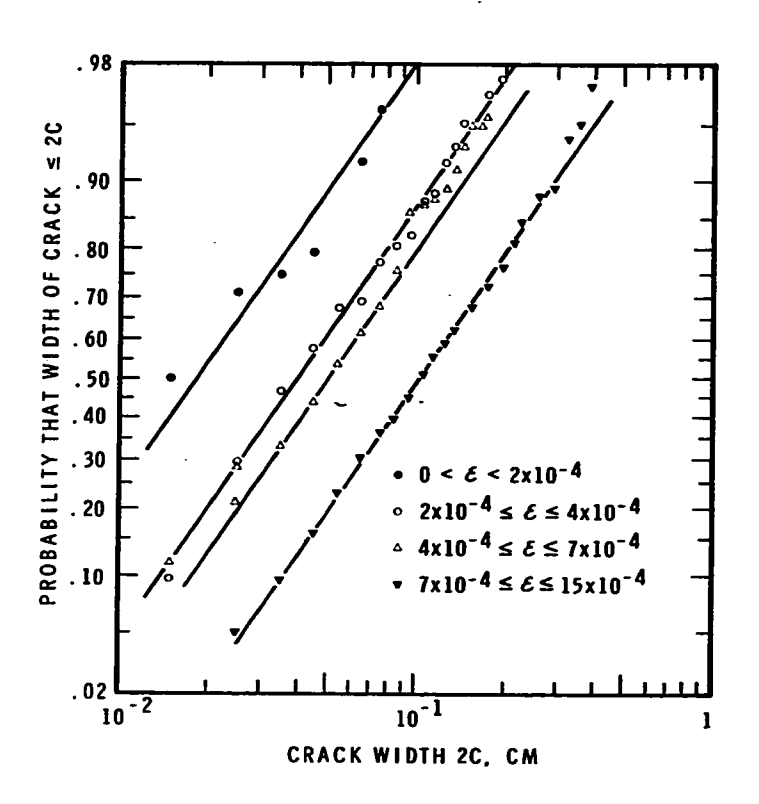


FIGURE 34
PROBABILITY DISTRIBUTION OF WIDTH OF CRACKS
FORMED IN GIVEN RANGE OF STRAIN

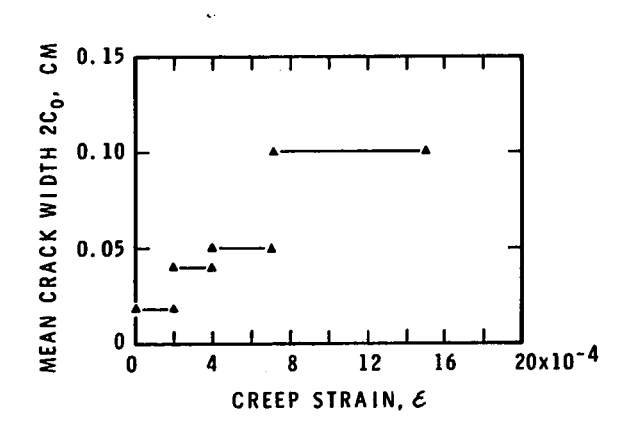


FIGURE 35 STRAIN DEPENDENCE OF THE LOGARITHMIC MEAN CRACK WIDTH

Initiation was probably a very localized event, and occurred at the most susceptible point in a region. Propagation, on the other hand, would involve a significantly larger volume. Although it might be expected that the probability for nucleation would increase with increase in energy available for propagation, the localization of the nucleating event would tend to make it independent of this energy. If this were the case, the distribution in crack widths would be similar to that for the energy, except for the possible modification of the energy distribution by the cracking activity (i.e. if regions in which cracks formed were not truly independent).

The energy available for propagation in a given region would be expected to increase with strain, at least until a crack formed or the secondary stage was attained. It would also be reasonable to expect that during the secondary stage of creep this energy would be normally distributed about a constant mean value. The log-normal distribution given in equation (39) does have characteristics that correspond to this behaviour. For small values of the mean crack width (i.e. small amount of energy of propagation), the distribution is strongly skewed toward the ordinate. As the mean crack width increases, the distribution tends to a normal one. No observations were made to determine if the mean crack width

was constant during the secondary stage of creep. This clearly must have been the case for stresses less than or equal to $10 \, \mathrm{kg/cm^2}$, as the cracking rate tended to zero in the secondary stage. The results indicate, therefore, that either crack initiation was independent of the energy available for propagation, or had a very special dependence on it.

The distributions shown in figure 32 are not easily calculated from the results. This calculation requires the following integration to be carried out.

$$P(c/\epsilon) = \frac{1}{n(\epsilon)} \int_{0}^{\epsilon} \frac{\partial n(\epsilon)}{\partial \epsilon} \int_{0}^{2c} p(c/\epsilon) dc d\epsilon$$
 (40)

where $P(c/\epsilon)$ is the probability of finding a crack of width \leq 2c at strain ϵ , $n(\epsilon)$ is the crack density and $p(c/\epsilon)$ the probability density for crack widths associated with the cracks formed during an increase in strain of d ϵ at strain ϵ .

The distribution for the strain dependence of the crack density is discussed in the following section.

7.4 Crack Density

Information presented in Section 7.1 on the spatial distribution of cracks indicated that the formation of a crack is not a truly independent event. The deviation of actual behaviour from random behaviour, although significant, was sufficiently small, however, that it would be reasonable to assume that a specimen could be subdivided into essentially independent regions. From this point of view, one could look at each test as being a set of concurrently run independent observations of the stress, strain, and temperature dependence of the probability for the formation of a crack within a given region.

One of the difficulties encountered in developing justification for making such an assumption, is to establish the size of the essentially independent regions. In the discussion given in Section 6.3 it was pointed out that tertiary creep was initiated for a compressive stress of $\sigma=12~{\rm kg/cm^2}$, when the crack density was about $1.6/{\rm cm^2}$. This would suggest that the regions have an area of about $0.6~{\rm cm^2}$ perpendicular to the long direction of the grains. This area would include about 6 grains, i.e. a grain and its immediate neighbors.

Whether or not a crack will form in a region will be dependent on the relative crystallographic orientation of the grains. As the orientation of the <0001> direction is random in the plane perpendicular to the long direction of the columns, all possible combinations can be expected to occur. The observations, therefore, are a sample of the population of combinations of relative orientation that are capable of producing cracks. They provide information on how this proportion of the

population depends on stress and temperature, and how it develops with strain and time.

The question can now be posed "what is the nature of the probability distribution for a crack to form within a given region?" One approach that may be valid is that of Weibull (1939, 1951). Weibull assumed that a solid (in the present case, a region) could be subdivided in an arbitrary manner into n volume elements. Let the probability of a crack being initiated in an element undergoing a strain d ε be λ (σ , ε , T) d ε ,

where σ and ϵ are the stress and strain at the element. The probability that a crack has been formed in the element after a strain ϵ is $\int_0^\epsilon \lambda d\epsilon$. The probability that a crack has not been formed is $1 - \int_0^\epsilon \lambda d\epsilon$. If there are n elements, the probability that a crack does not form within the region by strain ϵ is

$$1-P = \left(1 - \int_{0}^{\varepsilon} \lambda_{1} d\varepsilon\right) \left(1 - \int_{0}^{\varepsilon} \lambda_{2} d\varepsilon\right) \cdots \left(1 - \int_{0}^{\varepsilon} \lambda_{n} d\varepsilon\right) (41)$$

where $P(\sigma,~\epsilon,~T) \text{ is the probability distribution}$ for a crack to form in a given region, and $\lambda_{1} \text{ is the value of } \lambda \text{ for each element.}$

Now

$$\ln(1 - P) = \sum_{i=1}^{n} \ln(1 - \int_{0}^{\varepsilon} \lambda_{i} d\varepsilon)$$
 (42)

If n is sufficiently large, $\int_{0}^{\epsilon} \lambda_{i} d\epsilon << 1$ and

$$\ln(1 - P) \simeq -\sum_{i=1}^{n} \int_{0}^{\varepsilon} \lambda_{i} d\varepsilon$$
 (43)

Variations of λ within the region must be due to structural factors and variations in the stress and strain. If the variations in stress and strain are continuous, it should be possible to replace equation (41) by

$$\sum_{i=1}^{n} \int_{0}^{\varepsilon} \lambda_{i} d\varepsilon = \phi(\sigma, \varepsilon, T)$$
 (44)

where now σ and ϵ are the applied stress and strain respectively. Therefore,

$$P = 1 - \exp(-\phi) \tag{45}$$

The question can now be asked, "does φ have a simple dependence on ϵ ?" Assume $\varphi = \varphi_1 \epsilon^m$. Then

$$\log \ln(1 - P) = -\log \phi_1 - m \log \varepsilon$$
 (46)

The observations on the strain dependence of the crack density for $\sigma \leqslant 10 \text{ kg/cm}^2$ and $\overline{T} = -4.8^{\circ}\text{C}$, -9.5°C and -14.8°C , given in figure 19, were converted into probability distributions, (P), by dividing by the estimated maximum density. In figure 36, the logarithm of $\ln(1-P)$ is plotted against the logarithm

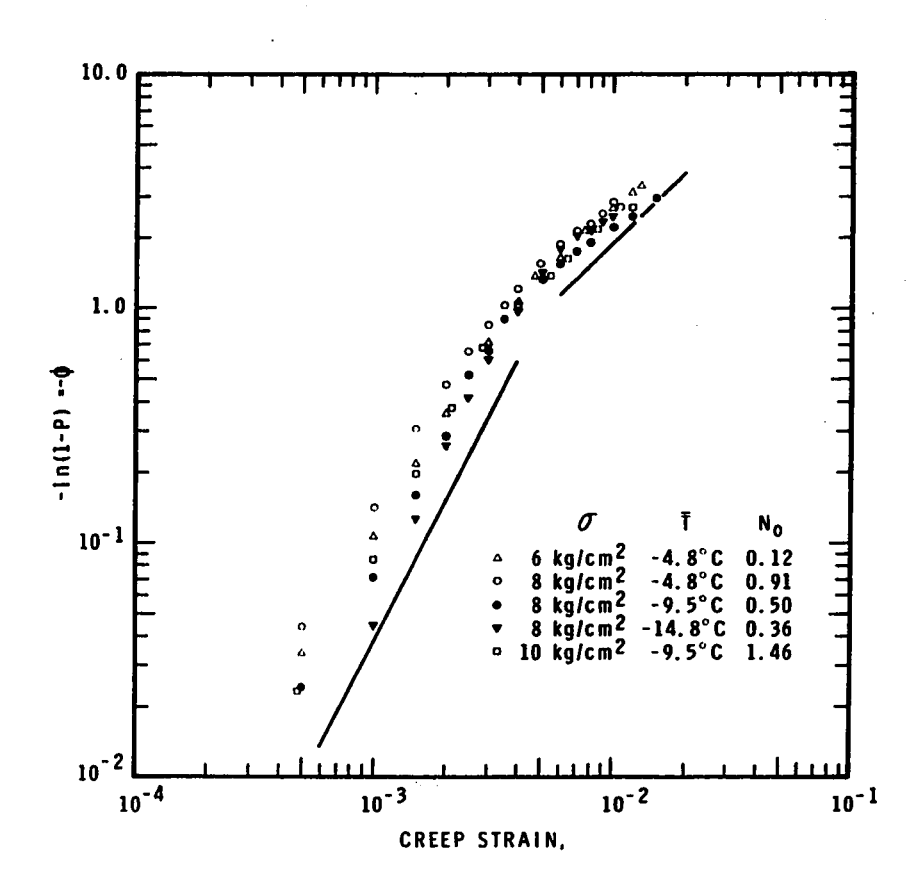


FIGURE 36 LOG [In(1-P)] VS LOG \mathcal{E} , σ = 10 kg/cm²; P IS THE PROBABILITY DISTRIBUTION FOR THE CRACKING ACTIVITY, N₀ IS THE ESTIMATED MAXIMUM CRACK DENSITY

of ϵ for each of the distributions. Given also in the figure is the estimated maximum density, N₈, for each case.

It can be seen that the observations define a curve rather than a straight line. Lines with slopes, m, equal to 1 and 2 are drawn on the figure. The line with a slope of 2 is approximately parallel to the observations for strains less than 4×10^{-3} ; the line with slope 1 for strains greater than 5×10^{-3} . This suggests that the observed distribution is made up of two independent distributions (Weibull, 1939).

Let the distribution with a slope of one be P_1 and the one with a slope of two be P_2 . Assume that they are present in the proportion α so that

$$P = \alpha P_1 + (1 - \alpha) P_2$$
 (47)

Let

$$P_1 = 1 - \exp(-A\varepsilon) \tag{48}$$

$$P_2 = 1 - \exp(-B\epsilon^2) \tag{49}$$

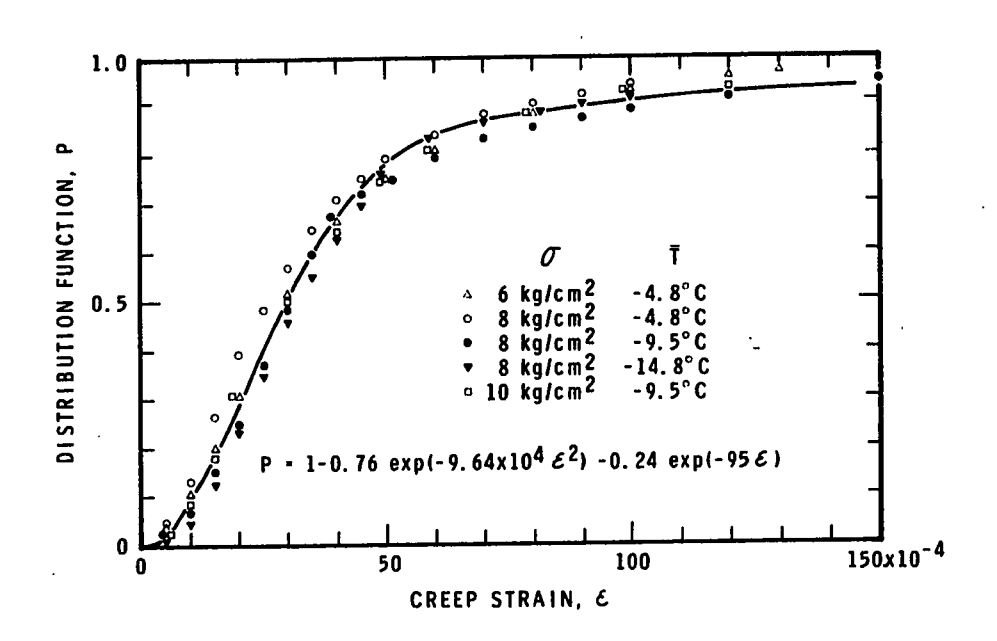
where A and B are functions of σ and T only. The substitution of equations (48) and (49) into (47) gives

1 - P =
$$\exp(-B\epsilon^2)$$
 + α [$\exp(-A\epsilon)$ - $\exp(-B\epsilon^2)$] (50)

The observed distributions are plotted against the strain in figure 37. From figure 37, the strains corresponding to $P=0.9,\ 0.5$ and 0.2, were estimated, and were used to determine A, B and α in equation (50). The resulting equation is presented and plotted in the figure. This equation does provide a good fit to the observations, and thereby, supports the validity of the assumptions that have been made. Figures 36 and 37 also show that α and T have a significant effect on No, but only a secondary effect, if any, on A, B and α for the range of stress and temperature covered.

The final equation is not unreasonable when considered from the physical point of view. $\phi = B\epsilon^2$ indicates that $\lambda_1 = B'\epsilon$, i.e. the probability for the nucleation of a crack in an element of a region increases directly with strain. This is the behaviour that would be expected for crack nucleation due to the pile-up of dislocations. For $\phi = A\epsilon$, λ_1 would be independent of the strain. This could occur if nuclei of various sizes were present, and these grew by a diffusion process until of sufficient size to initiate a crack. It is of interest to note that about 25% of the cracks occurred at grain boundaries. Observations were not made to determine if the grain boundary cracks corresponded to the P_1 distribution.

5.1



The probability density for the cracking activity is given by

$$\frac{\partial P}{\partial \varepsilon} = (1 - \alpha) B\varepsilon \exp (-B\varepsilon^2) + \alpha A \exp (-A\varepsilon)$$

$$= \frac{1}{N_0} \frac{\partial N}{\partial \varepsilon}$$
(51)

where $N(\sigma, \, \epsilon, \, T)$ is the observed crack density at strain ϵ and N_6 is the maximum crack density. Calculated values of $\frac{1}{N_6} \frac{\partial N}{\partial \epsilon}$ for $\overline{T} = -9.5^{\circ}C$ and $\sigma = 6$, 8 and 10 kg/cm^2 , are plotted in figure 38. Equation (51) is also plotted in the figure, using the values for α , A and B given in figure 37.

According to equation (51), there was a finite probability for crack formation when the load was applied. This finite probability is associated with the P₁ distribution. It was pointed out earlier that crack formation during the application of the load (see figure 24) was mainly at grain boundaries. If this initial cracking activity was part of the P₁ distribution, it would be a further indication that this distribution is associated with grain boundary cracks. The quiescent period immediately following the application of the load would simply reflect the initial knee in the probability distribution shown in figure 37.

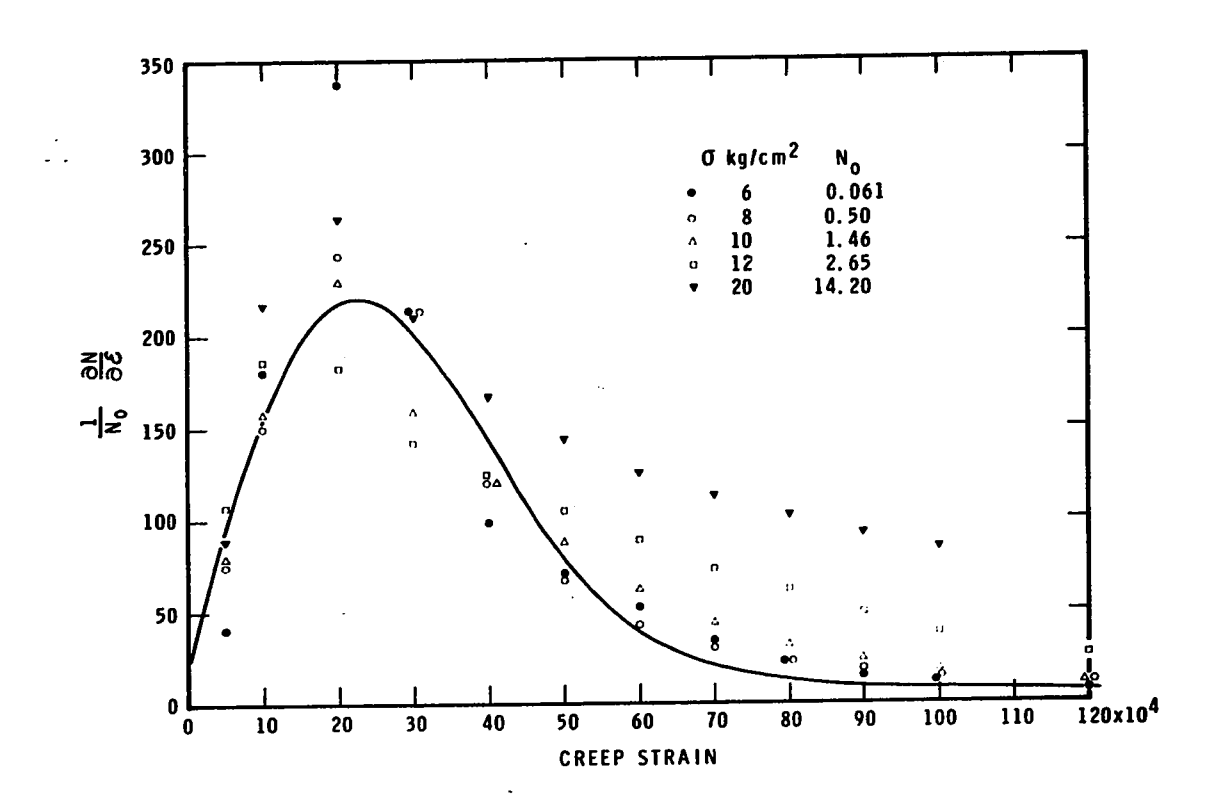


FIGURE 38 THE PROBABILITY DENSITY FOR THE CRACKING ACTIVITY, $\,$ T = -9.5°C

If the P_1 distribution is associated with grain boundary cracking, at least part of the elastic strain (which was about 4×10^{-4} for $\sigma = 20 \text{ kg/cm}^2$ and $\overline{T} = -4.8^{\circ}\text{C}$ in the present study) should probably be taken into consideration with respect to it (i.e. $\epsilon = 0$ for the P_1 distribution is at some strain between the unloaded and fully loaded condition). This would account for the finite probability for crack formation during the application of the load. As pointed out in Section 6.1, subtraction of this initial cracking activity from the subsequent activity had no effect on the calculation of the cracking rate, $\frac{\partial N}{\partial \epsilon}$, and only a small effect on the densities presented in figures 17, 18 and 19.

The observations indicated that the cracking activity was continuous for stresses greater than 12 kg/cm², and non-uniform once tertiary creep had been developed. It was not possible, therefore, to estimate a value for No for this stress condition. Equation (50) shows, however, that the crack densities at strain ε hold the same relation to each other as the maximum densities. It is possible, therefore, to use equation (34) (i.e. N = $(\sigma - C)^n$) to estimate the maximum crack densities that would have occurred if the failure condition (tertiary creep) had not developed. Values of No for $\sigma = 12$ and 20 kg/cm² and $\overline{T} = -9.5^{\circ}C$, were obtained in this way, assuming n in equation (34) to be equal to 3.3. The values calculated for $\frac{1}{N_0}$ $\frac{\partial N}{\partial \varepsilon}$ for

these two stresses are presented in figure 38. The maximum values for the probability density are seen to be in reasonable agreement with that given by equation (51). The densities for these stresses are appreciably greater than those given by the calculated curve, however, for strain greater than 50 x 10^{-4} . This is considered to reflect the failure condition.

The cracking rate does appear to continuously decrease with strain even for the larger stresses. It should be recalled, however, that the tertiary stage was well developed by a strain of 50 x 10⁻⁴ for stresses greater than 12 kg/cm², and that the cracking activity for this condition was often confined to zones approximately parallel to the planes of maximum shear (i.e. non-uniform). As these zones became highly cracked, the need for continued cracking would be reduced. This is so because once crack formation becomes non-random, the need for cracks to form would decrease as the non-cracked regions became smaller. This, as well as the difficulty of visually observing all cracking activity in the highly cracked regions, could explain the continuous decrease in cracking rate that was observed for the larger stresses.

Ninety-nine percent of the cracks associated with the P_2 distribution had formed by the time the strain was 70 x 10^{-4} . According to the interpretation that has been developed, therefore, the dislocation pile-ups must have been pretty well at

their steady state length by this strain. This is consistent with the observation that the new modes of deformation in previously undeformed type S2 ice are established mainly during the transient creep stage.

The analysis of the time and strain to the formation of the first three large cracks was made with the implicit assumption that they were nucleated by dislocation pile-ups. Observations made on their mode of propagation showed that both transcrystalline and grain boundary cracks were involved. This may have contributed to the scatter in the observations. Attention should be given to the mode of propagation in future studies of the time to formation of cracks in ice.

7.5 Discussion

Failure is a form of structural instability. The observations made indicated that for the type of material used, and the conditions imposed, it can be induced by the deterioration of the structure due to essentially independent events, i.e. a random process. Such events are local in character, and involve a conversion of energy. The energy conversion associated with each random event can occur rapidly, as in the formation of a crack, or slowly, as in the formation of a cavity. The process that is most significant in a region would depend on the relative orientation of the grains at the site, the nature of the imperfections present, the stress and the temperature.

The results presented on the statistical characteristics of the cracking activity provide additional insight concerning the failure mechanisms in ice discussed in Sections 3.5 and 3.6. Of particular significance is the probability of two independent crack distributions; one with a probability for crack initiation proportional to strain, and one with a probability independent of strain. The observations showed that when the stress was sufficiently large to induce the failure condition, the initial part of the probability distribution for the cracking activity still behaved as though there was a fixed total number of crack nucleating sites. Crack density observations for strains less than that associated with the onset of failure showed that this apparent total number of cracks depended mainly on stress and temperature.

The onset of instability associated with failure involved both the stress and the degree of deterioration of the structure. The higher the stress, the larger was the number of cracks formed in a given strain. Both the higher stress and the increased cracking activity must have contributed to the reduction observed in the strain to failure. According to the interpretation of the probability distribution for the crack density presented in Section 7.4, this implies that the higher the stress, the more significant, initially, was the role of grain boundary cracking. If the stress was sufficiently high,

presumably grain boundary cracking alone could cause the breakdown in structure necessary to induce instability.

This behaviour has been observed by the author under conditions of rapid rates of strain (unpublished). For strain rates approaching and greater than that associated with the ductile to brittle transition, the initial cracking activity was uniformly distributed over the specimens, and mainly at grain boundaries. In this brittle region, failure occurred abruptly by the formation of fault zones. The failure was explosive, and the ice from the fault zones highly shattered. At strains near the ductile to brittle transition, yielding sometimes occurred, followed by abrupt failure. This yielding did indicate that a contribution from the P2 distribution (i.e. cracks due to dislocation pile-ups) was required to break down the structure to the extent necessary for abrupt and complete failure. It was clear that within the ductile region, the stress and the cracking activity were not adequate to cause the structure to lose all of its resistance to deformation. Rates of strain were such that the non-cracked regions were able to conform to it and bonds between these regions were able to remain intact.

As the events responsible for the deterioration of the structure can be described statistically, it should be possible, in principle, to define the failure condition in terms of the

characteristics of the relevant distributions, and their dependence on stress, strain, temperature and time, without reference to the processes responsible for crack formation.

This would be roughly equivalent to measuring the pressure of a gas rather than claculating it from a knowledge of the motion of its molecules. A proper understanding of the failure process and how it is affected by stress, strain, temperature and time, can only be obtained, however, from a knowledge of how these factors affect the various modes of deformation responsible for it. Only with this understanding will it be possible to establish with confidence whether the results of laboratory observations of failure are valid for the more complicated situations encountered in engineering practice.

8. CONCLUSIONS

This study of the failure process was carried out on a columnar-grained material having hexagonal crystallographic symmetry. Each grain had a preferred crystallographic orientation such that its basal planes tended to be parallel to the columnar axis, but otherwise random in direction. Specimens were prepared so that the load was applied perpendicularly to the long direction of the columns. They were maintained at a temperature within 40C degrees of their melting point; no evidence was seen of structural changes due to thermal stress. When the loads were first applied, each grain had, effectively, only one direction of glide for dislocations, and that was in the basal plane perpendicular to the columnar axis. mation, therefore, was essentially two dimensional, and remained so for the range of strain covered in the tests. Attention was given to the deformation and failure behaviour that occurred due to a constant compressive stress. The conclusions derived from this study follow:

- (1) Crack formation is induced in columnar-grained type S2 ice when the compressive stress exceeds about 6 kg/cm². This critical stress increases with decreasing temperature.
- (2) Crack initiation prior to the failure condition is essentially a random process, and is probably independent of

the energy available for propagation. The energy available for crack propagation, as indicated by the crack width, probably has a distribution of the log-normal type, with a standard deviation independent of strain, at least during the initial part of the deformation.

- (3) The strain dependence of the crack density involves two
 Weibull type distributions, one of which is probably associated with cracks nucleated by dislocation pile-ups or
 similar type of stress concentration, and the second with
 grain boundary cracks. The probability for a crack to
 initiate at a site is proportional to the strain in the
 first case, and independent of it in the second.
- (4) Random crack formation results in a deterioration of the structure. At some stage, depending mainly on the stress, the deterioration is sufficient to cause structural instability. If the compressive stress is less than or equal to 10 kg/cm², deterioration of the structure due to crack formation is not sufficient to cause structural instability during the primary creep stage, and the secondary stage can develop. If the compressive stress is greater than or equal to 12 kg/cm², structural instability is induced during primary creep, and the primary stage is transformed directly to the tertiary stage.

- (5) The cracking activity is a depletion type process, and for stress less than or equal to 10 kg/cm², the sites available for crack initiation decrease with strain so that the cracking rate tends to zero in the secondary creep stage. For stress greater than or equal to 12 kg/cm², there is probably a continuous generation of new crack nucleating sites once structural instability has been established.
- (6) There is a maximum in the strain dependence of the cracking rate that occurs in the range of strain 10×10^{-4} to 25×10^{-4} . This maximum is probably associated with the cracks initiated by dislocation pile-ups or similar strain-dependent stress concentrations.
- (7) The apparent activation energy for creep decreases from about 0.91 eV (21 kcal/mole) within 15C degrees of the melting point, to a value tending to that for self-diffusion for temperature less than -35°C.
- (8) Dislocation pile-ups probably attain their maximum length within the first 70 \times 10⁻⁴ strain.
- (9) An edge effect exists for deformation and failure of ice. This edge effect extended inwards about two centimeters (about ten grain diameters) in the present study.

9. RECOMMENDATIONS FOR FUTURE RESEARCH

The work reported in this thesis was the first study that has been carried out on the cracking activity in ice during deformation, and the role that crack formation plays in establishing the failure condition. It has demonstrated that meaningful studies of the deformation behaviour of ice due to large stresses cannot be undertaken without giving attention to this activity, particularly its relationship to modes of deformation and recovery.

It was suggested in Section 6 that the stress, temperature, time and strain dependence of the crack density was determined by the relative contribution of the various modes of deformation and recovery. This is still to be proven by theory and experiment. Attention should be given to clearly establishing the significant modes of deformation and recovery in ice, their stress and temperature dependence and methods of measuring their contribution to the strain and internal stress. Attention should also be given to the temperature and stress dependence of the apparent activation energy of polycrystalline ice.

Information obtained from such studies would help establish if the relative contribution of the modes of deformation and recovery do change with temperature.

The present work has shown that ice is a useful material for the study of crack initiation. Studies should be undertaken to prove definitely if dislocations can be responsible for the nucleation of transcrystalline cracks in ice. Observations by the author did show that at least one edge of transcrystalline cracks was usually associated with a grain boundary. This suggests that initiation may be due to the coalescence of the dislocations at the head of a pile-up, or to the high tensile stress existing at the head of a pile-up in an adjacent grain. This question could be studied both theoretically and experimentally.

Further investigations should be carried out on the characteristics of the strain dependence of the crack density to confirm:

- (1) The cracking activity involves two independent distributions.
- (2) One of these distributions is associated with dislocation or similar type cracks, and the second with grain boundary cracks.
- (3) The cracking activity has a compound Weibull type distribution.

- (4) Cracking activity becomes insignificant in the secondary stage of creep.
- (5) Crack initiation is independent of propagation.

Theoretical studies are required on the cracking activity to determine if the characteristics of it can provide useful information concerning deformation processes (e.g. the characteristics of the crack density and crack orientation distributions). Attention could be given to the statistical description of the failure process in ice, particularly in relation to the ductile to brittle transition.

The crack width studies indicated a potentially useful method of studying the characteristics of the distribution in the energy available for crack propagation. This possible method could be explored both theoretically and experimentally. It should be confirmed if the "standard deviation" of the distribution in crack widths is independent of the strain. If this is so, it suggests the existence of a constant of a nature similar to the Boltzman constant in statistical mechanics.

Finally, it must be pointed out that the present study was carried out with type S2, columnar-grained ice subjected to a uniaxial compressive stress. The characteristics of the cracking activity of other types of ice are still to be investigated. The results of such studies would provide additional

appreciation of the influence of crystallographic orientation on the deformation and failure behaviour of polycrystalline materials. Attention should be given to relating the failure behaviour of ice to that of other materials. This could provide useful insight into behaviour that is all two often ignored in laboratory investigations of strength.

The whole subject of the failure behaviour of ice under biaxial and triaxial stress fields is still to be explored.

These studies are necessary to provide the proper understanding of the strength of ice required for the solution of engineering problems.

BIBLIOGRAPHY

Anantha, N.G. and Chalmers, B., 1967, Jour. App. Phys., 38, 4416.

Argon, A.S. and Orowan, E., 1964, Phil. Mag., 9, 1023.

Armstrong, R.W., 1961, J. Mech. Phys. Solids, 9, 196.

Armstrong, R., Codd, I., Douthwaite, R.M. and Petch, N.J., 1962, Phil. Mag., $\frac{7}{2}$, 45.

ASTM, 1965, Symposium of Fracture Toughness Testing and its Applications, ASTM Special Pub. No. 381. Philadelphia, U.S.A.

Balluffi, R.W. and Seigle, L.L., 1957, Acta Metal., 5, 449.

Barnes, W.H., 1929, Proc. Roy. Soc. Lond., Ser. A, 125, 670.

Bartenev, G.M. and Zuyev, Yu.S., 1968, Strength and Failure of Visco-elastic Materials, Pergamon Press, p. 164.

Basinski, Z.S. and Mitchell, T.E., 1966, Phil. Mag., 13, 103.

Beach, C.W., Munn, A.M. and Reeves, H.E., 1894-1895, Technograph, 9, 38.

Beevers, C.J. and Halliday, M.D., 1968, Jour. Mater. Sci., 3, 660.

Bell, G.G., 1911, Proc. Main Soc. Civil Eng., $\underline{1}$, 41.

Bernal, J.D. and Fowler, R.H., 1933, J. Chem. Phys., 1, 515.

Bilby, B.A. and Hewitt, J., 1962, Acta Metal., 10, 587.

Bishop, J.W. and Hill, R., 1951, Phil. Mag., 42, 1298.

Bjerrum, N., 1951, Dan. Mat. Fys. Medd., 27, 3.

Bjerrum, N., 1952, Sci., 115, 385.

Blakey, F.A. and Beresford, F.D., 1955, Civil Eng. and Pub. Works Rev., 50, 410.

- Boettner, R.C. and Robertson, W.D., 1961, Trans. Metal. Soc. AIME, 221, 613.
- Brace, W.F., 1960, Jour. Geophys. Res., 65, 3477.
- Brace, W.F. and Bombolalsio, E.G., 1963, Jour. Geophys. Res., 68, 3709.
- Brace, W.F., Paulding, B.W. and Scholz, C., 1966, Jour. Geophys. Res., <u>71</u>, 3939.
- Brace, W.F. and Orange, A.S., 1966, Sci., 153, 1525.
- Bridgman, P.W., 1949, Jour. App. Phys., 20, 1241.
- Briggs, A., Clarke, F.J.P. and Tattersall, H.G., 1964, Phil. Mag., 9, 1041.
- Bromer, D.J. and Kingery, W.D., 1968, Jour. App. Phys., 39, 1688.
- Brown, E., 1926, Experiments on the Strength of Ice, St. Lawrence Waterway Project, Rept. Joint Board Eng., App. F., Ottawa, 423.
- Bryant, G.W. and Mason, B.J., 1960, Phil. Mag., 5, 1221.
- Bullough, R., 1964, Phil. Mag., 9, 917.
- Butkovich, T.R., 1954, Ultimate Strength of Ice, Res. Paper No.

 11, Cold Regions Research and Eng. Lab., U.S. Corps of Eng.,
 Hanover, N.H.
- Butkovich, T.R., 1955, Crushing Strength of Lake Ice, Res. Paper
 No. 15, Cold Regions Research and Eng. Lab., U.S. Corps of
 Eng., Hanover, N.H.

- Butkovich, T.R., 1958, Recommended Standards for Small Scale

 Ice Strength Tests, Tech. Rept. 57, Cold Regions Research

 and Eng. Lab., U.S. Corps of Eng., Hanover, N.H.
- Butkovich, T.R. and Landauer, J.K., 1959, The Flow Law for Ice,
 Res. Rept. 56, U.S. Army Cold Regions Research and Eng.
 Lab., Hanover, N.H.
- Butkovich, T.R. and Landauer, J.K., 1960, Creep of Ice at Low Stresses, Res. Rept. 72, Cold Regions Research and Eng. Lab., U.S. Army Corps of Eng., Hanover, N.H.
- Byerlee, J.D., 1967, Jour. Geophys. Res., 72, 3639.
- Chen, W.T., 1964, Phil. Mag., 9, 1207.
- Clarke, F.J.P., Samble, R.A. and Tattersall, H.G., 1962, Phil. Mag., 7, 393.
- Cottrell, A.H., 1958, Trans. Metal. Soc., AIME, 212, 192.
- Cottrell, A.H., 1963, Tewksbury Symposium on Fracture, Eng. Faculty, Univ. of Melbourne, 1965, 1.
- Cottrell, A.H., 1964, Proc. Roy. Soc., 276, 1.
- Davidson, T.E., Uy, J.C. and Lee, A.P., 1966, Acta Metal., 14, 937.
- Davies, P.W. and Dennison, J.P., 1958-59, Jour. Inst. Metals, 87, 119.
- Davies, P.W., Williams, K.R. and Wilshire, B., 1968, Phil. Mag., 18, 197.
- Dengel, O. and Riehl, N., 1963, Phys. Kondens. Materie., $\underline{1}$, 191.
- Dengel, O., Jacobs, E. and Riehl, N., 1966, Phys. Kondens.

 Materie., <u>5</u>, 58.

- Dieter, G.E., 1961, Mechanical Metallurgy, McGraw Hill, New York, p. 200.
- Dillon, H.B. and Andersland, O.B., 1967, Physics of Snow and Ice, Inst. Low Temp. Sci., Hokkaido Univ. Japan, 1, 313.
- Dorsey, N.E., 1940, The Properties of Ordinary Water Substance, Rheinhold Pub. Corp., New York.
- Dower, R.J., 1967, Acta Metal., 15, 497.
- Eshelby, J.D., 1949, Phil. Mag., 40, 903.
- Eshelby, J.D., Frank, F.C. and Nabarro, F.R.N., 1951, Phil. Mag., <u>42</u>, 351.
- Feller, W., 1957, An Introduction to Probability Theory and its Application, Vol. I, 2nd edition. John Wiley, New York.
- Francois, D. and Wilshaw, T.R., 1968, Jour. Appl. Phys., 39, 4170.
- Fukuda, A. and Higashi, A., 1969, Physics of Ice, Proc. Int.
 - Symp. on Ice, Munich, Plenum Press, New York, p. 239.
- Garofalo, F., 1965, Fundamentals of Creep and Creep-Rupture in Metals, MacMillan, Toronto, p. 177.
- Gentile, A.L. and Drost-Hansen, W., 1956, Naturwiss, 43, 274.
- Gervais, A.M., Norton, J.T. and Grant, N.J., 1953, Trans. AIME, 197, 1487.
- Gibbs, G.B., 1965, Mem. Sci. Rev. Metall., 62, 775.
- Gibbs, G.B., 1968, Mat. Sci. and Eng., $\underline{2}$, 269.
- Gifkins, R.C., 1959, Fracture, Proc. Swampscott Conf., John Wiley, New York, 579.

Gifkins, R.C., 1963, Proc. 1st Tewksbury Symp., Univ. Melbourne, Melbourne, Australia, 44.

Gilman, J.J., 1953, Acta Metall., 1, 426.

Gilman, J.J., 1958, Trans. AIME, Metal. Soc., 212, 783.

Gittins, A. and Williams, H.D., 1967, Phil. Mag., 16, 849.

Glen, J.W., 1953, Nature, 172, 721.

Glen, J.W. and Perutz, M.F., 1954, Jour. Glac., 2, 397.

Glen, J.W., 1955, Proc. Roy. Soc. (A), 228, 519.

Glen, J.W. and Jones, S.J., 1967, Physics of Snow and Ice, Inst. Low Temp. Sci., Hokkaido Univ., Japan, $\underline{1}$, 267.

Glen, J.W., 1968, Phys. Kond. Materie., 7, 43.

Gold, L.W., 1958, Can. Jour. Phys., 36, 1265.

Gold, L.W., 1960, Can. Jour. Phys. 38, 1137.

Gold, L.W., 1963a, Ice and Snow, edited by W.D. Kingery, M.I.T. Press, 8.

Gold, L.W., 1963b, Can. Jour. Phys. 41, 1712.

Gold, L.W., 1965, Pt. I and II, Can. Jour. Phys., 43, 1414.

Gold, L.W., 1966, Can. Jour. Phys., 44, 2757.

Gold, L.W., 1967, Physics of Snow and Ice, Inst. Low Temp. Sci., Hokkaido Univ., $\underline{1}$, 359.

Gold, L.W., 1968, Ice Pressures Against Structures, T.M. 92,

Assoc. Comm. Geotech. Res., Nat. Res. Council, Ottawa, 13.

Granicher, H., Jaccard, C., Scherrer, P. and Steinemann, A., 1957, Far. Soc. Disc., No. 23.

Granicher, H., 1958, Z. Kristallogr., 110, 432.

- Granicher, H., 1963, Phys. Kondens. Materie., 1, 1.
- Greenwood, J.N., Miller, D.R. and Suiter, J.W., 1954, Acta Metal., $\underline{2}$, 250.
- Griffith, A.A., 1921, Phil. Trans. Roy. Soc., A, 221, 163.
- Griggs, D.T. and Coles, N.E., 1954, Creep of Single Ice Crystals,
 Rept. 11, U.S. Army Cold Regions Research and Eng. Lab.,
 Hanover, N.H.
- Griggs, D. and Handin, J., 1960, Observations on Fracture and a Hypothesis of Earthquakes, Rock Deformation, Mem. 79, Geol. Soc. Amer. Ed. D. Griggs and J. Handin.
- Groves, G.W. and Kelly, A., 1963, Phil. Mag., 8, 877.
- Groves, G.W. and Kelly, A., 1969, Phil. Mag., 19, 977.
- Haas, C., 1962, Phys. Letters, 3, 126.
- Hahn, G.T., Averbach, B.L., Owen, W.S. and Cohen, M., 1959, Fracture, Proc. Swampscott Conf. John Wiley, p. 91.
- Halbrook, T.R., 1962, Mechanical Properties of Ice, M.Sc. Thesis, Dept. Civil Eng., Michigan State Univ.
- Hansen, T.C., 1968, Causes, Mechanisms and Control of Cracking in Concrete, Pub. SP-20, Amer. Concrete Inst., p. 43.
- Harrison, J.D. and Tiller, W.A., 1962, Controlled Freezing of Water, Sci. Paper 925-11601-P1, Westinghouse Res. Lab., Pittsburgh, Penn.
- Harrison, J.D. and Tiller, W.A., 1963a, Jour. App. Phys., 34, 3349.
- Harrison, J.D. and Tiller, W.A., 1963b, Ice and Snow, Ed.
 - Kingery, W.D., M.I.T. Press, Cambridge Mass., 215.

Hauser, J.J. and Chalmers, B., 1961, Acta Metal., 9, 802.

Head, A.K. and Louat, N., 1955, Austr. Jour. Phys., 8, 1.

Head, A.K., 1960, Austr. Jour. Phys., 13, 613.

Herring, C., 1950, Jour. App. Phys., 21, 437.

Heslop, J., 1962-63, Jour. Inst. Metals, 91, 28.

Hesstvedt, E., 1964, The Interfacial Energy Ice/Water, Norwegian Geotech. Inst. Pub. 56, Oslo, Norway.

Higashi, A. and Sakai, N., 1961, Jour. Fac. Sci., Hokkaido
Univ., Japan, Ser. II, 5, 221.

Higashi, A., Koinuma, S. and Mae, S., 1964, Jap. Jour. App. Phys., 3, 610.

Higashi, A., Koinuma, S. and Mae, S., 1965, Jap. Jour. App. Phys., 4, 575.

Higashi, A., 1967, Physics of Snow and Ice, Inst. Low Temp. Sci., Hokkaido Univ., Japan, $\underline{1}$, 277.

Higashi, A., Mae, S. and Fukuda, A., 1968, Trans. Jap. Inst.

Metals, 9, 784.

Higuchi, K., 1958, Acta Metall., 6, 636.

Hillig, W.B., 1958, The Kinetics of Freezing of Ice in the

Direction Perpendicular to the Basal Plane, Growth and

Perfection of Crystals, John Wiley & Sons, New York, p. 350.

Hollomon, J.H., 1948, Fracture of Metals, Amer. Soc. Metals, 262.

Hull, D. and Rimmer, D.E., 1959, Phil. Mag., $\underline{4}$, 673.

Inglis, C.E., 1913, Trans. Inst. Naval Archit., 55, 219.

Irwin, G.R., 1948, Fracture of Metals, ASM, Cleveland.

Irwin, G.R., 1960, Fracture Mechanics, in Structural Mechanics, Pergamon Press, London.

Irwin, G.R., 1957, Jour. App. Mech., 24, 361.

Isenberg, J., 1968, Causes, Mechanisms and Control of Cracking in Concrete, Pub. SP-20, AC I, p. 29.

Jaccard, C., 1959, Helv. Phys. Acta, 32, 89.

Jaccard, C., 1965, New York Acad. Sci., 125, 390.

Jellinek, H.H.G. and Brill, R., 1956, Jour. App. Phys., 27, 1198.

Jellinek, H.H.G., 1958, Proc. Phys. Soc., 71, 797.

Jellinek, H.H.G., 1962, Plastic Deformation of Thick-Walled

Snow-Ice Cylinders Under Hydrostatic Pressure, Can. Jour.

Phys., 40, 1310.

Johnston, T.L., Davies, R.G. and Stoloff, N.S., 1965, Phil. Mag., 12, 305.

Johnston, W.G., 1960, Phil. Mag., <u>5</u>, 407.

Johnston, W.G., 1962, Jour. App. Phys., 33, 2716.

Jonas, J.J., 1969, Acta Metall., 17, 397.

Jonas, J.J., Sellars, C.M., Tegart, W.J. McG., 1969, Strength and Structure Under Hot Working Conditions, Review No. 130, Metall. Rev., 14, 1.

Jonas, J.J. and Müller, F., 1969, Can. Jour. Earth Sci., 6, 963.

Jones, R., 1952, Brit. Jour. App. Phys., 3, 229.

Jones, R., 1958, The Failure of Concrete Test Specimens in Compression and Flexure, Mechanical Properties of Non-Metallic-Brittle Materials, Butterworths, 1958.

Jones, S.J., 1967, Phys. Let., 25A, 366.

Jones, S.J. and Glen, J.W., 1967, The Mechanical Properties of Single Crystals of Ice at Low Temperatures, I.A.S.H.,

I.U.G.G., Snow and Ice Comm., Gen. Assembly Bern, 326.

Jones, S.J. and Glen, J.W., 1969, Phil. Mag., 19, 13.

Kaechele, L.E., 1967, A Statistical Investigation of Cleavage Microcrack Formation in Polycrystalline Iron, Ph.D. Dissertation, Div. of Eng. Mech., Stanford Univ., Stanford, Calif.

Kaechele, L.E. and Tetelman, A.S., 1969, Acta Metall., <u>17</u>, 463. Kamb, W.B., 1961, Jour. Glac., <u>3</u>, 1097.

Kamdar, M.H. and Westwood, A.R.C., 1968, Acta Metall., 16, 1335.

Kaplan, M.F., 1961, Jour. Amer. Concr. Inst., 58, 591.

Kenny, P. and Campbell, J.D., 1968, Prog. Mater. Sci., 13, 135.

Ketcham, W.M. and Hobbs, P.V., 1967, Jour. Crys. Growth, $\underline{1}$, 263.

Kocks, U.F., 1964, Phil. Mag., 10, 187.

Kräger, F.A., 1964, The Chemistry of Imperfect Crystals, John Wiley, p. 752. (North Holland and Interscience)

Krausz, A.S., 1961, Jour. Glac., <u>3</u>, 1003.

Krausz, A.S., 1963, Can. Jour. Phys., 41, 167.

Krausz, A.S., 1968a, Acta Metall., 16, 897.

Krausz, A.S., 1968b, Scripta Metall., $\underline{2}$, 615.

Krausz, A.S., 1969, Mat. Sci. and Eng., 4, 193.

Ku, R.C. and Johnston, T.L., 1964, Phil. Mag., $\underline{9}$, 231.

Kume, K., 1961, Jour. Phys. Soc. Japan, 16, 290.

Landau, L.D. and Lifshitz, E.M., 1958, Statistical Physics, Pergamon Press, London.

Livingston, J.D. and Chalmers, B., 1957, Acta Metall., 5, 322.

Lonsdale, K., 1958, Proc. Roy. Soc., A, 247, 424.

Low, J.R., 1954, Trans. ASM, 46A, 163.

Low, J.R., 1963, The Fracture of Metals, Prog. in Mater. Sci., 12, No. 1.

Louat, N. and Wain, H.L., 1959, Fracture, John Wiley, New York, p. 161.

Ludlow, W., 1884, Proc. Eng. Club Philadelphia, 4, 93.

Macklin, W.C. and Ryan, B.F., 1965, Jour. Atm. Sci., 22, 452.

Mae, S., 1968, Phil. Mag., 18, 101.

McClintock, F.A. and Walsh, J.B., 1962, Proc. Fourth U.S.

National Congress of App. Mech., 2, 1015.

McConnel, J.C., 1891, Proc. Roy. Soc. (Lond.), 49, 323.

McConnel, J.C. and Kidd, D.A., 1888, Proc. Roy. Soc. (Lond.), 44, 331.

McEvily, A.J. and Johnston, T.L., 1967, Int. Jour. Fract. Mech., 3, 45.

McLean, D., 1956-57, Jour. Inst. Metals, 85, 468.

McMahon, C.J., 1964, Micromechanisms of Cleavage Fracture in Polycrystalline Iron, SSC-161, Ship Structure Committee, Washington, D.C.

Michel, B., 1969, River Ice Engineering, (a) Winter Regime of
Rivers and Lakes, Monograph 111-Bla, U.S. Army Cold Regions
Research and Eng. Lab., Hanover, N.H.

Michel, B. and Ramseier, R.O., 1969, Classification of River and Lake Ice Based on its Genesis, Structure and Texture, Rept. S-15, Département de Génie Civil, Université Laval, Québec, Qué.

Mogi, K., 1966, Bull. Earthquake Res. Inst., 44, 215.

Morrisson, R.G.K., 1963, Trans. Can. Mining and Metal., 66, 394.

Muguruma, J., 1961, Jour. Electronmicroscopy, 10, 246.

Muguruma, J., 1963, Jour. Fac. Sci., Hokkaido Univ., Ser. II, $\underline{6}$, 11.

Muguruma, J. and Higashi, A., 1963, Jour. Phys. Soc. Jap., 18, 1261.

Muguruma, J., 1965, Nature, 208, 180.

Muguruma, J., Mae, S. and Higashi, A., 1966, Phil. Mag., 13, 625.

Muguruma, J., 1969, Brit. Jour. App. Phys., 2, 1517.

Mullendore, A.W. and Grant, N.J., 1963, Creep Rupture and the Tertiary Stage of Creep, High Temp. Structures and Materials, U.S. Office Naval Res., 169.

Murrell, S.A.F., 1964, Brit. Jour. App. Phys., 15, 1195.

Nabbaro, F.R.N., 1948, Report on Conf. on Strength of Solids, Phys. Soc. (Lond.), p. 75.

Nakaya, U., 1958, Mechanical Properties of Single Crystal Ice, Res. Rept. No. 28, U.S. Army Cold Regions Research and Eng. Lab., Hanover, N.H.

Orowan, E., 1934, Zs. Kristallogr., 89, 327.

Orowan, E., 1948-49, Fracture and Strength of Solids, Repts. Prog. in Phys., $\underline{12}$, 185.

Orowan, E., 1950, Fatigue and Fracture of Metals, Proc. M.I.T. Symp., 139.

Orowan, E., 1966, Rev. Geophys., 4, 395.

Owston, P.G., 1953, Jour. Chim. Phys., 50, C13.

Owston, P.G., 1958, Adv. Phys., 7, 171.

Pauling, L., 1935, Jour. Amer. Chem. Soc., 57, 2680.

Perey, F.G.J. and Pounder, E.R., 1958, Can. Jour. Phys., 36, 494.

Petch, N.J., 1953, Jour. Iron Steel Inst. (Lond.), 173, 25.

Petch, N.J., 1954, The Fracture of Metals, Prog. in Metals Phys., 5, 1.

Peterson, S.W. and Levy, H.A., 1957, Acta Cryst., 10, 70.

Peyton, H.R., 1968, Ice Pressures Against Structures, T.M. 92,

Assoc. Comm. Geotech. Res., Nat. Res. Council, Ottawa, 117.

Pines, B.Ya. and Sirenko, A.F., 1959, Sov. Phys., Solid State, $\underline{1}$, 247.

Price, P.B., 1963, Direct Observation of Glide, Climb and
Twinning in Hexagonal Metal Crystals, Electron Microscopy
and Strength of Crystals, Interscience Pub., 41.

Priestner, R. and Louat, N., 1965, Acta Metal., 13, 563.

Pugh, S.F., 1967, Brit. Jour. App. Phys., 18, 129.

Ramseier, R.O., 1967, Jour. App. Phys., 38, 2553.

Ramseier, R.O., 1968, Jour. Crystal. Growth, 4, 621.

Ratcliffe, R.T. and Greenwood, G.W., 1965, Phil. Mag., $\underline{12}$, 59.

Readey, D.W. and Kingery, W.D., 1964, Acta Metal., $\underline{2}$, 171.

Readings, C.J. and Bartlett, J.T., 1968, Jour. Glac., 7, 479.

Reed-Hill, R.E., 1964, Physical Metallurgy Principles, Van Nostrand, New York, p. 5.

Rice, J.R., 1965, 1st Int. Conf. Fract., Sendai, Japan, 1, 309.

Rice, J.R. and Drucker, D.C., 1967, Int. Jour. Fract. Mech., 3, 19.

Rice, J.R., 1968, Jour. App. Mechs., Trans. ASME, 35, 379.

Rohatgi, P.K. and Adams, C.M., 1966, Dendritic Freezing of Ice From Aqueous Solutions, Int. Inst. Refrig., Sub-Commission 6-B, 69.

Romualdi, J.P. and Batson, G.B., 1963, Amer. Soc. Civil Eng.,
Jour. Eng. Mech. Div., EM3, 89, 147.

Rüsch, Von H., 1959, Zement-kalk-gips, 12, 1.

Sack, R.A., 1946, Proc. Phil. Soc., 58, 729.

Sanders, J.L., 1960, Jour. App. Mechs., Trans. ASME, 27, 352.

Seigle, L. and Resnick, R., 1955, Acta Metal., 3, 605.

Sherby, O.D. and Burke, P.M., 1967, Prog. Mater. Sci., 13, 325.

Simmons, G. and Brace, W.F., 1965, Jour. Geophys. Res., 70, 5649.

Smekal, A., 1936, Ergeb Exakten Naturwiss, <u>15</u>, 106. (AERE Trans. 1023, Harwell, Eng. 1964).

Smith, E. and Worthington, P.J., 1964, Phil. Mag., 9, 211.

Smith, E. and Worthington, P.J., 1965, 1st Int. Conf. Fract.,
Sendai, Japan, 1, 12.

Smith, E., 1965, Int. Jour. Fract. Mech., 1, 204.

Smith, E., 1966a, Acta Metal., 14, 985.

Smith, E., 1966b, Acta Metal., 14, 556.

Smith, E. and Barnby, J.T., 1967, Metal. Sci. Jour., 1, 56.

- Smith, E., 1968a, Int. Jour. Fract. Mech., 4, 131.
- Smith, E., 1968b, Jour. App. Phys., 39, 4865.
- Smith, F.C. and Brown, R.Q., 1941, The Shearing Strength of Cement Mortar, Bull. Un. Wash. Eng. Exp. Station, No. 106.
- Sneddon, I.N., 1946, Proc. Roy. Soc. Lond., A, 187, 229.
- Speight, M.V. and Harris, J.E., 1967, Jour. Metal. Sci., $\underline{1}$, 83. Steinemann, S., 1954a, Jour. Glac., 2, 404.
- Steinemann, S., 1954b, Flow and Recrystallization of Ice, Pub.

 No. 39, Assoc. Int. d'Hydrol., Rome General Assembly,

 4, 449.
- Steinemann, S., 1958, Experimental Investigations of the Plasticity of Ice, Res. Trans. AMS T-G-166+, U.S. Air Force, Cambridge Res. Lab. (Bei. Zur. Geol. Karte der Schweiz, Geotech. Ser. Hydrol., No. 10).
- Stokes, R.J., Johnston, T.L. and Li, C.H., 1958, The Formation of Cracks in Magnesium Oxide Single Crystals, Honeywell Res. Centre, 1st Tech. Rept.
- Stokes, R.J., Johnston, T.L. and Li, C.H., 1959, Phil. Mag., 4, 137.
- Stokes, R.J., Johnston, T.L. and Li, C.H., 1961, Phil. Mag., 6, 9.
- Stroh, A.N., 1954, Proc. Roy. Soc. Lond., A, <u>223</u>, 404.
- Stroh, A.N., 1957, Adv. Phys., 6, 418.
- Stroh, A.N., 1958, Phil. Mag., 3, 597.

Sullivan, C.P., 1967, A Review of Some Microstructural Aspects of Fracture in Crystalline Materials, Welding Res. Council Bull. 122, New York, N.Y., 56 pages.

Taylor, G.I., 1938, Jour. Inst. Metals, <u>62</u>, 307.

Taylor, G.I., 1958, G.I. Taylor Scientific Papers, Cambridge
Univ. Press, 1, 586.

Tegart, W.J. McG., 1964a, Phil. Mag., 9, 339.

Tegart, W.J. McG., 1964b, Jour. Glac., 5, 251.

Tegart, W.J. McG., 1966, Elements of Mechanical Metallurgy,

MacMillan, Toronto.

Tetelman, A.S. and McEvily, A.J., 1967, Fracture of Structural Materials, John Wiley, New York.

Truby, F.K., 1955, Jour. App. Phys., 26, 1416.

Udd, J.E., 1963, Trans. Can. Mining and Metal., 66, 461.

Voitkovskii, K.F., 1960, The Mechanical Properties of Ice,

Trans. A.F. Cambridge Res. Lab., -62-838. (Mekhanicheskie svoistva 1'da, Izdatel'stvo Akademii Nauk SSR, Moscow).

Von Mises, R., 1928, Z. Angew. Math. Mech., 8, 161.

Waddington, J.S., 1968, Phil. Mag., 17, 51.

Waddington, J.S. and Lofthouse, K., 1967, Jour. Nucl. Mater., 22, 205.

Wakahama, G., 1967, Physics of Snow and Ice, Low Temp. Inst., Hokkaido Univ., Japan, $\underline{1}$, 291.

Walsh, J.B. and Brace, W.F., 1964, Jour. Geophys. Res., <u>69</u>, 3449. Walsh, J.B., 1965a, Jour. Geophys. Res., 70, 381.

Walsh, J.B., 1965b, Jour. Geophys. Res., 70, 399.

Walsh, J.B., 1965c, Jour. Geophys. Res., 70, 5249.

Webb, W.W. and Hayes, C.E., 1967, Phil. Mag., 16, 909.

Weeks, W.F. and Lofgren, G., 1967, The Effective Solute Distribution Coefficient During the Freezing of NaCl Solutions,

Physics of Snow and Ice, Inst. Low Temp. Sci., Hokkaido Univ., 1, 579.

Weeks, W.F. and Assur, A., 1968, Ice Pressures Against
Structures, T.M. 92, Assoc. Comm. Geotech. Res., Nat.
Res. Council, Ottawa, 25.

Weertman, J., 1968, Dislocation Climb Theory of Steady State Creep, Presented Meeting ASM, Oct., (to be published in Trans. ASM).

Weibull, W., 1939, Proc. Roy. Swedish Inst. Eng. Res., Paper No. 153.

Weibull, W., 1951, Jour. App. Mech., 18, 293.

Westwood, A.R.C., 1961, Phil. Mag., $\underline{6}$, 195.

Wiederhorn, S., 1963, Jour. App. Phys., 34, 2125.

Williams, J.A., 1967, Acta Metal., 15, 1119.

Williams, J.A., 1968, Scripta Metall., 2, 273.

Wollan, E.O., Davidson, W.L. and Shull, C.G., 1949, Phys. Rev., 75, 1348.

Workman, E.J., 1953, Phys. Rev., 92, 544.

Wronski, A. and Fourdeux, A., 1964, Jour. of Less Common Metals, $\underline{6}$, 413.

Zajac, A., 1962, Jour. App. Phys., 33, 2059.

Zener, C., 1948, Fracture of Metals, ASM, 3.

Zhurkov, S.N. and Sanfirova, T.P., 1958, Sov. Phys., Tech. Phys., 3, 1586.

CLAIM OF ORIGINAL WORK

This is the first study to be undertaken of the role that crack formation plays in bringing about the failure condition in ice during compressive creep. It is demonstrated that failure is due to the breakdown of the structure by the formation of stable transcrystalline and grain boundary cracks. Following are listed results that have not been previously demonstrated:

- (1) Crack formation occurs in columnar-grained ice when the compressive stress exceeds about 6 kg/cm^2 .
- (2) In the stress range of 6 to 10 kg/cm², the cracking activity is confined primarily to the primary creep stage, and tends to zero in the secondary creep stage. For compressive stress greater than 12 kg/cm², crack formation causes the failure condition to develop during the primary creep stage.
- (3) Cracking activity in ice is essentially a random process prior to the onset of the failure condition.
- (4) The cracking activity, and in particular the crack density, is related in a meaningful way to stress, strain, temperature and time.

(5) The cracking activity in ice is probably associated with two independent processes - one with a probability for crack nucleation that increases linearly with strain, and one with a probability that is independent of strain. The latter process is probably associated with grain boundaries, and the former with stress concentrations of the type developed by dislocation pile-ups.

To the author's knowledge, no study of crack density has been carried out in sufficient detail on other materials to allow the analysis and interpretation that was possible in the present work.